The Structure and Function of Lung Surfactant: Effect of Amyloid Fibril Formation

by

Francis Hane

A thesis

presented to the University of Waterloo

in fulfillment of the

thesis requirement for the degree of

Master of Science

in

Biology

Waterloo, Ontario, Canada, 2009

AUTHOR'S DECLARATION

I hereby declare that I am the sole author of this thesis. This is a true copy of the thesis, including any required final revisions, as accepted by my examiners.

I understand that my thesis may be made electronically available to the public.

Abstract

The alveoli of mammalian lungs are covered in a thin lipid film referred to as pulmonary surfactant. The primary purpose of pulmonary surfactant is to reduce the surface tension of the air/liquid interface allowing breathing with minimal effort required.

We investigated the effect of addition of cholesterol and amyloid-β peptide on structure and function of Bovine Lung Extract Surfactant (BLES) and model lipid films.

In our first experiment, we have demonstrated the effect of amyloid-β and cholesterol on lipid films of DPPC, DPPC-DOPG and BLES. We saw that cholesterol inhibits multilayer formation in all monolayers. Amyloid-β increases multilayer formation in DPPC and DPPC-DOPG, but reduced multilayer formation in BLES. When cholesterol and amyloid-β is added to BLES, 1% amyloid-β is inconsequential, whereas 10% amyloid-β allows BLES to regain some of its surfactant function.

In our second experiment, we observed that for bothanionic DOPG and cationic DOTAP films which are in the fluid phase, amyloid-β interacts with the bilayer much quicker than in zwitterionic DPPC which is in the gel phase. Approaching 24 hours, we see small fibrils form on the bilayer, but these fibrils are considerably smaller than those formed when amyloid-β is incubated in solution. For fluid phase bilayer membrane, disruption is also observed.

Acknowledgments

I would not have been able to complete this degree without the support of numerous people and I therefore wish to acknowledge their support. First of all, my wife and children, who have graciously sacrificed in order for me to complete this degree. Secondly, I wish to thank my supervisor, Dr. Zoya Leonenko for taking a chance on me and giving me freedom in my research and giving me the flexibility of completing my research on my schedule. Also, I'd like to thank Dr. Leonenko for her guidance and her relentless efforts at teaching me how to discuss results, and teaching me the value of attention to detail. Lastly, I am indebted to my fellow graduate student, Brad Moores, and my undergraduate assistants, Liz Drolle, Erin Faught, Vince Choi, and Janet Simons, for answering my diverse questions on subjects that they are far more knowledgeable.

TABLE OF CONTENTS

List of Figures

Chapter 1
Introduction

1.1 The Pulmonary Surfactant System

1.1.1. **Introduction to the Pulmonary Surfactant System**

Pulmonary surfactant is a complex protien-lipid mixture that forms a monolayer existing in mammalian lungs and serves to reduce the surface tension of the air/liquid interface to reduce the work required of breathing.

Pulmonary surfactant is by definition a lipid detergent, usually consisting of a mixed lipid-protein monolayer lining the alveoli in the air/liquid interface. The primary purpose of surfactant is to lower the surface tension of this interface to near zero values (Holm, Enhorning and Notter 1988). Experimental measurements indicate that the equilibrium surface tension is approximately 23 mN/m at beginning of expiration (Floros 2005). While this low surface tension is necessary to allow minimal effort while breathing, surfactant must change its properties during the breathing cycle to increase its surface tension to a higher value to prevent alveolar collapse (Clements 1957).

Surfactant is secreted by exocytosis from the lamellar bodies which are formed by alveolar type II cells in the lung epithelium. Tubular myelin is a complex of bilayer structures formed when laminar bodies are hydrated within the alveolar liquid (Johannsen 1997).

1.1.2. **Composition of the Pulmonary Surfactant System**

Pulmonary surfactant is primarily a lipid-based system with small amounts of associated proteins referred to as the surfactant proteins A, B, C, and D, named in order of their discovery. Historically surfactant has been considered a lipid monolayer, but this idea is now seen as an oversimplification (Johannsen 1997). The composition of surfactant can vary and is influenced by diet, age, and physical fitness (Crewels, van Golde and Haagsman 1997).

1.1.2.1. Lipids

The primary lipid (70-80%) in pulmonary surfactant has been shown to be phosphatidylcholine (PC), in which 50-70% is saturated PC (Crewels, van Golde and Haagsman 1997). Of this PC lipid layer, dipalmitoylphosphatidylcholine (DPPC) is considered the primary variant lipid. DPPC is capable of reducing surface tension levels approaching zero; however, DPPC alone fails as an effective surfactant because it is slow to re-spread when compression is relieved and it is slow to adsorb from an aqueous suspension (Poulain and Clements 1995). DPPC molecules in a monolayer are oriented with the fatty acid tails pointed up (towards the air interface). The polar headgroups are in the subphase with the fatty acid tails tilted between 21.5-29 degrees depending on humidity (Katsaras, Yang and Epand 1992). In order for lung surfactant to maintain its biophysical properties, the lipids are required to both allow the surfactant surface tension to reduce to very low values, as well as re-spread rapidly during the respiratory cycle. The individual components of surfactant are each good at lowering surface tension (DPPC) or fluidizing the monolayer (PG, PC, proteins); none of the individual components exhibits both properties (Ding, et al. 2001).

1.1.2.2. Proteins

Within the pulmonary surfactant system proteins compose approximately 10% of the surfactant system (Johansson, Curstedt and Robertson 1994). These proteins serve a variety of roles within the surfactant system. The surfactant proteins can be divided into two classes: the hydrophilic proteins and the hydrophobic proteins.

The first protein identified was the hydrophilic Surfactant Protein A. SP-A consists of 248 amino acid residues and has a molecular weight between 28-36 kDa depending on the species (Crewels, van Golde and Haagsman 1997). The following is a list of function which SP-A is responsible for (Crewels, van Golde and Haagsman 1997):

1. Formation of tubular myelin
2. Regulation of phospholipid insertion into the monolayer
3. Modulation of uptake and secretion of phospholipids by type II cells
4. Activation of alveolar macrophages
5. Binding and clearance of bacteria and viruses
6. Chemotactic stimulation of alveolar macrophages.

The other hydrophilic surfactant protein is SP-D. There is some academic debate over whether SP-D is a true surfactant protein since it is also found in gastric tissue (Crewels, van Golde and Haagsman 1997). SP-D is the largest of the surfactant proteins consisting of 355 amino acid residues and having a molecular weight of 43 kDa. Along with SP-A, SP-D plays an important role in pathogen defense, which is its primary purpose (Crewels, van Golde and Haagsman 1997).

The surfactant proteins B and C (SP-B, SP-C) are hydrophobic proteins. Both SP-B and SP-C are considerably smaller than SP-A and SP-D with SP-C containing 35 amino acid residues. In addition, both SP-B and SP-C are only soluble in organic compounds such as chloroform or methanol (Perez-Gil 1993). Both SP-B and SP-C require intracellular post translational modification to form their mature forms (Beers, et al. 1994). Specifically, SP-C needs to gain two thio-ester side chains in order to maintain its biophysical properties (Johannsen 1997). SP-B is high in cysteine which allows it to form a unique pattern of disulfide bonds to assist in stabilizing the protein. The most important property of SP-B is in enhancing the biophysical properties of the surfactant and assisting in rapid insertion of phospholipids into the air/liquid interface. This results in a stable surface film (Hawgood, et al. 1987). SP-C has similar roles in the maintenance of surfactant as SP-B: it is responsible for rapid formation of the monolayer and molecular ordering of the monolayer. These roles require SP-C to have extreme structural and stability properties (Johannsen 1997). SP-C is one of the most hydrophobic proteins discovered: this hydrophobicity is the result of a significant portion of the protein being made up of the highly hydrophobic amino acid valine resulting in an alpha-helical stretch which spans the DPPC layer (Morrow, et al. 1993). NMR studies of SP-C confirm that SP-C has no tertiary structure (Johannsen 1997). SP-C is also the only surfactant protein that lacks homologous proteins. SP-C contains two palmitoyl groups post-translationally bound to two amino acid residues. This palmitoylation of SP-C increases membrane affinity of the protein, influences protein structure and plays a role in membrane fusion by enhancing re-spreading and stability of DPPC (Qanbar 1996).

1.1.3. **Function of Pulmonary Surfactant**

The primary function of the pulmonary surfactant system is to reduce the surface tension of the air/liquid interface to near zero at the beginning of expiration. No single component of surfactant contributes solely to the required biophysical properties necessary for effective surfactant function (Ding, et al. 2001). The tension of the surface film varies with area, where exhalation results in decreased surface area and decreased surface tension, preventing the alveoli from collapsing (Clements 1957). The pressure within the alveoli can be estimated by the expression,

$$P = 2\gamma/r,$$

where P is the pressure, γ is the surface tension and r is the radius of the alveoli (King 1982). Knowledge of individual surfactant components will assist with understanding how the complete surfactant system operates. As mentioned earlier, surfactant is composed primarily of phospholipids. These phospholipids include phosphatidylcholine (saturated and unsaturated), primarily dipalmitoylphosphatidylcholine (DPPC) and phosphatidylglycerols (PG). A mixture of these lipids is necessary to make up the lipid portion of an effective surfactant. These two lipids have different characteristics. During the breathing cycle, DPPC is required to lower the surface tension of the air/liquid interface (Clements 1964). While DPPC is effective in lowering surface tension, it is inadequate to complete the task of respreading the surfactant into an even lipid layer; PG on the other hand is effective in spreading this surfactant (Hallman 1975). Incidentally, PG is one of the last compounds developed during natal development. A premature infant is often born without sufficient PG. This lack of PG is causal to Infant Respiratory Distress Syndrome (Hallman 1975).

The process of lowering the surface tension in surfactant films is accelerated when surfactant proteins are included in the lipid film (King 1972). A good lung surfactant will adsorb within milliseconds during a deep breath. During expiration, when the surface film is compressed and below the equilibrium surface tension, there is a net desorption of various components from the film (King 1972). A given material in the alveolar subphase will not integrate into the air/liquid interface unless surfactant surface tension is below the equilibrium value for the material (King 1972). SP-A acts together with SP-B and SP-C to promote rapid formation of the surfactant film (Rooney, Young and Mendelson 1994). Surfactant protein B reduces surface tension by increasing the lateral stability of the phospholipid monolayer (Cochrane and Revak 1991). It has been shown by Mathialagen et al that SP-B is more influential in reducing surface tension than SP-C, suggesting that SP-B is more efficient in removing unsaturated phospholipids (which inhibit the reduction of surface tension) from the surfactant surface (Mathialagan 1990). As mentioned earlier, SP-C contains two palmitoyl groups post-translationally bound to cystienes 5 and 6. This palmitoylation of SP-C increases membrane affinity of the protein, influences protein structure, and plays a role in membrane fusion by enhancing re-spreading and stability of DPPC (Qanbar, et al. 1996). SP-C is also responsible for maintaining lipids in the vicinity of the air/liquid interface. Meanwhile SP-B assists in ordering monolayer collapse, ensuring a reduction in surface tension (Ding, et al. 2001).

While the surfactant proteins assist in the function of surfactant, the serum proteins (or blood proteins) inhibit the function of surfactant. The presence of serum proteins in the surfactant has been shown by Holm, et al to increase surface tension by up

to a factor of two. These results suggest that these proteins may be mechanistically responsible for limiting effective surfactant function (Holm, Enhorning and Notter 1988).

As stated earlier, effective surfactant must be able to change its properties during the breathing cycle: surfactant must have a very low surface tension at the beginning of expiration to allow oxygen diffusion, and then surface tension must increase at the end of expiration to prevent alveolar collapse. The explanation of the method by which surfactant accomplishes this remarkable task has evolved over the course of surfactant research. It was previously thought that as the surface area of the alveoli decreases (during expiration), the surfactant must "squeeze-out" unsaturated lipids and proteins (Ding, et al. 2001). This would lead to a surfactant rich in DPPC, resulting in an increase in surface tension preventing alveolar collapse. These "squeezed-out" components would temporarily reside in microscopic "reservoirs" on the phospholipid layer. During inspiration, the components within the reservoirs would be released and spread along the air/liquid interface. It was theorized that SP-C stabilized these reservoirs (Amrein, von Nahmen and Sieber 1997) by incorporating their alpha helix into one bilayer and stretching their palmitoyl groups into neighboring bilayers. Through the use of atomic force microscopy (AFM), Ding et. al have expanded on this "squeeze-out" theory and somewhat rendered it obsolete. In fact, during expiration, the lipid monolayers form multiple, discrete layers to compensate for the reduction in alveolar surface area (Ding, et al. 2001). Therefore, these other components are not "squeezed-out", but rather they remain at the surface and fold and "unzip" in order to maintain low surface tensions and re-spreading readily at the collapsed state without changing surfactant composition. Proteins located within the phospholipid folds may provide a method of incorporating

new material into the air/liquid interface upon alveolar expansion (Ding, et al. 2001). The research conducted by Oosterlaken, et al indicates that the insertion rates of lipids into the monolayer were not affected by the composition of the monolayer, but only affected by the protein content (Oosterlaken 1991). Furthermore, because of surface pressures can be reduced to very low values without loss of proteins from the monolayer, it can be concluded that there is a lipid/protein interaction (Oosterlaken 1991).

1.1.4. **Relevant Pathologies**

Acute Respiratory Distress Syndrome (ARDS) is a respiratory condition resulting from pulmonary surfactant failure. This failure can be attributed to a number of factors including: presence of serum (blood proteins) within the alveoli (perhaps as a result of an acute lung injury), amyloidosis of the surfactant protein C, as well as other unknown factors. Research by Gregory et al showed that the presence of serum proteins within the air/liquid interface may cause ARDS (Gregory, et al. 1991) by changing the chemical composition and function of pulmonary surfactant (Holm, Enhorning and Notter 1988). This failure of lung surfactant occurs when the surfactant fails to adequately reduce the surface tension of the air/liquid interface. A by-product of this surfactant failure is considerably lower lung surface, responsible for gas exchange (Petty, et al. 1979).

Mortality for patients suffering from ARDS remains high. ARDS typically requires replacement surfactant therapy (Floros 2005). This surfactant may be either a natural animal extract, such as Bovine Lung Extract Surfactant (BLES) or an artificial surfactant made up of DPPC, PG, and various surfactant proteins, which is currently under development and is an active area of research. In addition, the use of the coagulant antithrombin III, as a treatment for ARDS, is being investigated (Floros 2005). This is

because the presence of the serum protein fibrinogen destroys surfactant activity because it initiates the coagulation cascade. However, lysis of the clot allows surfactant function to be restored (Floros 2005).

Neonatal Respiratory Distress Syndrome (RDS) is similar to ARDS, except that it occurs in premature infants where surfactant is not development. In fact, ARDS used to be an acronym for Adult Respiratory Distress Syndrome to distinguish it from the infant version. NRDS is usually caused by pre-term births or a genetic condition. Since, the pulmonary system is the last mammalian system to develop during gestation, it stand's to reason that the pulmonary system is the system most affected by a pre-term birth. Specifically, the surfactant system is among the last to develop within the pulmonary system. Typical treatment of RDS is artificial surfactant or BLES therapy. Breathing is assisted through the use of a high frequency oscillating ventilator which provides sufficient oxygen to the lungs, while keeping tidal volume low and peak end expiratory pressure (PEEP) within acceptable limits. If a pre-term birth is expected, the mother is given various hormones to assist with fetal surfactant biosynthesis (Floros 2005).

Various genetic disorders may also result in IRDS. Nogee, et al observed SP-C mutation in infants with chronic lung disease. This mutation would result in a decrease in lipid stability compromising surfactant function (Nogee, et al. 2002). Nogee also discovered that a frameshift mutation in the gene producing SP-B resulted in no SP-B production and 100% infant mortality of those infants suffering from this genetic disorder (Nogee, et al. 2002).

Another disorder, known as Pulmonary Alveolar Proteinosis (PAP) is associated with the amyloidosis of SP-C. Pulmonary Alveolar Proteinosis is the result of

the surfactant protein C forming amyloid fibrils under certain conditions (Gustafsson, et al. 1999) (Dluhy, et al. 2003). The structure of these fibrils is similar to fibrils formed by other amyloid proteins, such as amyloid-β and α-synuclein. When SP-C plaques form, SP-C ceases to function as an effective distributer of DPPC and leads to a breakdown of the effective function of the surfactant (Wüstneck 2004). It appears that this SP-C amyloidosis occurs at high lipid/protein concentrations. This condition is a contributing factor in (ARDS).

1.1.5. **Current Developments in Research**

The latest developments in surfactant research have revolved around the role of cholesterol and electrostatic interactions between protein and lipid. In 2005, Gunesakara et al reported that cholesterol is very influential in molecular ordering of the surfactant films, even at low concentrations (Gunasekara, et al. 2005). Using atomic force microscopy and Kelvin probe force microscopy, Leonenko et al reported that BLES with significantly elevated levels of cholesterol (20%) had considerably smaller tip/film adhesion forces than BLES with regular (5%) levels of cholesterol. This evidence suggests that the adhesive properties of the film were changed by the additional cholesterol. In this case, one can assume that with the addition of cholesterol, the lipid molecules are not mobile enough to easily rearrange and fold into lipid multilayers. In this case, the surface tension is higher on contraction. Furthermore, it is believed that if the conversion from lipid monolayer to lipid bilayer is inhibited by cholesterol, the unsaturated lipids are unable to form a bilayer and thus are unable to reduce the surface tension. This increased concentration of cholesterol results in the lipid film collapsing during alveolar compression (Leonenko, Gill, et al. 2007). Studies conducted using

Kelvin Probe Force Microscopy (KPFM) have provided further insight into the lipid monolayer to bilayer conversion. KPFM has shown that the second layer of the surfactant film has a more positive surface potential than the first monolayer while the third layer has the same surface potential as the first layer (Leonenko, Rodenstein, et al. 2006).

1.2 Amyloidosis

1.2.1. **Introduction to Amyloidosis**

Amyloidosis is defined as an abnormal process in which a protein, which is normally in an alpha-helical state unfolds, re-conforms in a β-sheet conformation and aggregates to form insoluble fibril-like formations (Serpell 2000). These amyloid fibrils are then deposited either systemically or in specific organs, destroying surrounding cells (Johannson 2005). Amyloid fibrils can be observed by staining with the Congo Red dye and showing birefringence under polarized light. They will appear as 5-10 nm fibrillar structures detectable by electron microscopy or x-ray diffraction (Serpell 2000). Despite significant research into the amyloidosis process, no clear reason has emerged on the formation and kinetics of this process (Carrell and Gootu 1998). This amyloidosis process is implicated in at least twenty different pathologies, each one affected by the aggregation of a different protein. These diseases include the neuro-degenerative disorders Alzheimer’s, Huntington's, Parkinson's, and Creutzfeld-Jacob's. Pulmonary Alveolar Proteinosis (PAP) is believed to be caused by the amyloidosis of the Pulmonary Surfactant Protein C (SP-C) (Johannson 2005). Whether this fibril formation is causal to the pathology or whether this amyloidosis is the result of an abnormal intra-alveolar metabolism has yet to be determined (Johannsen 2003).

1.2.2. **Amyloid-β**

Amyloid-β is a 40-43 amino acid length peptide, part of the protein associated with Alzheimer's disease. Amyloid-β is a proteolytic product of the Amyloid Precursor Protein (APP). Amyloid- β consists of a hydrophilic, extracellular region located at residues 1-28, and a hydrophobic, transmembrane alpha-helical coil at residues 29-42 (Bokvist, et al. 2004).

The gene for APP is found on chromosome 21, and is expressed in a variety of cells the glial, endothelial, epithelial and spleen. The symptoms of Alzheimer's disease are as a result of APP being expressed in neuronal cells (Bokvist, et al. 2004). The function of APP is unknown at this point, but past research has suggested that APP may have a role as an autocrine factor to stimulate the proliferation of ce11 (Saitoh, et al. 1989), and as a modulator of ce11 adhesion. Once amyloid-β is cleaved from APP, it is a soluble monomeric peptide in an aqueous environment, and is removed (in healthy persons). In pathological cases, amyloid-β may aggregate to a certain degree to become neurotoxic (Bokvist, et al. 2004).

In Alzheimer's disease, amyloid-β misfolds to form amyloid fibrils. It is believed that these amyloid fibrils and their intermediates are causal to the symptoms found in patients with AD (Selkoe 2000). Several mechanisms have been suggested as to why amyloidosis results in specific pathologies. Research by Lin and associates indicates that oligomeric amyloid-β forms ion channels in lipid membranes resulting in higher levels of intracellular calcium (Lin, Bhatia and Lal 2001). Perturbations in membrane fluidity have been suggested by groups Kremer (Kremer, Pallitto, et al. 2000)and Muller (Muller, et al. 1998). Free radical production has been suggested by Butterfield (Butterfield,

Varadarajan and Koppal 1999) . Changes in lipid metabolism have been suggested by Koudinov (Koudinov, Berezov and Koudinova 1998).

1.2.3. **Mechanisms of Action**

Although much research has been conducted on the conformational change of Amyloid-β a clear answer still eludes the research community. Amyloid-β fibril formation has been shown to involve an α-helix to β-sheet transition. However, not all

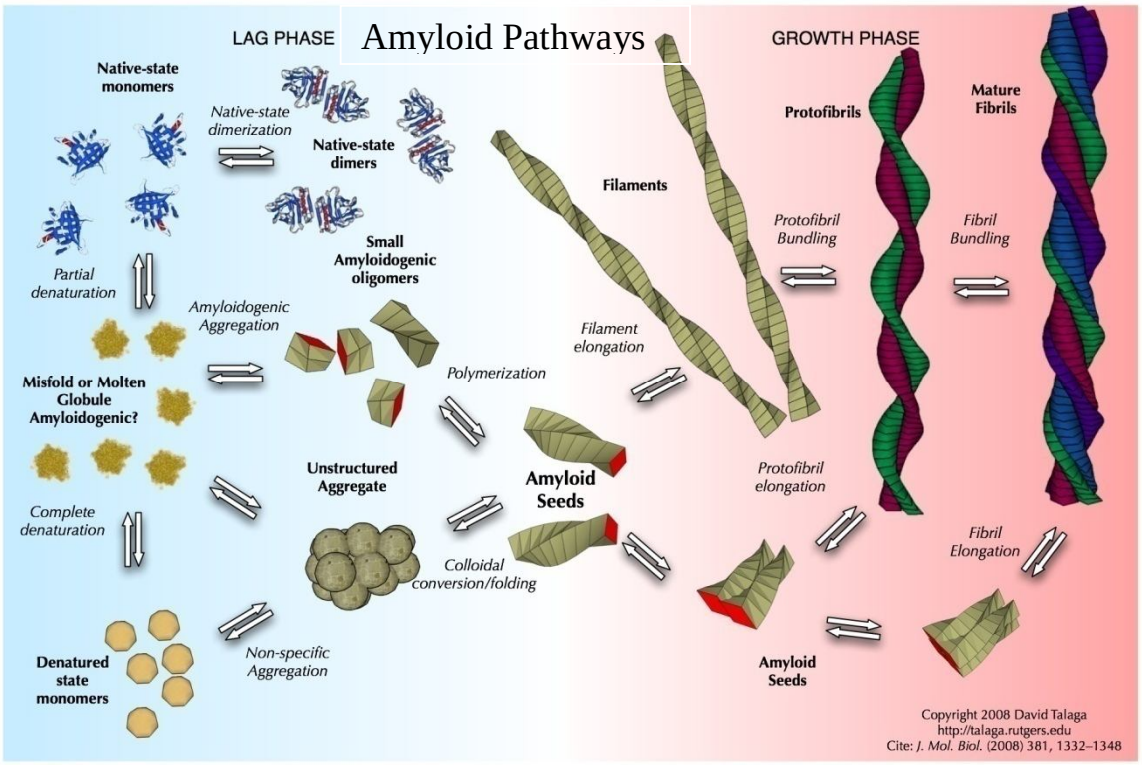

Figure 1 - Possible pathways in amyloid fibril formation adapted from (Giurleo, He and Talaga 2008)

protein's form amyloid deposits by this conformational change. α-synuclein has no defined structure in its native state, yet still forms amyloid fibrils (Johannsen 2003). Certain proteins show very similar secondary structures once amyloid process is

complete despite radically different primary structures: this suggests that the amyloidosis process for each different protein involves a different biochemical mechanism (Booth, et al. 1997). In solution, amyloid-β readily transforms into a β-sheet conformation (Szyperski, et al. 1998) despite that molecular dynamics simulations show that the helix is highly resistant to unfolding (Kovacs, et al. 1995). Figure 2, shown below, shows a schematic of the process of fibril formation. Structure N is the native state and Structure U is a completely unfolded state. Structure I is the intermediary state which undergo a conformational transition to a β-sheet structure (O). These β-sheets form protofibrils

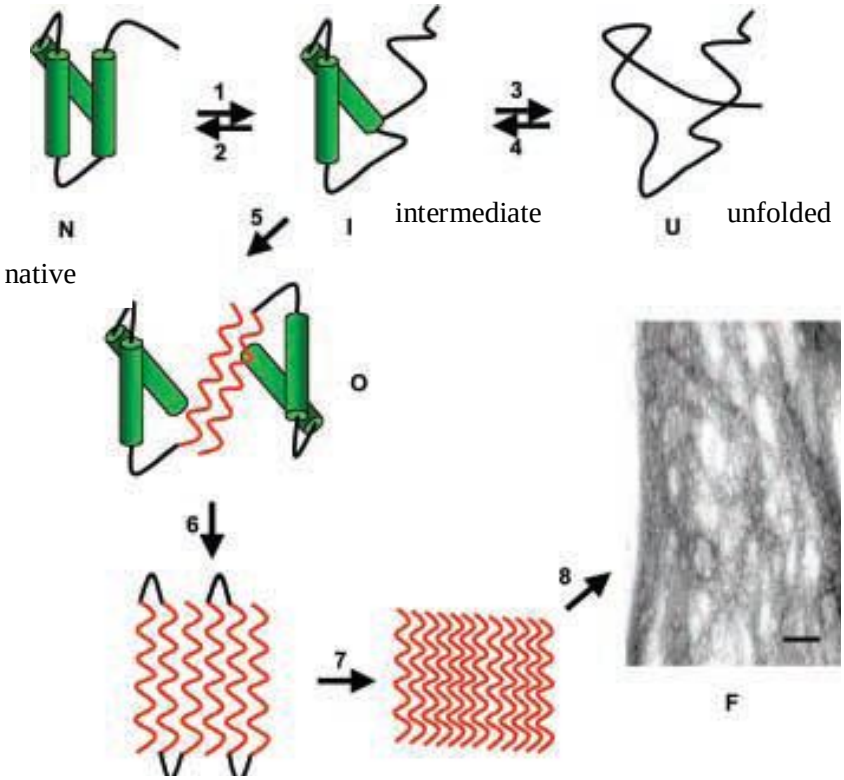

Figure 2 - Proposed mechanism for amyloid fibril formation adapted from (Johannsen, Molecular determinants for amyloid fibril formation: lessons from lung surfactant protein C 2003)

which aggregates to form amyloid fibrils. The electron micrograph depicts the fibrils. The scale bar represents 50 nm (Johannsen 2003).

1.2.4. **Amyloid Fibrils**

Amyloid fibrils have been shown to associated with a wide variety of diseases including Alzheimer's, Parkinson's, the prion disease and about 20 others disease of various severity. Despite a similar end product, there seems to be no commonality among primary protein structure linking these proteins.

The original work done on amyloid fibril structure stretches back to 1935, when Astbury, using x-ray diffraction, found that there existed a difference in length and width of egg white when stretched, suggesting a fibre like structure (Astbury and Dickinson 1935). Later, researchers were able to obtain a cross-β x-ray diffraction pattern. This structure was found in the deposits of pathological tissues (Sunde and Blake 1997). Today, various methods including x-ray diffraction, NMR, atomic force microscopy, and electron microscopy have shown that fibrils formed by different properties share similar properties, including a structure made up of unbranched protofilaments (Nelson 2006). The classical biophysical definition of an amyloid fibril is a protein structure which exhibits red-green birefringence when exposed to circularly polarized light. Identification of amyloid fibrils is also made by determining binding to Congo red or Thioflavin T. X-ray diffraction patterns of amyloid fibrils show characteristic signals produced at 4.7 and 10 angstroms corresponding to interstrand and stacking distance between the β-sheets. Amyloid fibrils are approximately 100 Å in diameter and composed of 20–35 Å wide protofilaments.

While amyloid-β has a poorly defined monomeric structure due to its insolubility and difficulty in crystallization, recent advances have allowed researchers to solve the structure of amyloid fibrils (Luhrs, et al. 2005). However, to date, only one amyloid-β 3D

structure has been resolved (Nelson 2006). There is general agreement amongst (Nelson 2006) that amyloid-β peptides have a β sheet secondary structure which stack in an anti-parallel fashion to form β sheets which run perpendicular to the fibril axis (Kirchner, Abraham and Selkoe 1986). Figure 3-Model of β sheet amyloid structure adapted fromA shows the Van der Waals interactions between β sheets while Figure 3B and C shows the position of the β sheets relative to the direction of the fibril.

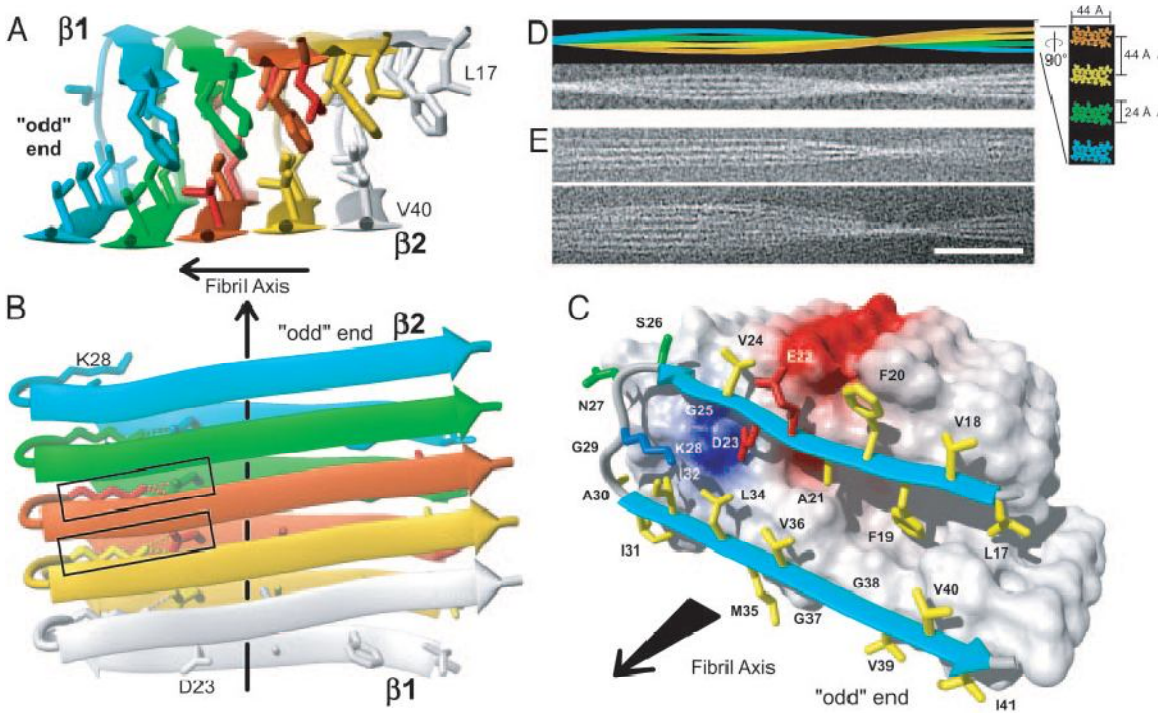

Figure 3-Model of β sheet amyloid structure adapted from (Jimenez, et al. 2002)

These sheets appear to form from amino acid sequences 18-26 and 31-43 (Luhrs, et al. 2005). Intermolecular interactions amongst the side chains are formed between the odd-numbered residues of strand 1of the *n*th molecule and the even-numbered residues of strand 2 of the (*n* -1)th molecule (Luhrs, et al. 2005). These anti parallel sheets are held together by hydrogen bonds. All fibrils have been shown to form a left handed helix (Bauer, et al. 1995), (Goldsbury, et al. 1997), (Ionescu-Zanetti, et al. 1999), (Harper, Liber and Lansbury 1997). Figure 4 - Model of Amyloid Fibril adapted fromFigure 4 -

Model of Amyloid Fibril adapted from shows a model of an amyloid-β fibril. Notice the anti-parallel β sheet structure stacked together to form a protofilament. Four protofilaments are wrapped together to form a mature amyloid fibril.

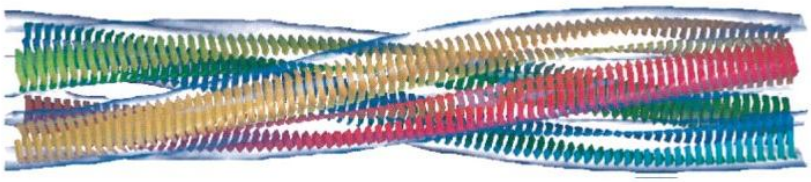

Figure 4 - Model of Amyloid Fibril adapted from (Jimenez, et al. 2002)

While all fibrils have similar morphologies and properties, small variations in structure occurs in amyloid fibrils of different proteins (Balbirnie, Grothe and Eisenberg, 2001) (Diaz-Avalos, et al. 2003) (Petkova, et al. 2005). Even within the same preparations, fibril morphology can vary. This difference has been attributed to the number of protofilaments found in the amyloid fibril (Jimenez, et al. 2002). Research by Jimenez suggests that individual protofilaments, are relatively flat as opposed to being highly twisted as previously suggested (Jimenez, et al. 2002). Comparing various fibrils structures suggests that small local changes in β-sheet twist are important in the long range coiling of protofilaments (Jimenez, et al. 2002).

Work by Nelson has provided the first truly atomic model of the amyloid fibril (Nelson, Sawaya, et al. 2005). In this research,

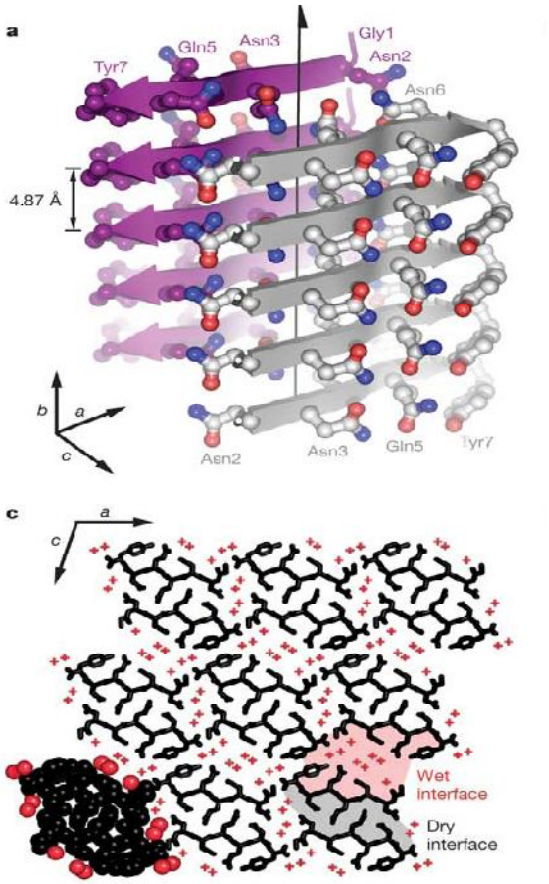

Figure 5-Proposed Atomic Model of B sheet interactions adapted from (Nelson, Sawaya, et al. 2005)

Nelson, et al showed that side chains protruding from the two sheets forms a tight, dry, "steric zipper". Figure 5-Proposed Atomic Model of B sheet interactions adapted from Notice the difference between wet and dry interfaces.

Side chains from each strand nestle between side chains from the opposing sheet. This is referred to as the "dry" interface. In this interface, van der Waals interactions hold the sheets together, while hydrogen bonds bind neighbouring molecules in the same sheet. Disruption of this "steric zipper" may be a target for future drug therapy. In the

"wet" interface, water molecules line neighbouring sheets. Within each sheet, hydrogen bonds hold together each segment to its neighbouring segment, through stacks of the backbone and side chains, demonstrating the stability of these fibril structures.

Present research has not yet identified one single theory explaining all the properties of amyloid fibrils. However, some models do answer many of the properties of the different fibrils (Nelson 2006). The major recent models of fibril formation are the refolding model, natively disordered model, and the gain of interaction model (Nelson 2006). In the refolding model, it is assumed that the peptide is either in the native or fibril form. In this model, the peptide must completely unfold from its native state and refold into its fibril form. In this model, the sequence of side chain interactions are unimportant. In the natively disordered model, it is assumed that certain proteins are naturally disordered in their native state. It is this disordered section of the protein that forms the cross-β spine of the amyloid fibril. The third class of model is the gain of interaction model. This model hypothesizes that the conformational change in a certain area of the peptide exposes a previously unexposed surface. It is this newly exposed surface that binds to another molecule and allows the fibril to continue its growth.

1.2.5. **Factors Affecting Fibril Formation**

A number of factors have been identified in increasing the kinetics of conformational change in amyloid forming peptide. Jimenez and colleagues showed that low pH increases the rate of amyloid fibril formation (Jimenez, et al. 2002). Also, the presence of ions, the protein-lipid ratio, and the presence of cholesterol and gangliosides have been shown to affect the rate of fibril formation (Maltseva, et al. 2005). Lastly,

extensive studies have shown the effect of lipids in amyloid fibril formation (Bokvist, et al. 2004).

1.3 Lipid-Protein Interactions

1.3.1. **Amyloid-B Membrane Lipid Interactions**

For most amyloid forming proteins associated with amyloid diseases, neither the reason for unfolding and aggregation, nor the specific function is known. Most research looking into the protein misfolding problem has been conducted in solution. However, researchers have recently been investigating the effect of membrane lipids on the protein misfolding problem.

One of these attempts is described by Bockvist and colleagues, who have identified two methods in which amyloid-β interacts with lipid membranes (Bokvist, et al. 2004). The first is method is that of peptide insertion into the lipid membrane, the second method occurs when aggregated amyloid-β binds to the membrane lipid.

In the first case, Bockvist showed that because of electrostatic interactions, peptide insertion increases as the charge of the lipid membrane decreases: maximum insertion occurs with negatively charged lipid membranes. This electrostatic effect augments the hydrophobic effect where the α-helical section of the peptide wants to insert itself into the bilayer. This finding correlates well with research by Maltseva, who showed that electrostatic interactions with negatively charged lipids increases peptide adsorption and other hydrophobic surfaces (Maltseva, et al. 2005) and Ege, who proposed that the strong electrostatic interaction between the peptide and the negatively charged lipids, drives the peptide deep into the lipid membrane (Ege and Lee 2004). However, amyloid-β has difficulty incorporating into lipid bilayers at high surface pressures (Ege

and Lee 2004). When incorporated into the membrane bilayer, amyloid-β peptide is stabilized and somewhat prevented from aggregating as it is bound in the membrane; amyloid fibril formation is therefore somewhat inhibited (Bokvist, et al. 2004).

Using a Langmuir Blodgett trough, Ji and associates measured the level of amyloid-β insertion into lipid monolayers (Ji 2002). Ji found that both cholesterol and low pH increase amyloid-β insertion into the lipid monolayers. Ji hypothesized that amyloid-β insertion is partial to lipid rafts which have been found to have higher than normal concentrations of cholesterol. Research by Ege and associates (Ege and Lee 2004) demonstrates that as lipid packing density increase, peptide insertion into lipid monolayers decreases proportionally. While there is general agreement that amyloid-β peptides prefer to bind with anionic lipids, research by Ege suggests that cationic lipids can bind just as readily. Also, Ege has noted that oligomeric forms of amyloid-β inserts more readily into lipid monolayers than monomeric forms (Ege and Lee 2004).

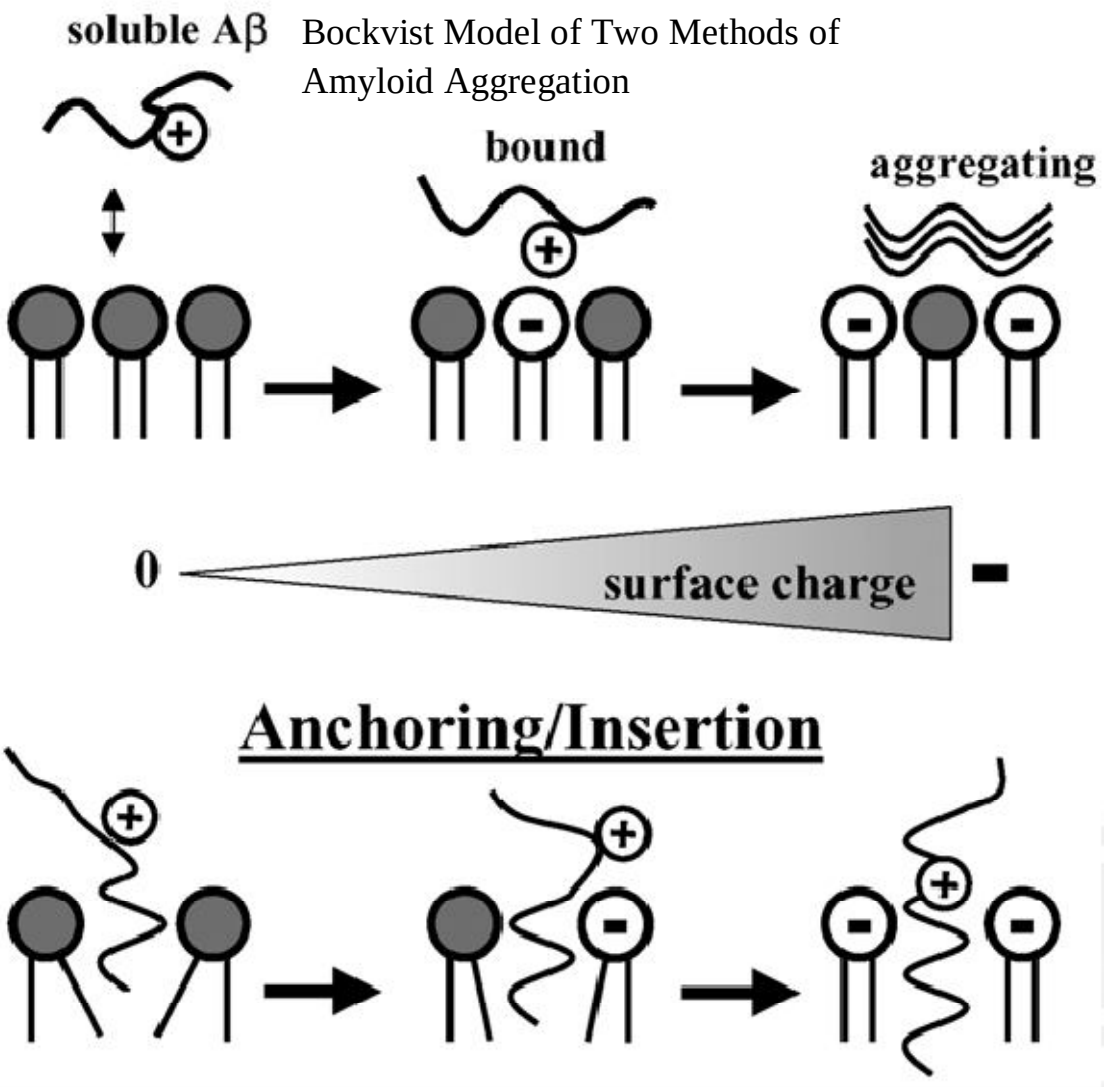

Figure 6 - Schematic model of Amyloid-β interacting with Membranes adapted from (Bokvist, et al. 2004)

The second mechanism identified by Bockvist occurs where amyloid-β is allowed to misfold into β-sheets in bulk solution and then forms amyloid fibrils. In this case, the presence of acidic lipids causes an increase in the surface concentration of the amyloid-β peptide increasing the conversion rate from α-helix to β-sheet through a direct membrane surface interaction (Bokvist, et al. 2004). In this case, amyloid-β is associated with ion channel activity resulting in neuronal apoptotic cell death. In this case, it has been shown by Maltseva that the β-sheets are oriented parallel to the surface (Maltseva, et al. 2005).

Using circular dichroism and caloimetry, Terzi (1994) suggested a lipid induced peptide aggregation of amyloid-β at the membrane of anionic lipids as opposed to membrane penetration. The theory proposed by Terzi is that the anionic lipids attract the cationic amyloid-β peptide to the surface electrostatically creating a parallel alignment of the peptide chains.

It has been proposed that monomeric amyloid-β may reinsert itself into the membrane as a possible mechanism to prevent aggregation and oligomerization (Ji 2002).

1.3.2. **Effect of Membrane Lipids on Amyloidosis**

Research has shown that the amyloidosis process is influenced by membrane lipids, especially negatively charged lipids (Maltseva, et al. 2005). In solution, amyloid-β reaches a reversible equilibrium of random coil, β sheet structures. Conversely, research by Terzi, has demonstrated that in the presence of negatively charged membrane lipids, this random and coil-β sheet equilibrium shifts almost completely toward the β sheet conformation. It was hypothesized by Terzi that this equilibrium shift is a result of the cationic amyloid-β peptide being attracted to the anionic lipids in the membrane forming a higher local surface concentration of the peptide on the surface. A combination of an increased surface concentration with the aligning of the peptide creates ideal conditions for the formation of amyloid fibrils. This process may act as a catalyst, reducing the activation energy required to correctly position the peptide chains, or the membrane shifts the thermodynamic equilibrium to favour β sheet conformation (Terzi 1994). Another theory proposed by Terzi (Terzi 1995) suggests that amyloid-β inserts into the hydrophobic region of the lipid membrane and forms β sheets within that region. This

possibility is supported by the observation that the membrane mimicking solvent trifluoroethanol induces a β-sheet structure. Further research by Choucair (Choucair, et al. 2007) provides evidence to the membrane mediation of fibril formation. In their research, Choucair and associates used a combination of atomic force microscopy and fluorescence to elucidate the effects of membranes on fibril formation. During the course of this research Choucair found that when the amyloid-β peptide is added to the lipid, the peptide started to accumulate on the lipid bilayer within 15 minutes, compared to the time of greater than 1 hour for the peptide to aggregate in solution. Choucair also found no evidence of the amyloid-β peptide inserting into the lipid bilayer.

Work by Choucair, et al shows that amyloid-β fibrils bind preferentially to gel-phase domains (Choucair, et al. 2007). While considerable research shows that amyloid-β binds preferentially to anionic lipids, Kremer demonstrates that amyloid-β changes membrane fluidity equally amongst different lipids (Kremer 2001) (Kremer, Sklansky and Regina, Profile of Changes in Lipid Bilayer Structure Caused by Beta-Amyloid Peptide 2001). Using neutron diffraction, Dante demonstrated that the amyloid section 25-35 deeply penetrates the lipid bilayer resulting in a perturbation of the bilayer (Dante, Hauss and Dencher 2003).

Research by Bockvist shows that the presence of acidic lipids electrostatic forced between the peptide and the lipid membrane keeps the peptide in a transmembrane position, thereby preventing aggregation (Bokvist, et al. 2004).

Our research is based on the following hypotheses: a) lipid surfaces and their structural and electric inhomogeneity play an important role in amyloid fibril formation;

b) structure and physical properties, which define function of the surfactant film may be considerably changed by fibril association. To test these hypotheses, changes in structural properties and surface activity of surfactant films and lipid films upon amyloid fibrillization are investigated in model lipid monolayers, bilayers, and BLES surfactant films. We believe that non-uniform nanoscale structure (both multilayers visible in AFM and non-uniform surface potential distribution discovered by KPFM) of BLES surfactant affect the effectiveness of SP-C fibril formation and fundamentally determine their interaction with the pulmonary surfactant film. The goal of this research is to investigate the structure and physical properties of model lipid monolayers and BLES surfactant films upon amyloid fibril formation on the lipid films, using atomic force microscopy (AFM) and Kelvin probe force microscopy (KPFM) to elucidate how non-uniform morphology and surface potential affects molecular mechanisms.

1.4 Methods

1.4.1. **Atomic Force Microscopy**

Atomic Force Microscopy (AFM) is a form of Scanning Probe Microscopy and was invented in the early 1980's. The developers of the Scanning Tunnelling Microscope, the precursor to the AFM, Gerd Binning and Heinrich Rohrer won the Nobel Prize in Physics in 1986. The concept of the AFM is simple: a sharp probe, called a tip attached on the end of a flexible beam called a cantilever scans the surface of the sample, driven by piezoelectric crystals to raster. In direct contact mode (DC), the tip comes close to the sample surface and the cantilever deflects as a function of the total interactions between the tip and sample. A laser measures this cantilever deflection and through a feedback loop, moves the z-axis of the piezo to keep a constant deflection and therefore force on

the sample. In the intermittent contact mode, the cantilever is oscillated at it's resonance frequency. As the tip rasters the surface, any interaction between tip and the sample results in a change of amplitude of the cantilever oscillation. This change in amplitude is registered and the resulting topology is determined.

Atomic Force Microscopy has a horizontal resolution which is a function of tip radius, usually around a few nanometers. Vertical resolution is usually approximately 0.1 nm. AFM gives only topological information; certain features on the side or under the sample are not resolved using the Atomic Force Microscope.

AFM has been used to image lipids, proteins, inorganic materials, and larger structures such as bacteria. In addition to imaging, AFM can be used to measure forces in the order of piconewtons. For example, researchers have used the AFM to measure the energy required to unfold proteins, separate membranes proteins from lipid membrane, and measure the forces required to separate two strands of DNA.

When the AFM is combined with the Kelvin Method, the instrument is called the Kelvin Probe Force Microscope and is used to determining local surface potential distribution in non metallic surfaces.

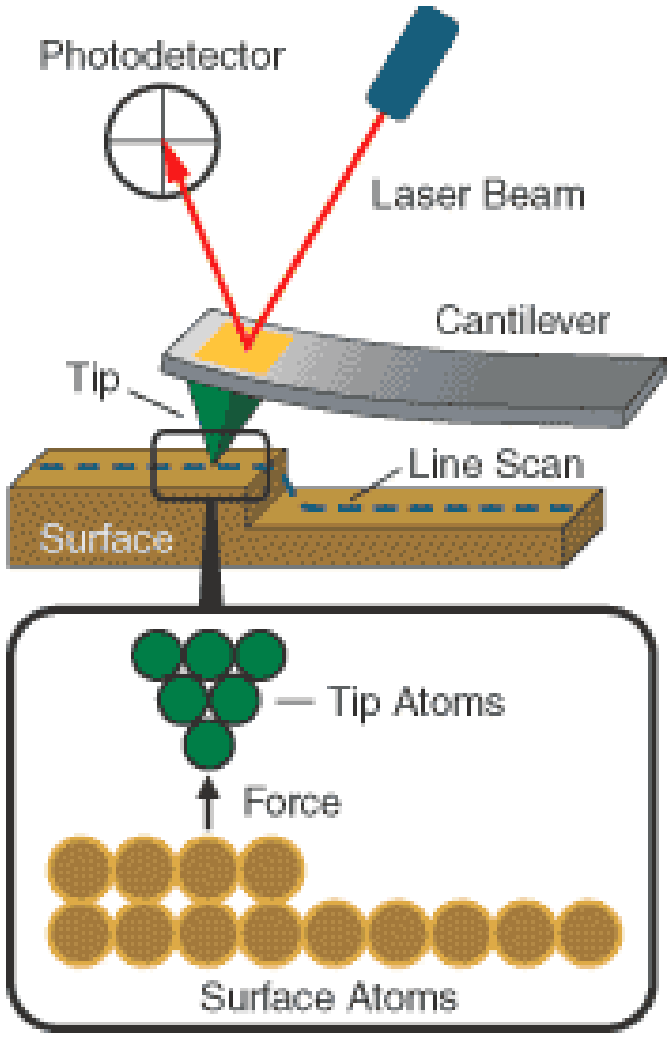

Figure 7 - Model of Atomic Force Microscope

1.4.2. **Langmuir-Blodgett Monolayer Technique**

The Langmuir-Blodgett (LB) monolayer technique is used to form a thin film composed of surfactant or lipid molecules, which is only one molecule thick. An LB film is formed using a device called the L-B trough. The L-B trough has 2 barriers on either side of the trough. A Wilhelmy balance is used to measure the surface pressure of the material. The trough is filled with water and a substrate (mica, glass, or silica) is placed through the interface. The film material is placed on the air/water interface and the material solvent is allowed to evaporate leaving only the film material remaining on the

interface. The barriers are then closed to achieve the required surface pressure. Once the required surface pressure is reached, the substrate is slowly raised, depositing a monomolecular film on the substrate. The substrate may then be lowered and raised again to form multilayers. The L-B trough may also be used to obtain surface pressure-area isotherm to observe how the surface pressure is affected by trough area.

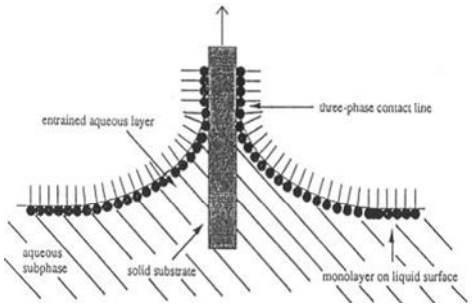

Figure 8 - Langmuir Blodgett Trough and cartoon of LB deposition

Chapter 2

Effect of Cholesterol and Amyloid-β on Monolayer Function

2.1 Description of Experiment

Cholesterol has been shown to affect the multilayer formation of lipid films and Bovine Lung Extract Surfactant (BLES). It has been also shown that the increased amount of SP-C leads to amyloidosis and diseased state of surfactant. The goal of our research was to determine how both factors affect the surfactant function and performance of model lipid monolayers. As SP-C is not readily available, we used amyloid-β (1-40) peptide as a substitute for SP-C. We further build on this research to determine the affect of the amyloid-β protein on these lipid and BLES films. We mixed lipids with cholesterol at 0% and 20% concentrations and with amyloid-β (1-40) at concentrations of 0%, 1% and 10%. These mixtures were deposited on the Langmuir-Blodgett trough. Surface Pressure Area isotherms were collected. L-B trough barriers were compressed to their plateau and the lipid material was deposited on mica substrate. We used Atomic Force Microscopy to image these films to elucidate the effect of cholesterol and amyloid-β on multilayer formation.

2.2 Materials and Methods

Sample Preparation

DPPC (Avanti Polar Lipids) and DPPC with 20% cholesterol by weight were dissolved in chloroform at a concentration of 1 mg/mL. Amyloid- β 1-40 (Genscript Corporation, Piscataway, USA) was dissolved in DMSO and sonicated for 10 minutes.

The DPPC in chloroform solution, was mixed with amyloid-β to obtain solutions with 1% and 10% amyloid-β by weight.

DPPC and DOPG (also referred to as eggPG) was mixed weighed and dissolved in chloroform at a ratio of DPPC:DOPG 80:20 and a concentration of 10 mg/mL. Amyloid-β (1-40) was prepared as noted above and mixed with the DPPC:DOPG solution

Bovine Lung Extract Surfactant (BLES, a kind gift from BLES biochemicals) was extracted into chloroform from Goerke's buffer. 0.5 mL BLES in buffer (concentration 27 mg/mL) was mixed with 0.5 mL methanol and 0.5 mL chloroform and centrifuged for 10 minutes at 100g. The bottom phase was removed and 0.5 mL chloroform was added to the remaining solution. Again the solution (was centrifuged at 100g for 10 minutes and the bottom phase was again removed and added to the previous bottom phase. The final concentration of the BLES solution was 27 mg/mL. Amyloid-β was prepared as indicated above.

Langmuir-Blodgett Deposition

A piece of freshly cleaved mica was placed in the arm of the LB trough and lowered into the subphase. Approximately 5 µL Protein-lipid solutions were deposited on the interface on a Langmuir-Blodgett trough (LB trough) using a 5 µL syringe. Exact volume's of solution were adjusted to achieve a surface pressure of 25 mN/m with the barriers fully open. The lipid was allowed to spread on the interface for a period of 10 minutes. The LB trough barriers were compressed at 10 cm^2/min to collect surface pressure-area isotherms. The mica was raised at a rate of 2 mm/min through the interface.

The mica was allowed to air dry for 10 minutes, than affixed on a glass microscope slide using double sided tape.

Imaging

The lipid multilayers were imaged in air using a JPK Nanowizard II (JPK Instruments, Berlin) Atomic Force Microscope using a 42 N/m Nanoworld cantilever with a resonance frequency of approximately 250 kHz in air in intermittent contact mode.

2.3 Results

2.3.1. **BLES Multilayer Formation**

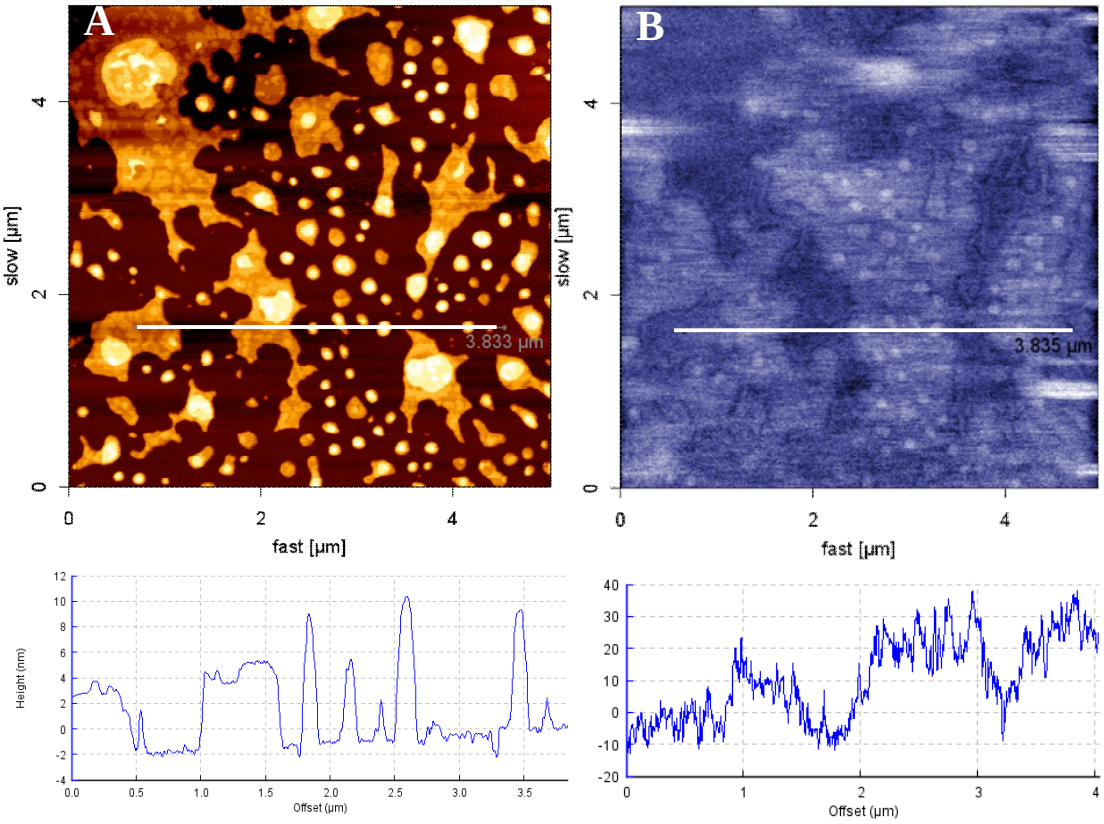

Figure 9 - AFM and Kelvin Probe Force Microscopy Image of BLES (Hane, et al. 2009)

Figure 9 - AFM and Kelvin Probe Force Microscopy Image of BLES shows an AFM and Kelvin Probe Force Microscopy Image of BLES. We observe discrete multilayer formations, of 5 nm in height. In the multilayer in top left of image A, we also observe domains within the first monolayer. In the KPFM image on the right, we observe multilayer potential below that of the monolayer. However, lighter areas indicate areas of higher surface potential. We believe these lighter areas are locations where SP-C is present.

2.3.2. **Effect of Cholesterol on BLES and Thin Lipid Films**

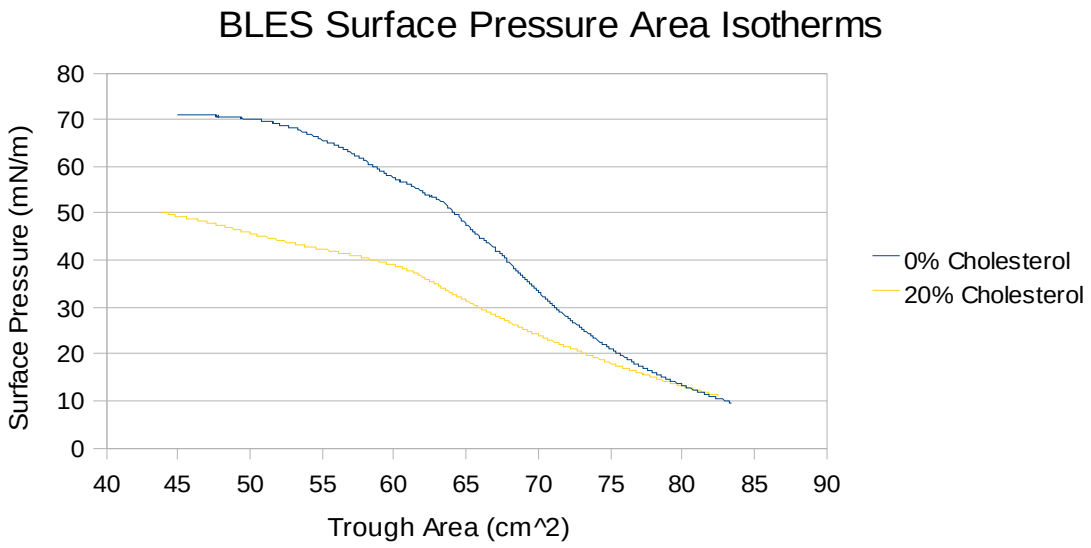

Figure 10 - Surface Pressure - Area Isotherm of BLES, effect of cholesterol

Figure 10 - Surface Pressure - Area Isotherm of BLES, effect of cholesterol shows the effect of cholesterol on the surface pressure-area isotherm of BLES with and without 20% cholesterol. When cholesterol is absent in BLES, surface pressure is allowed to increase to 70 mN/m. (The corollary of statement is that surface tension is reduced to appoach 0 mN/m, since surface tension is the difference between surface pressure and bulk surface tension.) With 20% cholesterol composition, the maximum surface pressure of BLES is asymptotic at approximately 48-50 mN/m as trough area decreases. This result is in agreement with results obtained by Gunasakara (Gunasekara, et al. 2005)and Leonenko (Leonenko, Gill, et al. 2007).

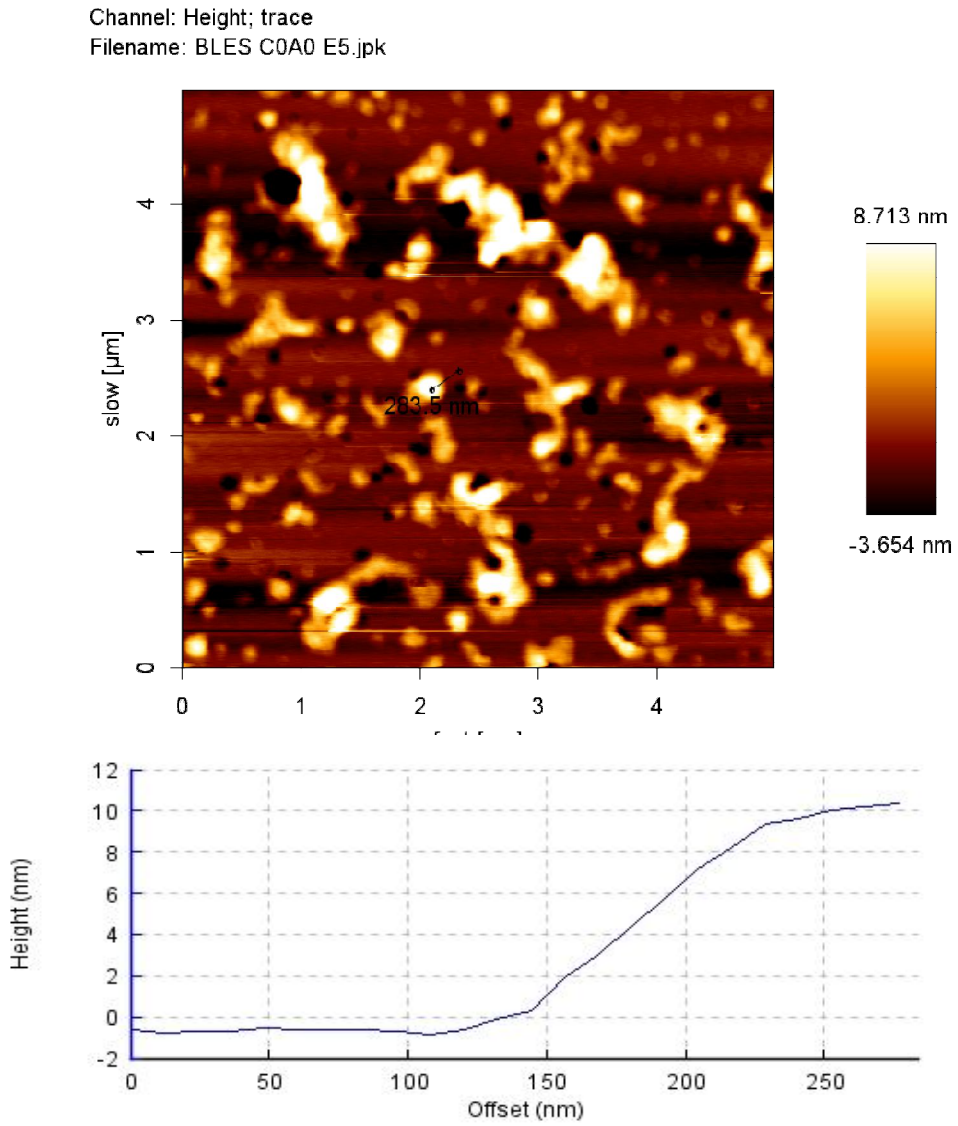

Figure 11 - BLES without cholesterol

Figure 11 - BLES without cholesterol shows an AFM image of a BLES monolayer compressed to 67 mN/m with no cholesterol. Notice discrete multilayer formations of 5 nm in height, corresponding to a lipid bilayer or multiples of them. Multilayers are numerous and well distributed. Cross section shows a height of the second multilayer of 10 nm.

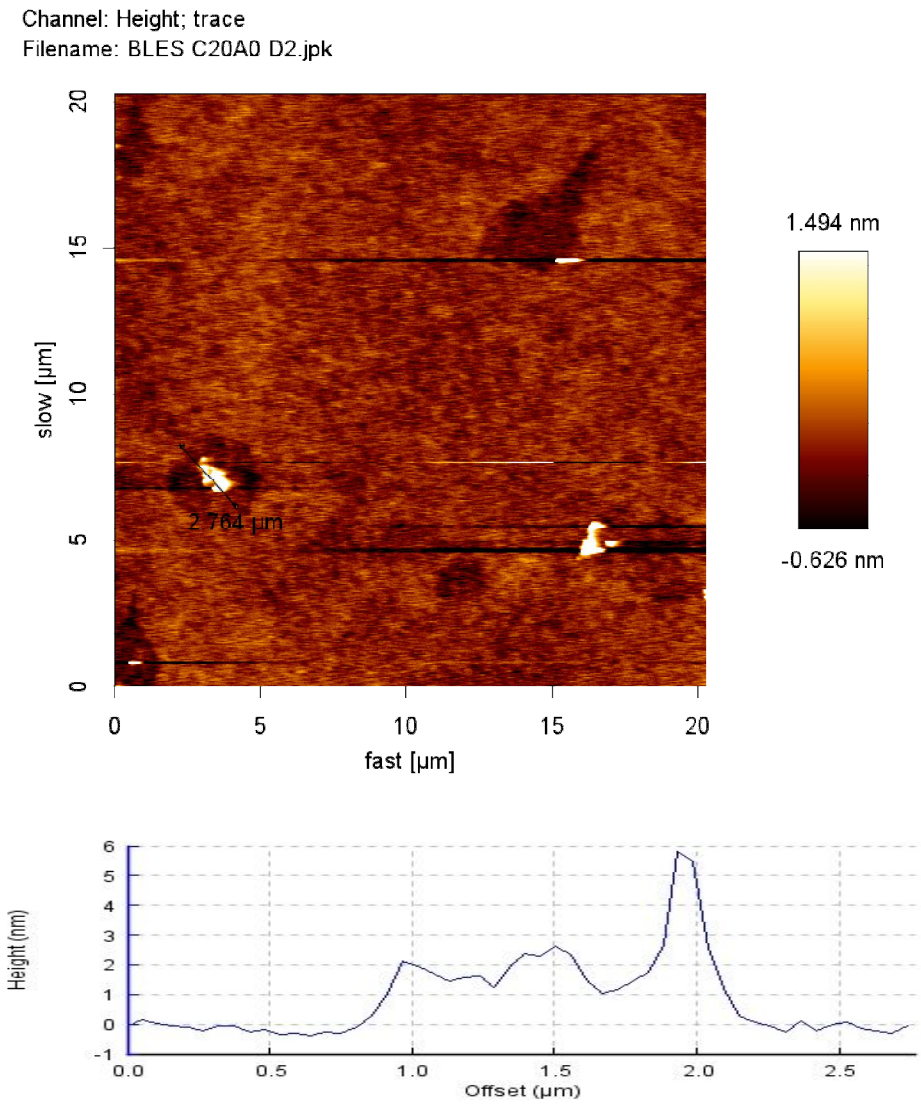

Figure 12 - BLES with 20% cholesterol

Figure 12 - BLES with 20% cholesterol shows an AFM image of a BLES monolayer compressed to 25 mN/m. There is an absence of defined multilayer formations. Notice cross section of few lipid protrusions. Surface is uneven and continuous in height.

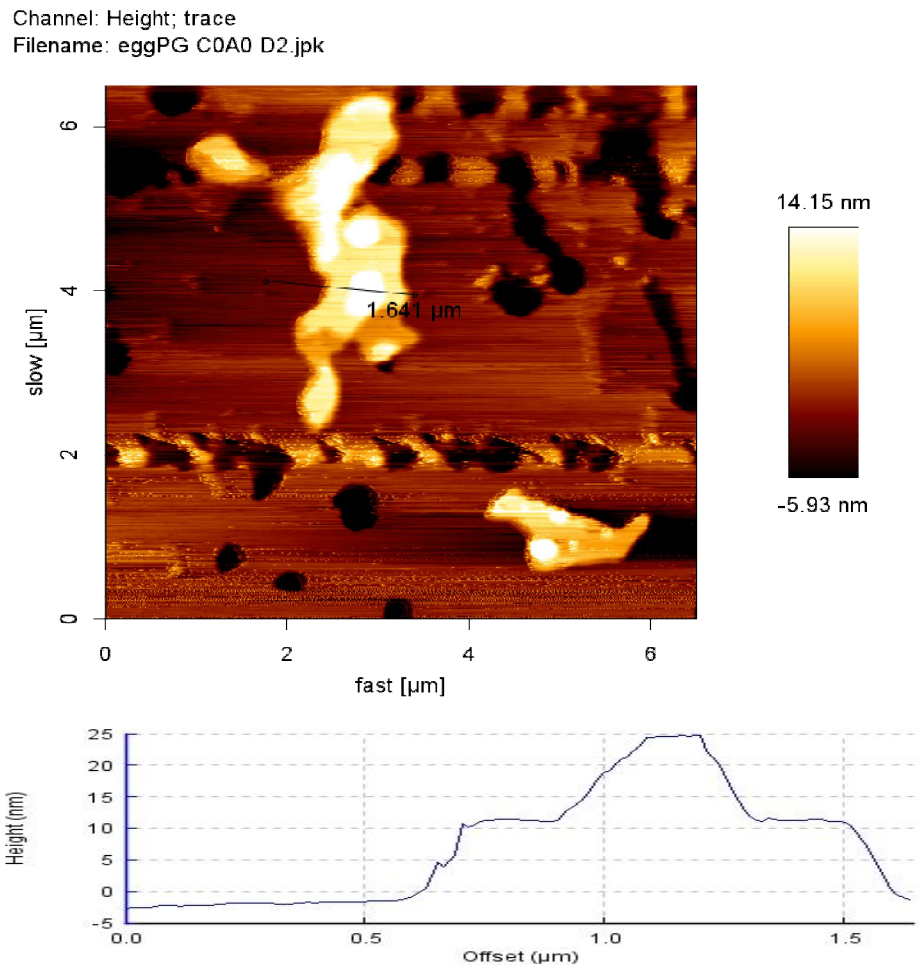

Figure 13 - DPPC-DOPG composition, no cholesterol

Figure 13 - DPPC-DOPG composition, no cholesterol shows an AFM image of a DPPC-DOPG monolayer compressed to 59 mN/m with no cholesterol. Similar to BLES, model lipid mixture forms discrete multilayer formations of 5 nm in height, corresponding to a lipid bilayer. Multilayers are numerous and well distributed. Cross section shows discrete multilayers of height 5(small plateau), 10, and 25 nm.

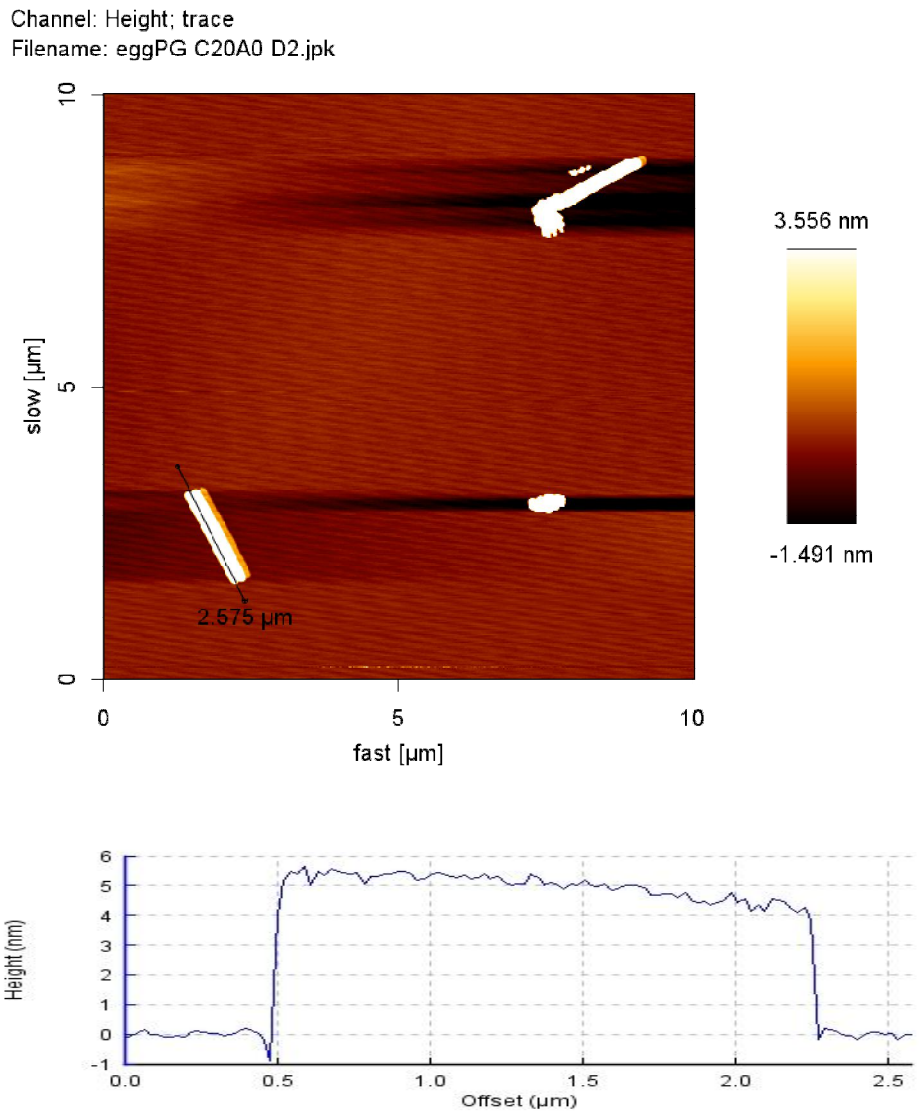

Figure 14 - DPPC-DOPG composition with 20% cholesterol

Figure 14 - DPPC-DOPG composition with 20% cholesterol shows an AFM image of a DPPC-DOPG (80:20 ratio) monolayer compressed to 55 mN/m. We observed unusual rod-like single bilayer formations with a height of 5 nm when the monolayer was compressed. The length of these rods varied from 1-5 µm in length and a consistent width of 0.5 µm.

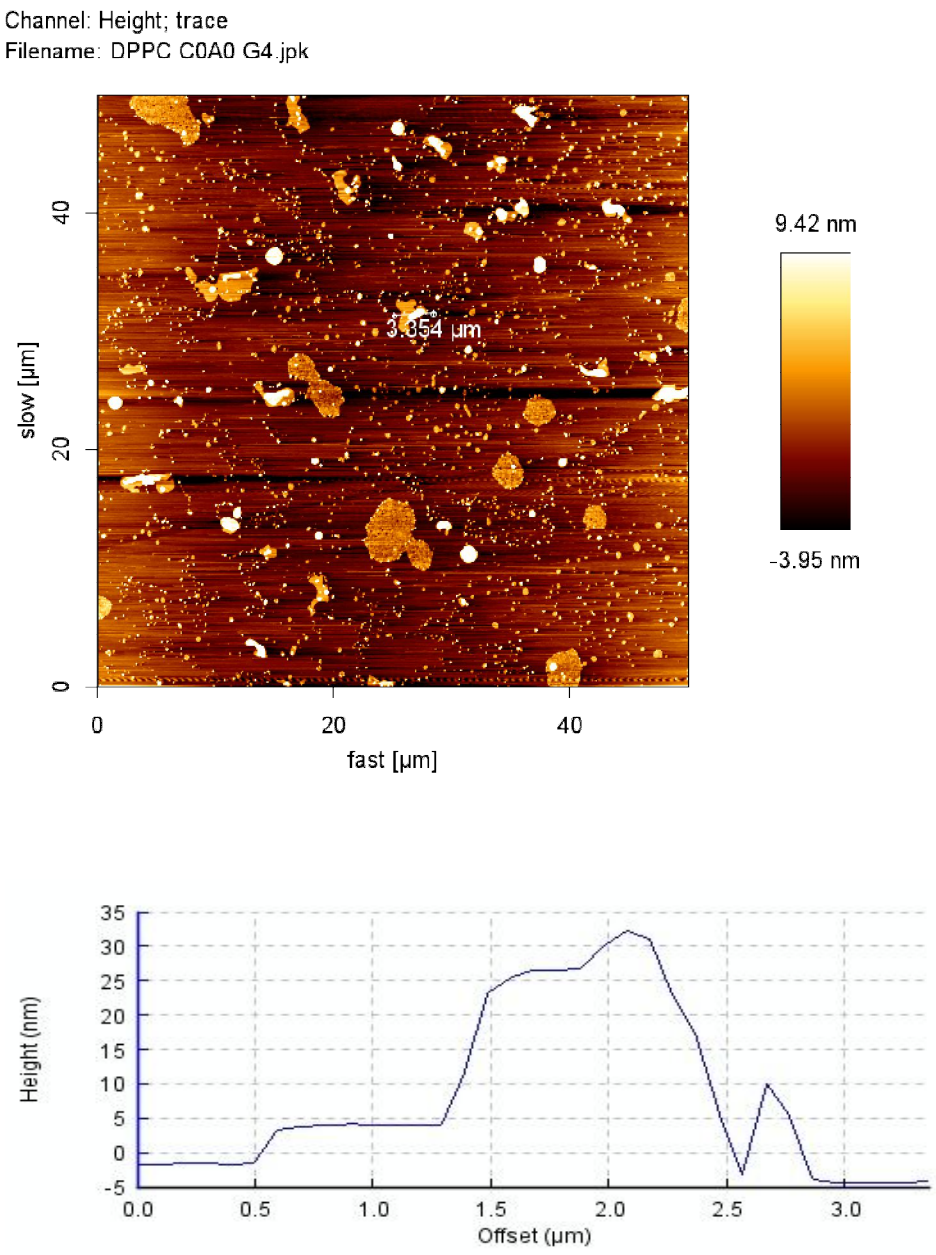

Figure 15 - DPPC with no cholesterol

Figure 15 - DPPC with no cholesterol shows an AFM image of a DPPC monolayer compressed to 40 mN/m, with no cholesterol. We observed numerous, well distributed, amorphous multilayer formations. Cross section shows discrete multilayers of height 5, 25, 30 and 10nm.

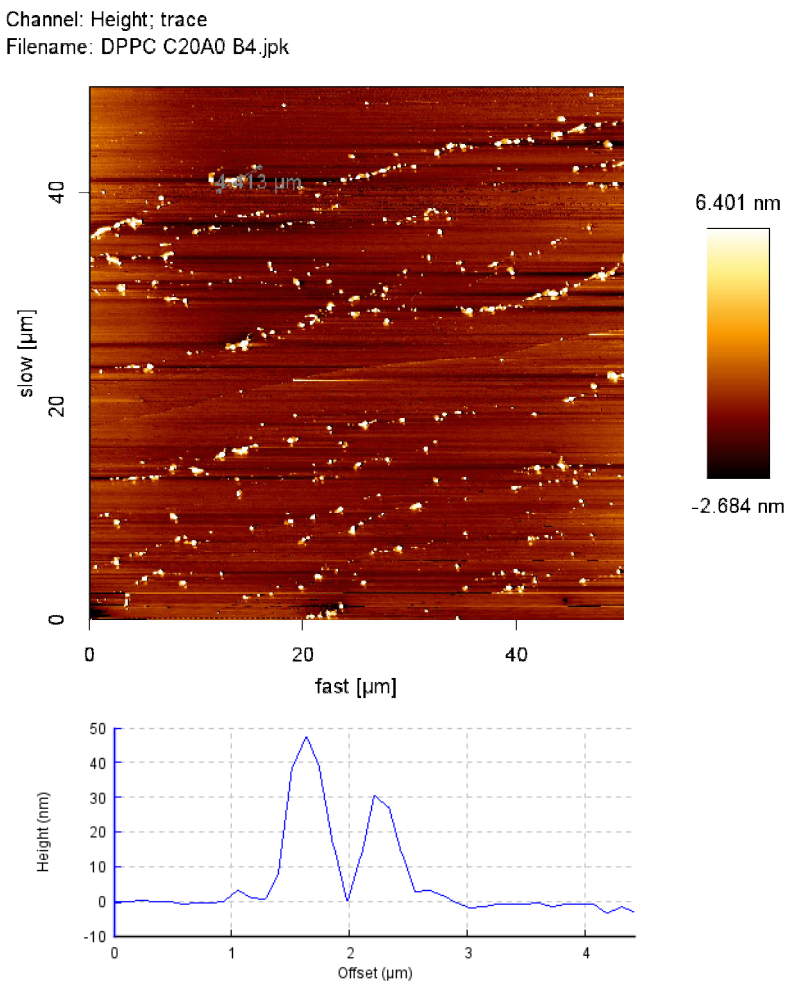

Figure 16 - DPPC with 20% cholesterol

Figure 16 - DPPC with 20% cholesterol shows an AFM image of a DPPC monolayer with 20% cholesterol compressed to 50 mN/m. We observed an absence of typical discrete lipid multilayer formations. We observe small patches of lipid material with heights to 50 nm. These may be multilayers, but the are much smaller and less discrete than multilayer patches found in DPPC without cholesterol. In summary: cholesterol in BLES and model lipid films suppresses multilayer formation observed by AFM, and does not allow it to achieve higher compressions in the Langmuir isotherms.

2.3.3. **Effect of Amyloid-B on BLES and Thin Lipid Films**

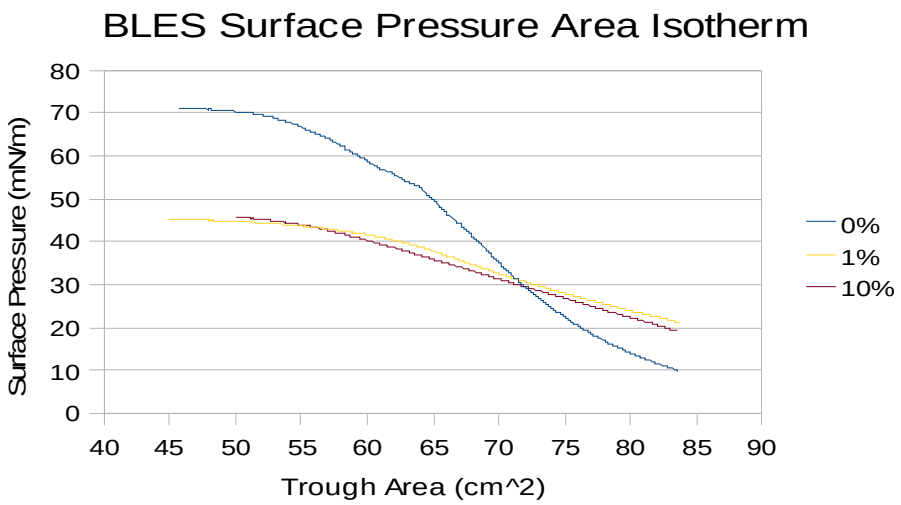

Figure 17 - Surface Pressure-Area Isotherms of BLES with differing concentrations of Amyloid-β

Figure 17 - Surface Pressure-Area Isotherms of BLES with differing concentrations of Amyloid-β shows the surface pressure-area isotherms of BLES with varying concentrations of amyloid-β. Notice that without the presence of amyloid-β, the surface pressure of BLES reaches around 70 mN/m (corresponding to a surface tension of 0 mN/m). Once amyloid-β is added in either 1% or 10% concentrations, the maximum surface pressure is reduced to approximately 45 mN/m.

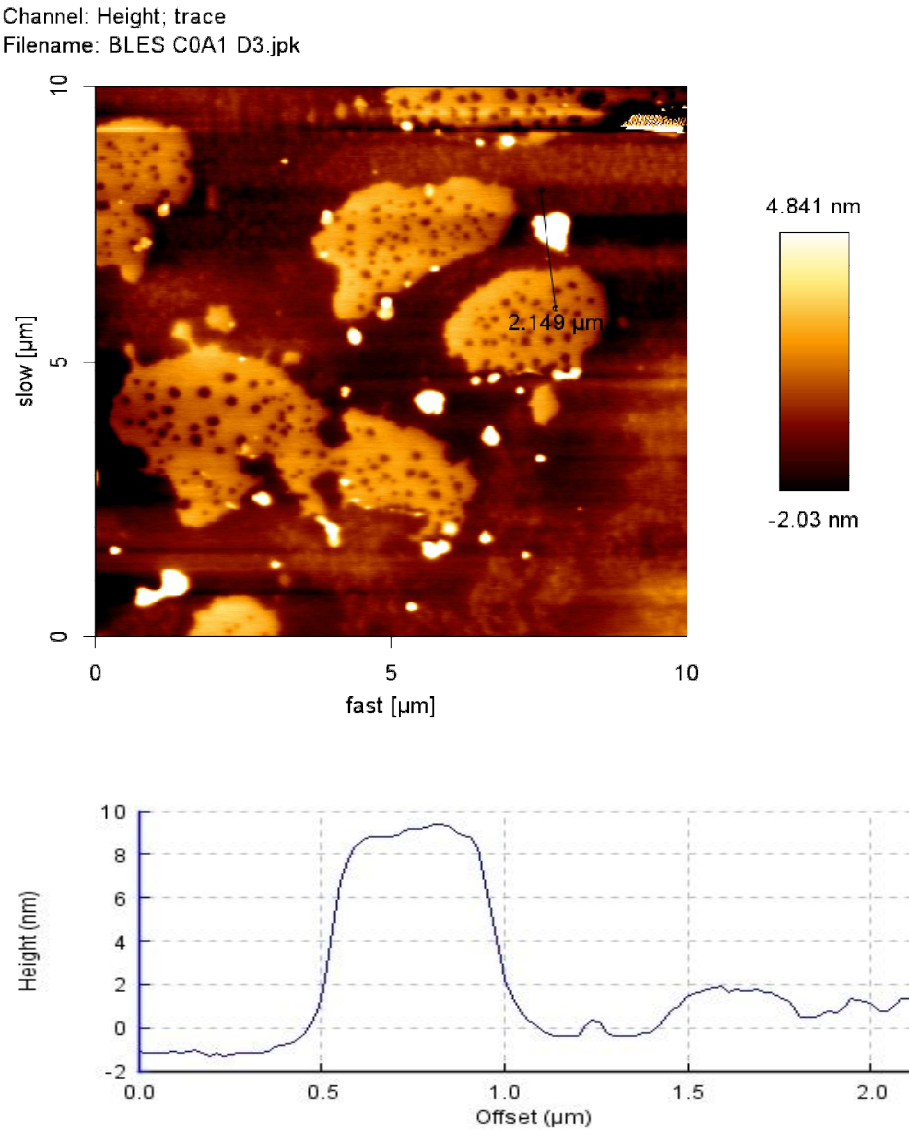

Figure 18 - BLES with 1% Amyloid-B

Figure 18 - BLES with 1% Amyloid-B shows an AFM image of BLES monolayer with 1% amyloid-β compressed to 48 mN/m. While amorphous patches may resemble multilayer patches, note the difference in height. The bright white patches have a height of 10 nm, which falls within discrete 5nm steps. However, the image shows the height of the lower patches of lipid to be only 2nm in height, which does not correspond to a 5 nm high bilayer.

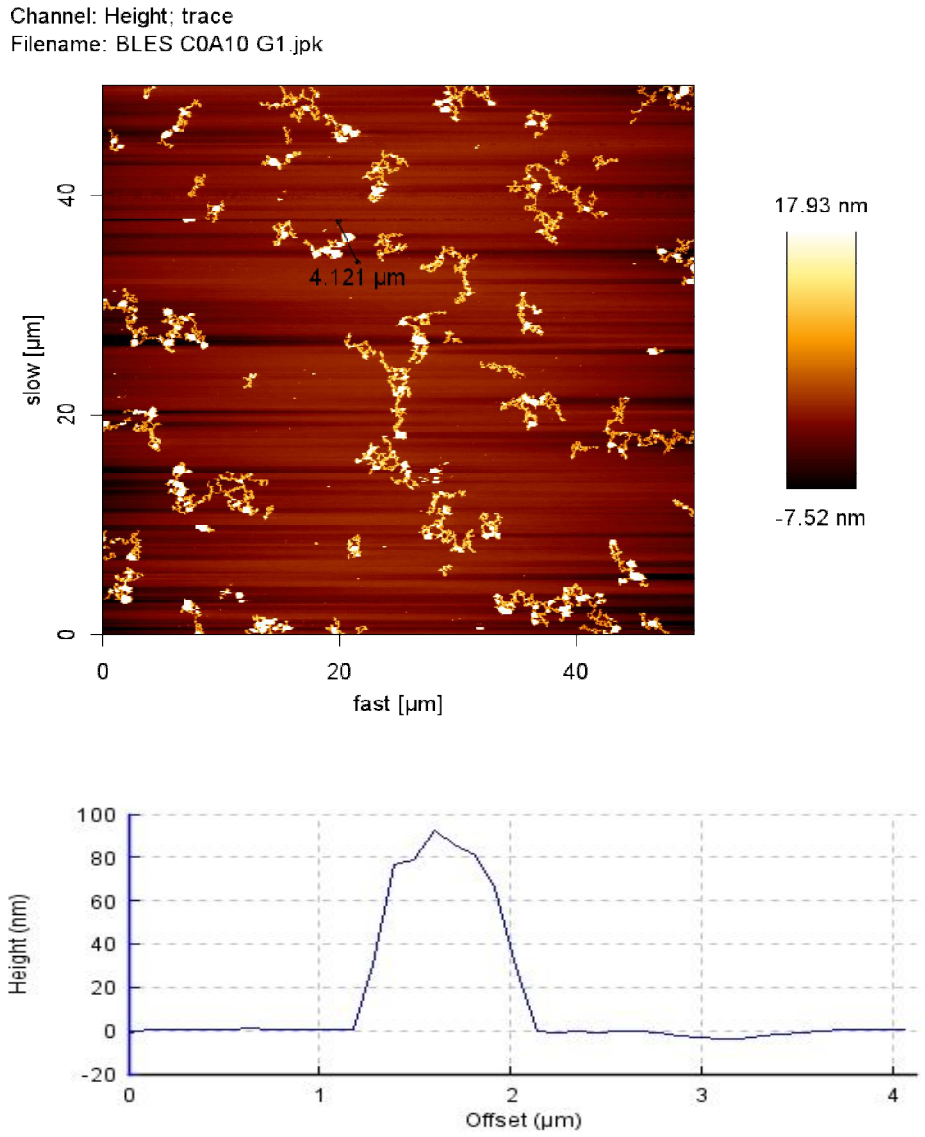

Figure 19 - BLES with 10% Amyloid-B

Figure 19 - BLES with 10% Amyloid-B shows an AFM image of BLES monolayer with 1% amyloid-β compressed to 47 mN/m. We observe small, thread like formations with a height varying from 20 nm continuously to 100 nm. These formations are likely protein or protein-lipid mixtures, being “squeezed-out” of the monolayer at higher compressions.

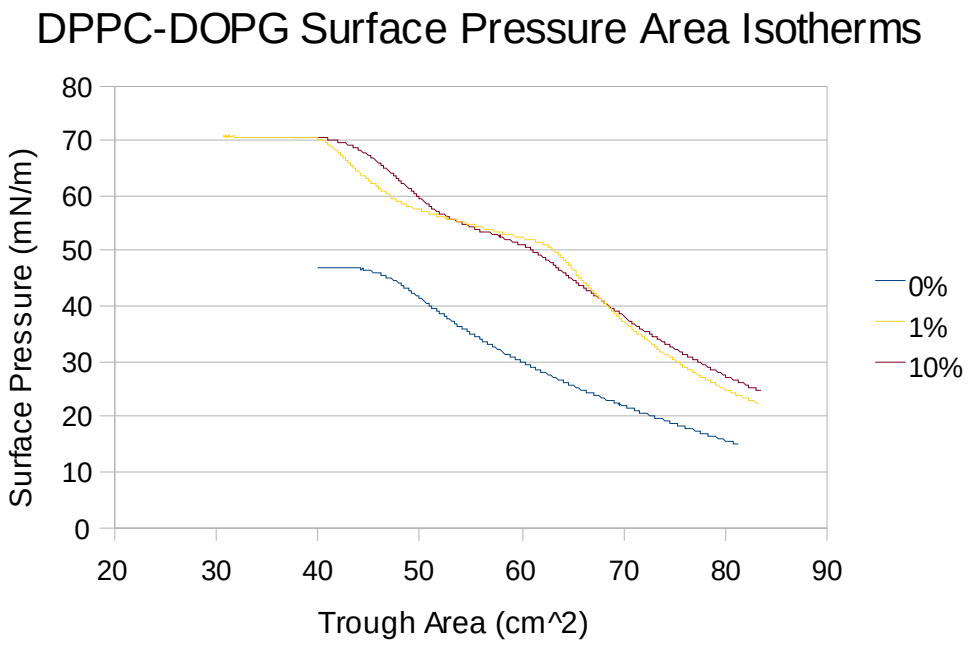

Figure 20 - Surface Pressure-Area Isotherms of DPPC-DOPG with different concentrations of Amyloid-β

Figure 20 - Surface Pressure-Area Isotherms of DPPC-DOPG with different concentrations of Amyloid-β shows a surface pressure-area isotherm of a lipid composition of DPPC-DOPG at a 80:20 ratio. Without any peptide, the maximum surface pressure achieved by the composition is 48 mN/m. Once 1% or 10% amyloid-β is added to the lipid, the maximum surface pressure increases to 70 mN/m.

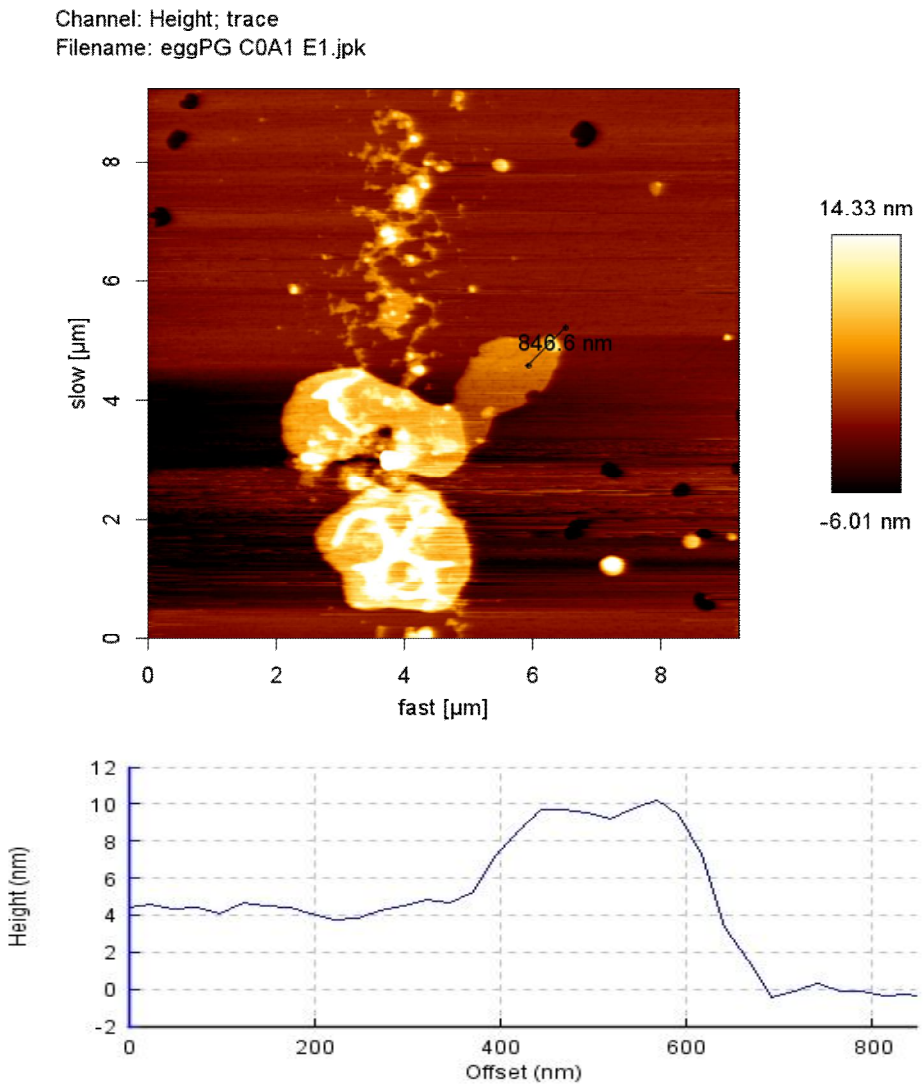

Figure 21 - DPPC-DOPG composition 1% Amyloid-β

Figure 21 - DPPC-DOPG composition 1% Amyloid-β shows an AFM image of BLES monolayer with 1% amyloid-β compressed to 69 mN/m. We observe large, discrete multilayers of variable heights reaching 3 bilayers high.

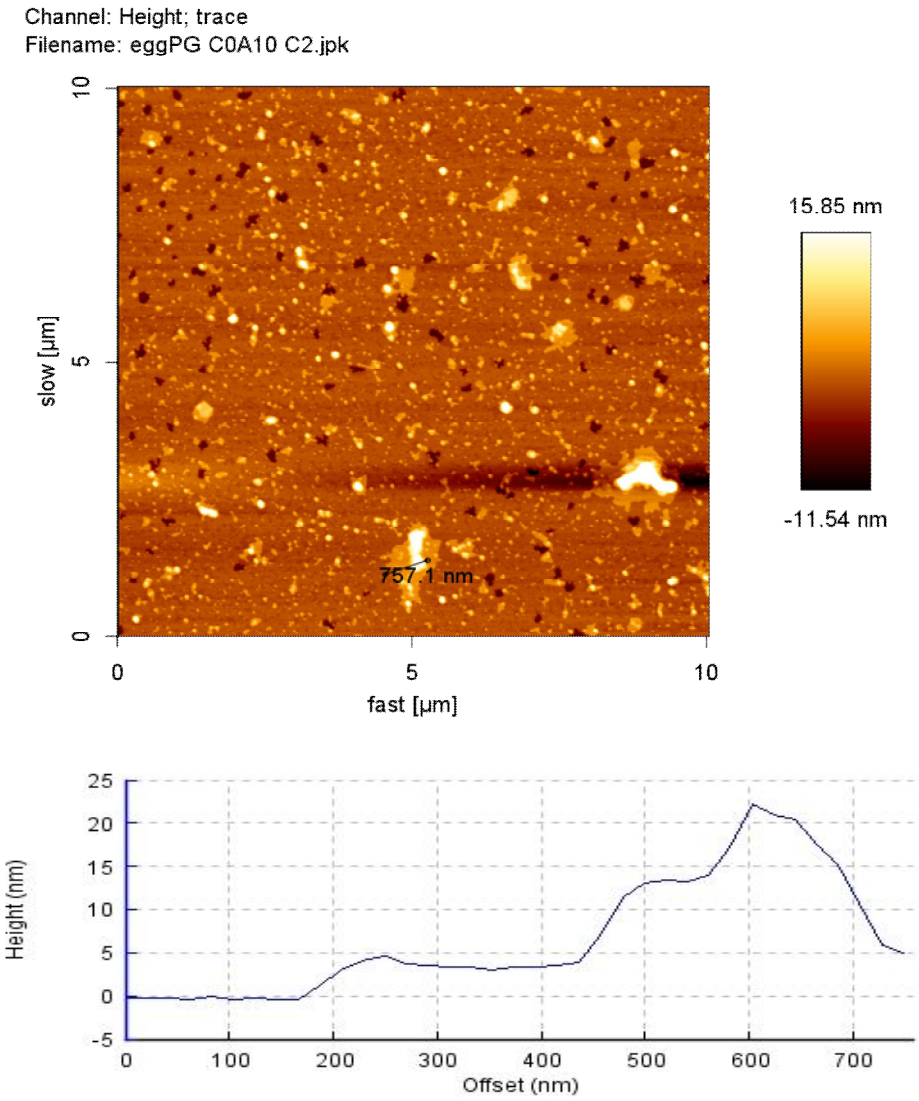

Figure 22 - DPPC-DOPG composition 10% Amyloid-β

Figure 22 - DPPC-DOPG composition 10% Amyloid-β shows an AFM image of BLES monolayer with 10% amyloid-β compressed to 70 mN/m. We observe numerous, well distributed, multilayer formations of variable shapes. Discrete bilayers are 5, 10, 15, 20 nm high. Some holes in the lipid monolayer are also present.

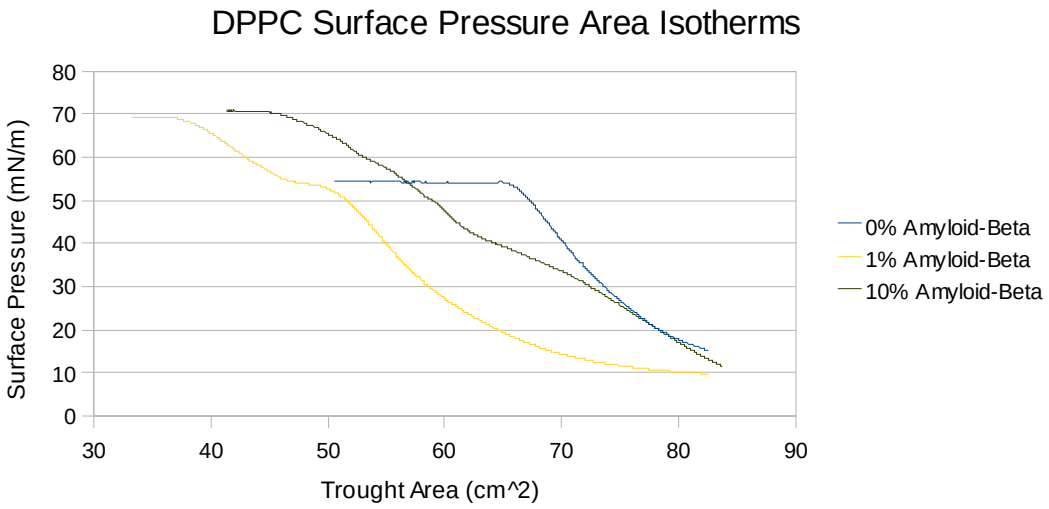

Figure 23 - Surface Pressure-Area Isotherms of DPPC with different concentrations of Amyloid-β

Figure 23 - Surface Pressure-Area Isotherms of DPPC with different concentrations of Amyloid-β is a surface pressure-area isotherm of DPPC with varying concentrations of amyloid-β added. Absent amyloid-β, the maximum surface pressure of DPPC is 55 mN/m. Once 1% and 10% of amyloid-β is added to the DPPC, the maximum surface pressure of DPPC increases to 70 mN/m.

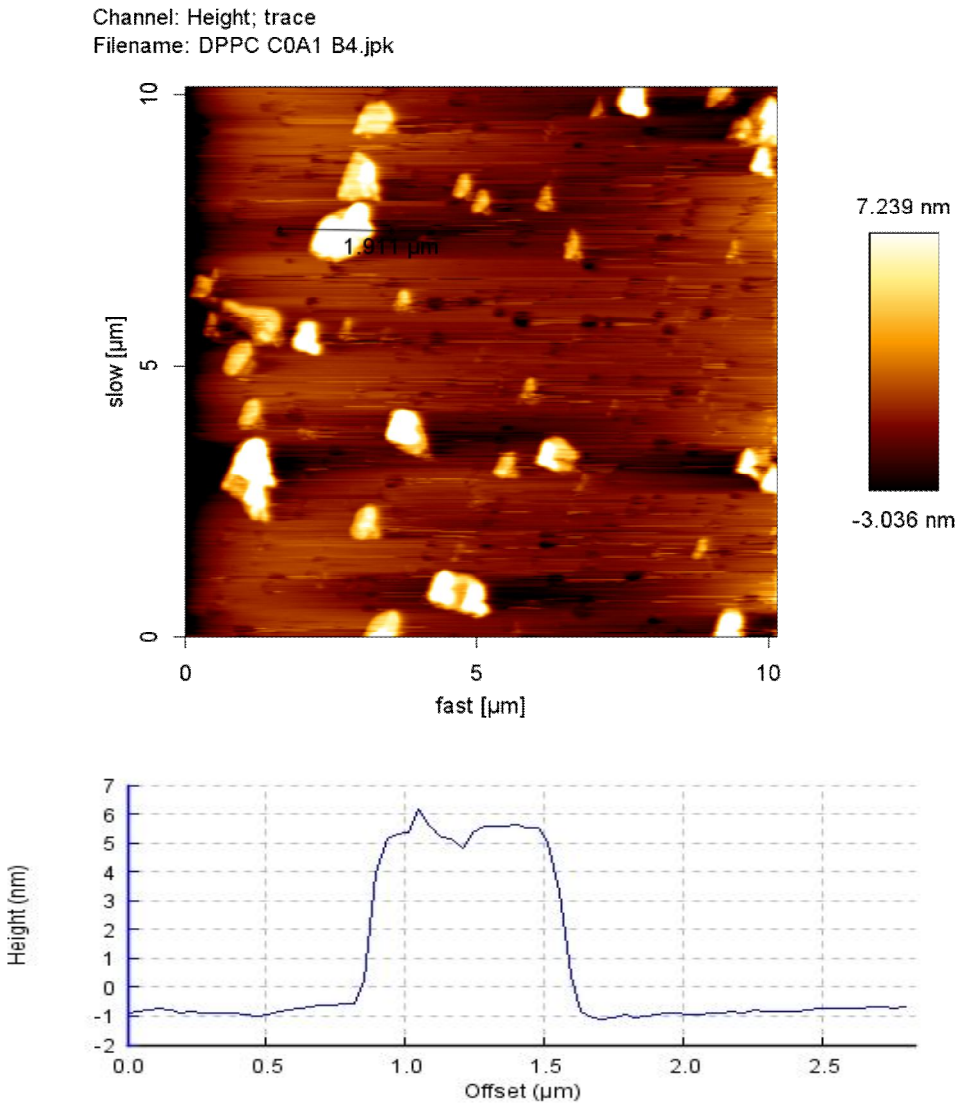

Figure 24 - DPPC 1% Amyloid-β

Figure 24 - DPPC 1% Amyloid-β shows an AFM image of a DPPC monolayer with 1% amyloid-β compressed to 65 mN/m. We observe numerous, well distributed, multilayer formations of various shapes. Discrete bilayers are 5, and 10 nm high.

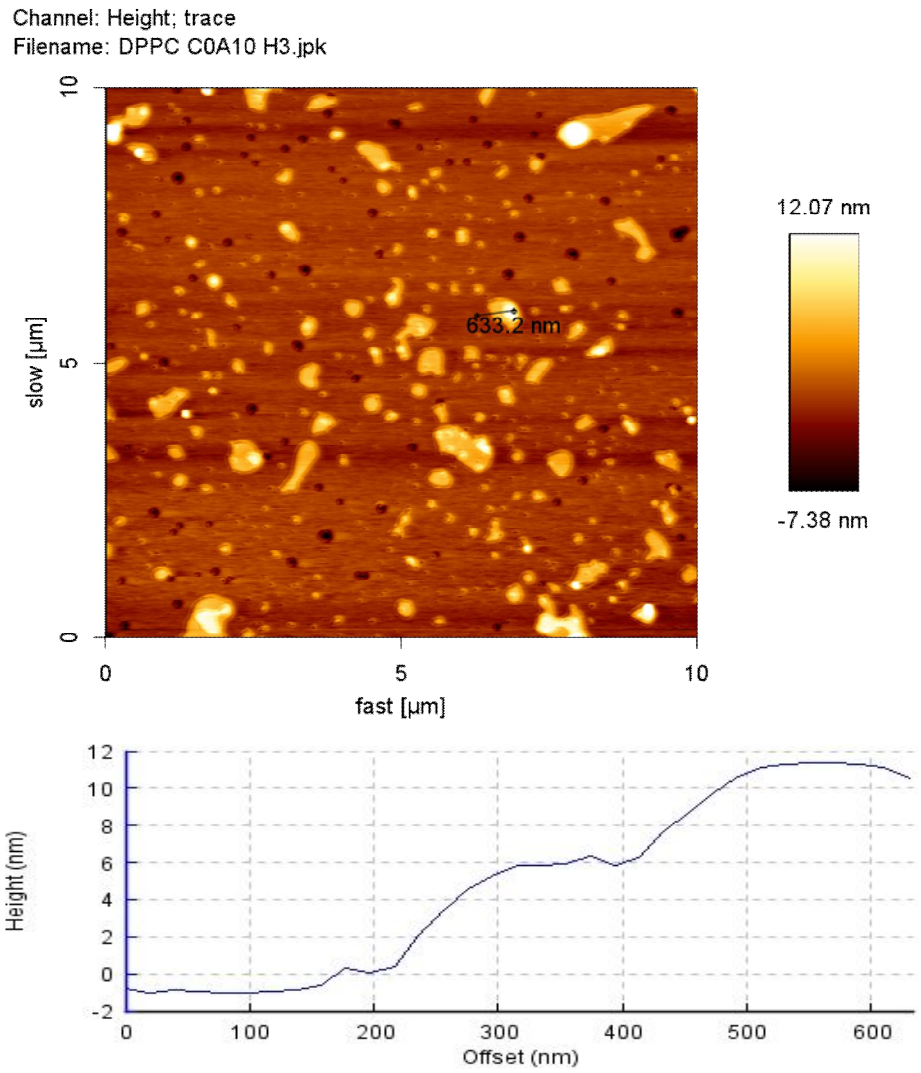

Figure 25 - DPPC 10% Amyloid-β

Figure 25 - DPPC 10% Amyloid-β shows an AFM image of a DPPC monolayer with 10% amyloid-β compressed to 70 mN/m. We observe numerous, amorphous limpid multilayers in discrete heights of 5 and 10 nm. We also observe small holes in the lipid monolayer.

2.3.4. **Effect of Cholesterol and Amyloid-β on BLES and Thin Lipid Films**

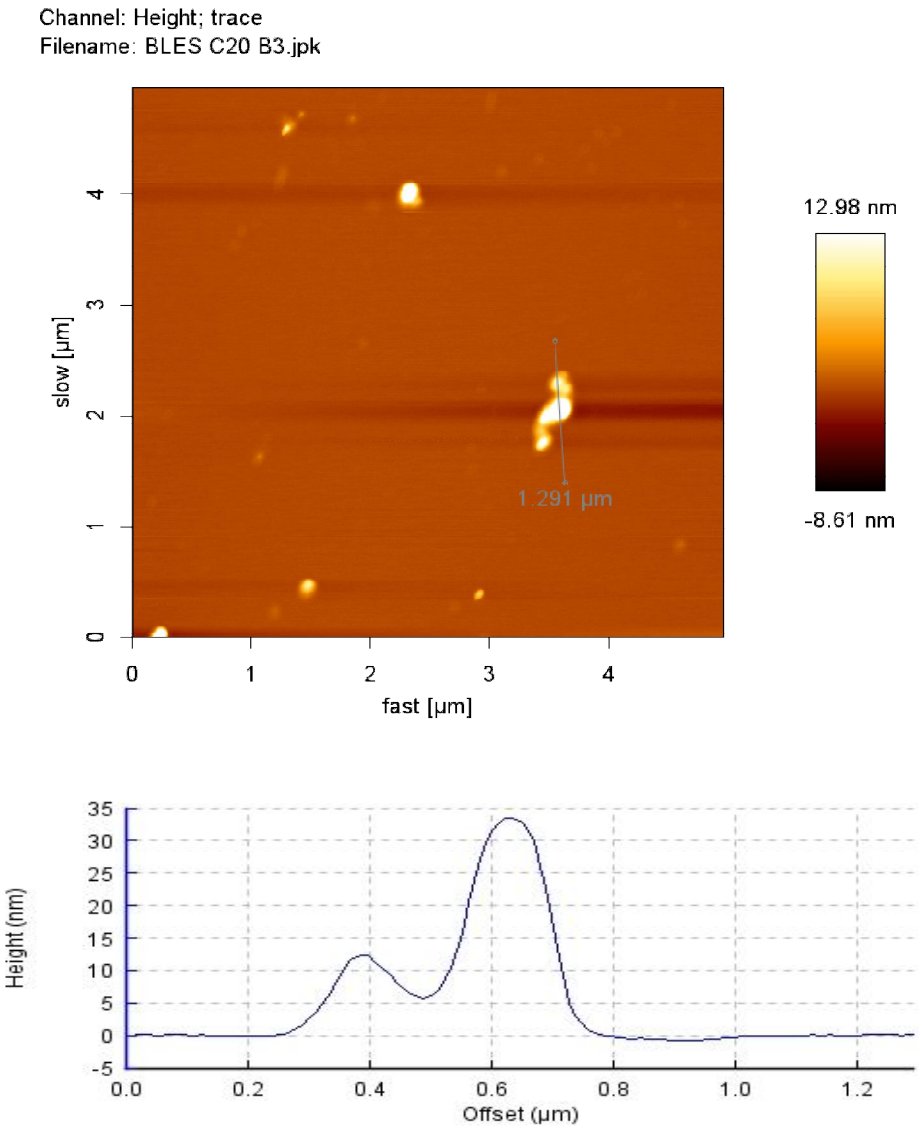

Figure 26 - BLES with 20% cholesterol and 1% Amyloid-β

Figure 26 - BLES with 20% cholesterol and 1% Amyloid-βshows an AFM image of a BLES monolayer with 20% cholesterol and 1% amyloid-β compressed to 48 mN/m, which is a maximum compression possible in the presence of cholesterol. We observe no perceptible multilayer formations, but only small, infrequent patches of lipid material varying continuously between 0 and 35 nm. This is not indicative of any multilayer formation, but rather non-structured aggregates.

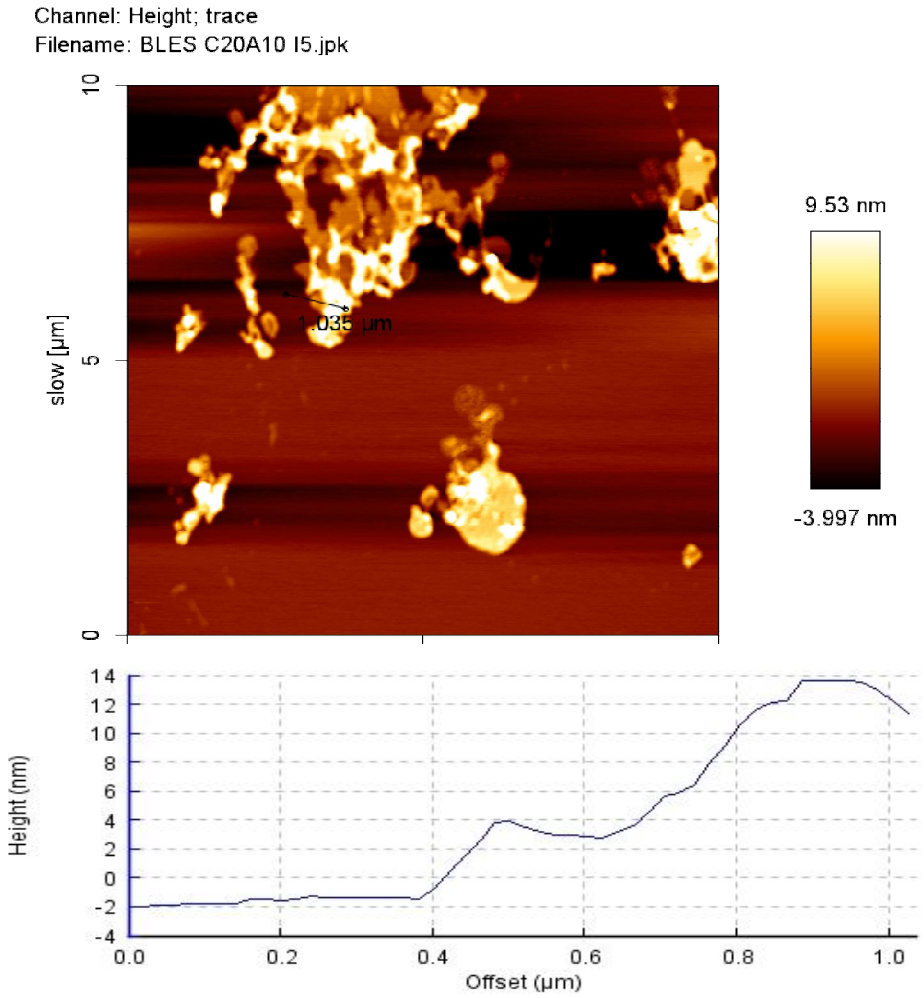

Figure 27 - BLES with 20% cholesterol and 10% Amyloid-β

Figure 27 - BLES with 20% cholesterol and 10% Amyloid-β shows an AFM image of a BLES monolayer with 20% cholesterol and 1% amyloid-β compressed to 48 mN/m. We do observe flat multilayer formations, and at the same time amorphous clusters on the top of the multilayers.

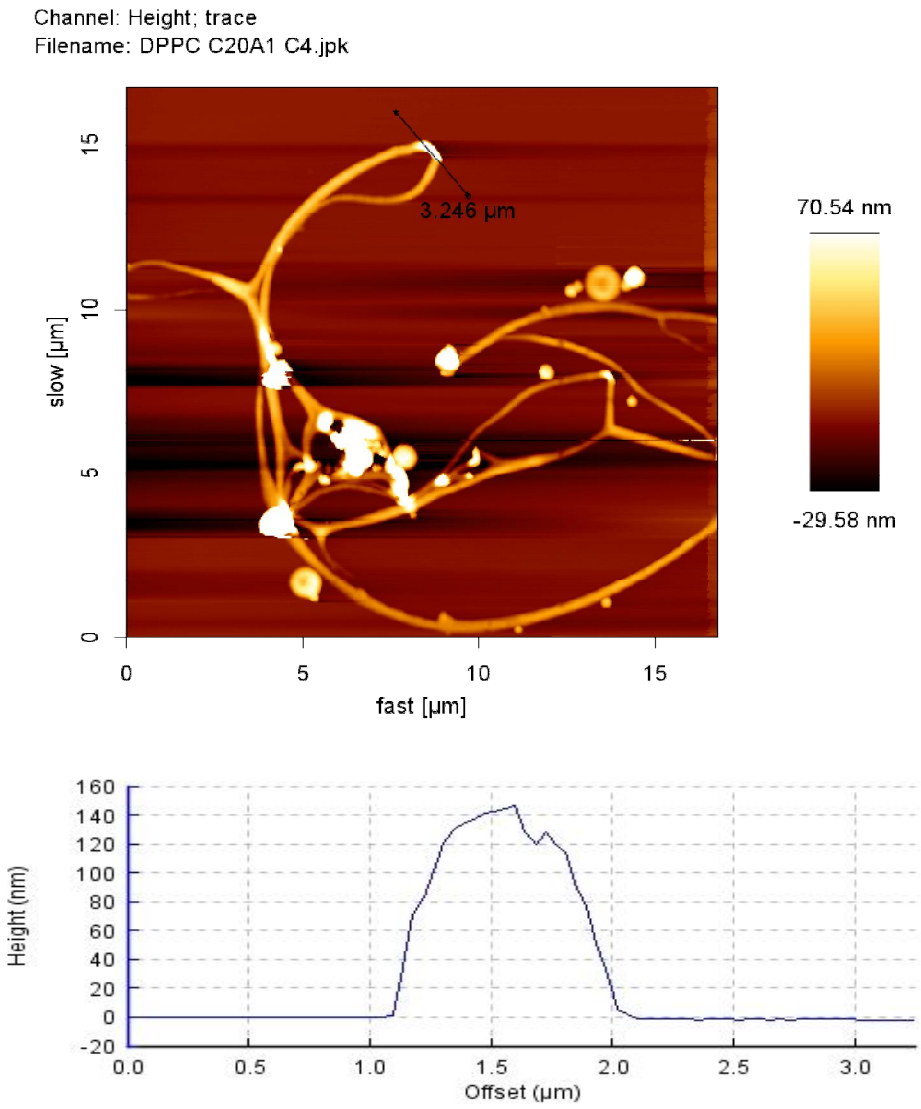

Figure 28 - DPPC-DOPG composition with 20% cholesterol and 1% Amyloid-β

Figure 28 - DPPC-DOPG composition with 20% cholesterol and 1% Amyloid-β shows an AFM image of a DPPC monolayer with 20% cholesterol and 1% amyloid-β compressed to 47 mN/m. We observe, long, whispy structures terminating with large circular aggregates approaching 200 nm in height. The composition of the long, curly structures is unknown, the larger aggregates are most likely composed of peptide or peptide-lipid aggregates.

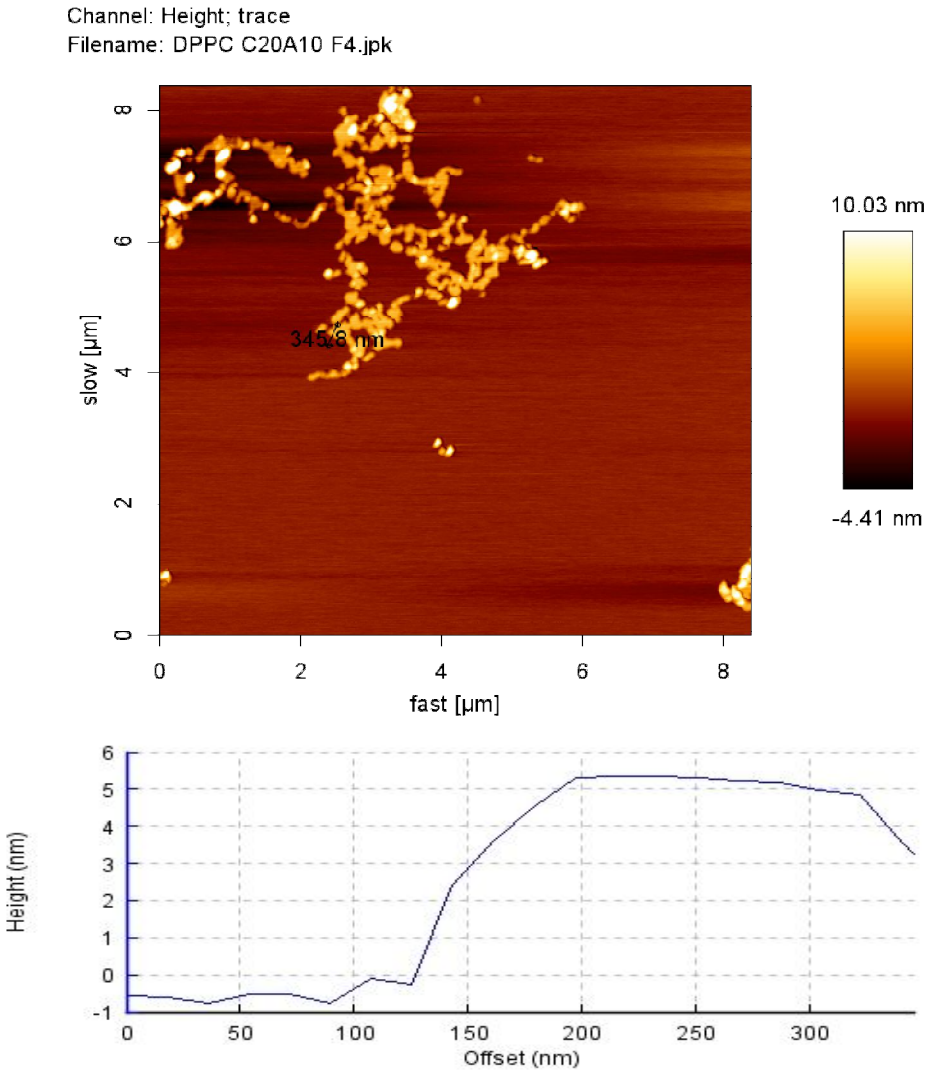

Figure 29 - DPPC-DOPG composition with 20% cholesterol and 10% Amyloid-β

Figure 29 - DPPC-DOPG composition with 20% cholesterol and 10% Amyloid-β shows an AFM image of a DPPC monolayer with 20% cholesterol and 1% amyloid-β compressed to 50 mN/m. We observe small round clusters, of what we believe, are composed of a protein-lipid mixture. Maximum height of the smaller clusters is 5-10 nm, while larger clusters are upwards of 30 nm high. Boundaries of these clusters are continuous which is unlike the discrete multilayers observed in BLES or DPPC-DOPG lipid films.

2.3.5. **Effect of Compression on Multilayer Formation**

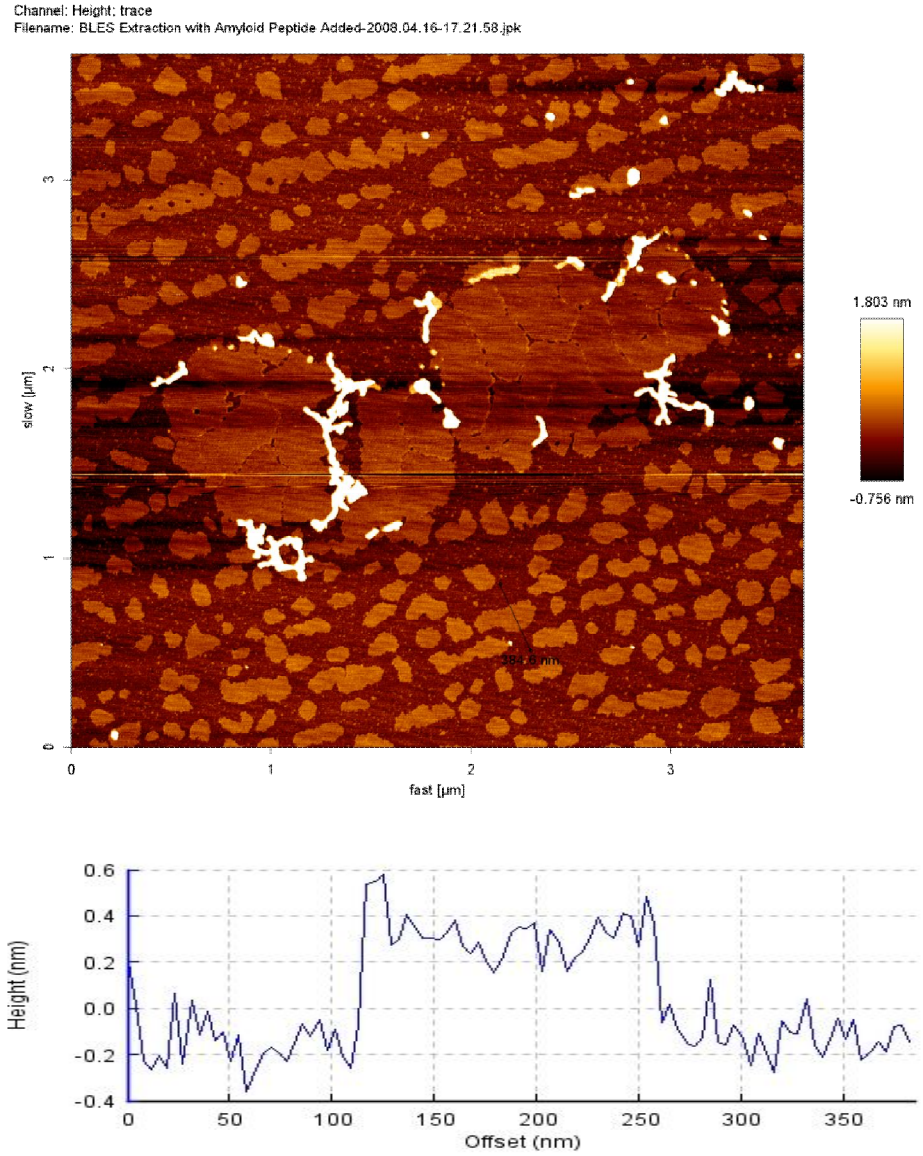

Figure 30 - BLES monolayer with 1% Amyloid-β compressed to 25 mN/m

Figure 30 shows a BLES monolayer with 10% amyloid-β compressed to 25 mN/m. We observe round liquid condensed-liquid expanded domains with a height difference of 0.2-0.4 nm. Observing the larger liquid expanded domains, we can see they are made up of smaller domains, that have been fused together forming larger domains. At the phase interface, we observe aggregations of peptide.

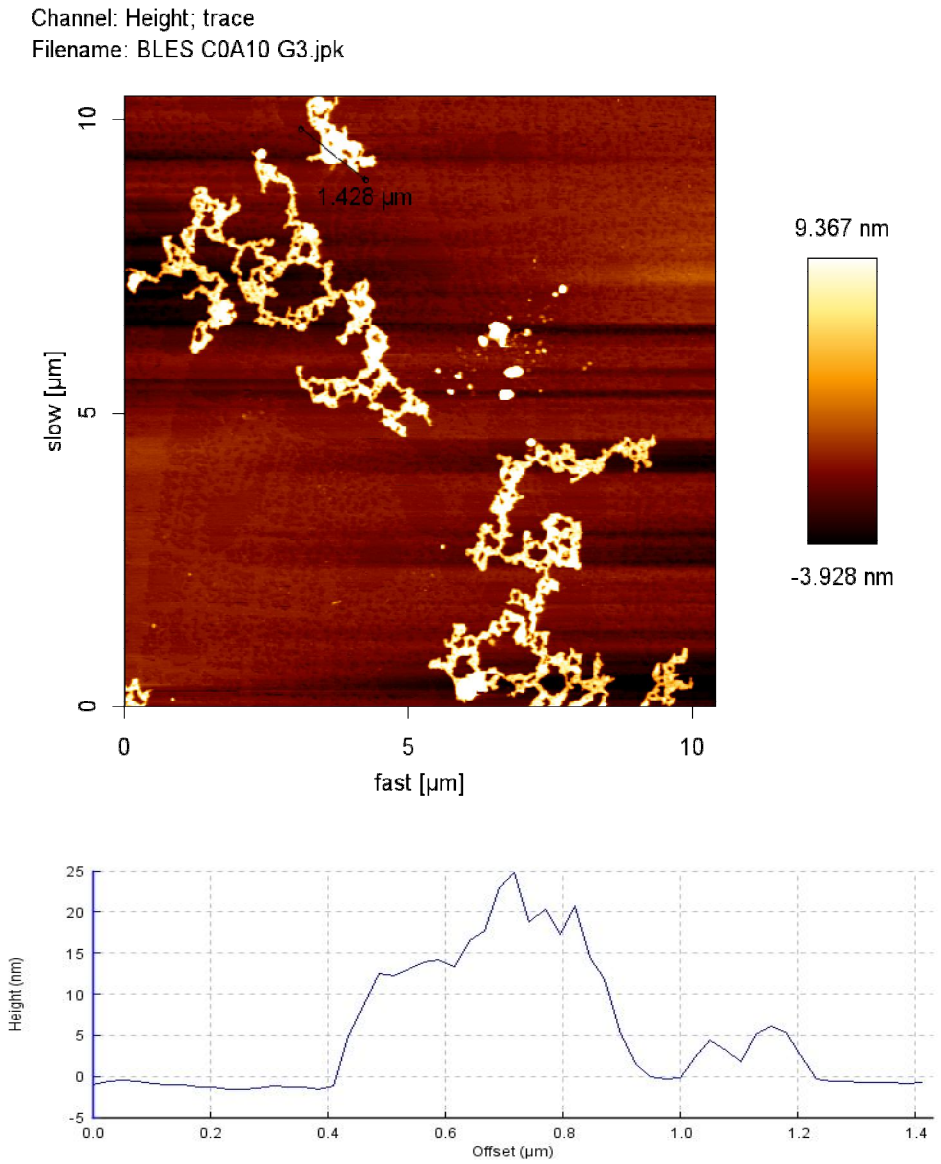

Figure 31 - BLES monolayer with 1% Amyloid-β compressed to 50 mN/m

Figure 31 - BLES monolayer with 1% Amyloid-β compressed to 50 mN/m shows a BLES monolayer with 10% amyloid-β compressed to 50 mN/m. We observe long microtubular aggregates connected to each other. The height of this clusters varies continuously, but approaches 40 nm in some areas. They are not flat as the multilayers we observed earlier without peptide. Most likely these clusters are peptide-lipid aggregates, which might be forced out of the monolayer at higher compressions. If we

look closely at the monolayer, we observe very small liquid expanded domains. These domains are less visible because of the z-scale required to accurately asses the peptide aggregates.

2.4 Discussion

2.4.1. **Effect of cholesterol on thin lipid films**

We found that for all investigated films, BLES, pure DPPC, or mixed DPPC-DOPG, high concentrations of cholesterol impairs surface tension reducing properties, which are required for proper function of pulmonary surfactant. In surface pressure-area isotherms (Figure 10), we notice a remarkable plateau at around 48 mN/m, with no further increase in surface pressure. This is a result of the cholesterol inhibiting multilayer formation causing excess material to drop into the liquid subphase as opposed to forming multilayers. Figure 11 shows a typical BLES multilayer formation. Gunasekara (Gunasekara, et al. 2005) and Leonenko (Leonenko, Gill, et al. 2007) showed that the addition of cholesterol to BLES resulted in the abolishment of surface activity of BLES. Our data is in good agreement with data reported earlier by these authors on BLES and extend these to the DPPC-DOPG mixture. Keating (Keating, et al. 2007) showed that mice ventilated with BLES and cholesterol showed lower arterial oxygen concentrations. Our of DPPC with cholesterol is in good agreement with Hoon, et. al (Hoon, Takizawa and Urisu n.d.).

2.4.2. **Effect of Low Concentrations (1%) of Amyloid-B on BLES and DPPC, DPPC-DOPG lipid films**

Addition of low concentrations of amyloid-β peptide showed an improvement in multilayer formation in both DPPC and DPPC-DOPG films. Isotherms showed a significant increase in maximum surface pressure upon the addition of 1% amyloid-β. It has been shown earlier that these features are interconnected with each other in BLES films, and thus successful formation of multilayer structures is associated with proper

functioning of BLES surfactant. Examination of topographical AFM images shows that multilayer surface coverage increased in both DPPC and DPPC-DOPG mixtures upon the addition of 1% amyloid-β. As well, higher multilayers tended to form in DPPC-DOPG mixtures, similar to BLES films. Therefore we illustrated here that small amount of amyloid-β peptide in model lipid films can serve the same purpose as SP-C protein in BLES, and can improve multilayer formation and therefore the function of the DPPC, or DPPC-DOPG mixed film, as a simple model of pulmonary surfactant. Previous research by Dante (Dante, Hauss and Dencher 2003) showed using neutron diffraction that amyloid-β incorporates deeply into POPC lipid films and perturbs the lipid bilayer. Our data obtained here are consistent with this finding. According to the proposed model (Leonenko, Gill, et al. 2007) (Amrein, von Nahmen and Sieber 1997), we believe that it is possible that the alpha-helical section of the amyloid-β peptide incorporates into the lipid bilayer, the random coil section may act as an anchor, allowing the peptide to become a molecular hinge, similar in function to SP-C.

Next, 1% of amyloid-β was incorporated into the BLES. Surface coverage of BLES multilayers with peptide present remained similar (Figure 18) to BLES without peptide added (Figure 11). Isotherm data showed a decrease in maximum surface pressure from 70 mN/m to around 50 mN/m (Figure 17).

The addition of 1% amyloid-β to DPPC (Figure 24) and DPPC:DOPG (results not shown) result in an increase of maximum surface pressure from around 48 mN/m to around 70 mN/m once peptide is added (Figure 23). Existing literature indicates that both DPPC and DOPG should reach surface pressures approaching 70 mN/m, however on our trough, we were unable to achieve surface pressure of greater than 55 mN/m. We were

able to achieve higher surface pressures with 1% amyloid-β added. While quantitative analysis was difficult, we can qualitatively say that amyloid-β added to thin lipid films improves surface activity of the film. This leads us to believe that, amyloid-β allows the film to achieve higher surface pressures more readily with less compression. The interesting result from this experiment is the counterintuitive result that surface pressure area isotherms of BLES (Figure 17) showed a decrease in maximum surface pressure with the addition of low concentrations of amyloid-β from 70 mN/m without peptide to around 48 mN/m with the peptide added. This means that the ability of lipid films to reduce surface tension is improved upon the incorporation of small amounts of amyloid β, while it is reduced for BLES. This could be due to the fact that SP-C at concentration of approximately 0.5%-1%, which is similar to amyloid-β, is already present in BLES mixture, and therefore additional increase in the total amount of peptide is not favourable.

2.4.3. Effect of High Concentrations (10%) of Amyloid-B on BLES and DPPC, DPPC-DOPG lipid films

As with low concentrations of amyloid-β, high concentrations of amyloid β showed a higher maximum surface pressure plateau in both DPPC and DPPC-DOPG mixtures of approximately 70 mN/m (Figure 25 and Figure 22). High concentrations of amyloid-β in DPPC and DPPC-DOPG showed multilayer formation surface coverage and height to be similar to low concentration compositions, however the morphology of the multilayers was occasionally different. Multilayers in 10% amyloid mixtures tended to be more circular in shape, whereas 1% amyloid mixtures yielded multilayers which tended to have various shapes and sizes (Figure 24, Figure 21).

Addition of 10% amyloid-β to BLES showed a decrease in maximum surface pressure plateau at 48 mN/m, compared to a maximum surface pressure of 70 mN/m in BLES without any peptide added (Figure 17). This phenomenon leads us to conclude that the addition of high concentrations of amyloid-β makes it unfavourable for the peptide to be incorporated into the lipid monolayer. At higher compressions (47 mN/m), AFM images showed no multilayer formation, but unique patterns of peptide aggregates. Little multilayer formation was observed, as compared to BLES without any peptide added. These aggregates reached heights of up to 50 nm.

2.4.4. **Effect of Cholesterol and Amyloid-β on BLES and DPPC, DPPC-DOPG lipid films**

Since BLES contains numerous proteins whose function is to improve surfactant function, and cholesterol inhibits surfactant function in BLES, it can be predicted that cholesterol would also inhibit multilayer formation in lipids with alpha-helical peptides added. BLES, DPPC and DPPC-DOPG all showed no multilayer formation and lower (48 mN/m) surface pressure area isotherm plateau's when cholesterol and 1% amyloid-β were added to the lipid mixture (isotherm not shown). Research by Ji concluded that (Ji 2002) there is a stronger interaction between amyloid-β and cholesterol than between amyloid-β and lipids. This would explain our results of difficulties in incorporation of peptide into monolayers rich in cholesterol.

However, when we added 10% amyloid-β to BLES, we saw a return of multilayer formation suggesting that at high concentrations, (Figure 27) amyloid-β may counteract the destructive effect of cholesterol return some surfactant function to BLES.

2.4.5. **Effect of Compression on BLES multilayer formation**

Our data showing the aggregation of peptide on the gel/fluid phase boundary at low compressions (Figure 30) correlate well with the data shown by Choucair (Choucair, et al. 2007) who showed preferential binding of amyloid fibrils on gel phase domains on the lipid membrane. Ege (Ege and Lee 2004) allowed peptide to bind to the monolayer from the subphase observed using fluorescence microscopy that the phase boundary became "fuzzy", suggesting that these are the preferred locations for the peptide. As surface pressure is increased, the remainder of the lipid materials is compressed into gel phase and domain boundary disappears (Figure 31). At this point, the unincorporated peptide is left to reside at the surface of the monolayer rather than incorporating. By comparing figures Figure 30 and Figure 31, we notice, what appears to be more peptide in the sample with higher compression (Figure 31). Ege also showed that the level of peptide insertion is inversely proportional to the packing density of the lipids (Ege and Lee 2004). We believe that in BLES, this occurs because peptide is being "squeezed out" or "unincorporated" out of the monolayer and is either dropped into the subphase or pushed to the air surface. This should be fairly obvious conclusion: as surface pressures increase, the peptide cannot insert as easily into the lipid monolayer.

Maltseva used a combination of grazing incidence x-ray diffraction and internal reflection absorption spectroscopy to study the interaction of lipid monolayers and amyloid-β (Maltseva, et al. 2005). The results Maltseva obtained show that at surface pressures higher than 30 mN/m, the peptide was squeezed out of the lipid monolayer. These data are consistant with our results.

Chapter 3
Binding of Amyloid-β to Lipid Membranes

3.1 Description of Experiment

The amyloidosis process varies depending on the environment of amyloid-β. In solution, amyloid-β forms fibrils which increase in length and width as a function of time. We believe that the interaction of amyloid forming peptide is important for the mechanism of amyloid formation, especially at the initial stages. Amyloid-β allowed to incubate on lipid membranes will not yield the same results as amyloid-β which is left to aggregate in aqueous solution without the presence of lipid membranes. In this experiment, we deposited amyloid-β on lipid bilayers of DPPC (zwitterionic), DOPG (anionic) and DOTAP (cationic) and allowed the peptide to incubate for various periods of time. At the end of incubation, we imaged supported bilayers in water using atomic force microscopy to observe any possible fibril or oligomeric formation in or on the lipid bilayer.

3.2 Materials and Methods

Lipid Bilayer Preparation

DPPC, DOPG and DOTAP lipids were purchased from Avanti Polar Lipids (Alabaster AL). Lipid vesicle solution was prepared by adding 0.5 mg of lipid in 1 mL of ultrapure water. The lipid solution was stirred for 15 minutes, followed by 10 minutes of ultrasonic sonication. This stirring/sonication procedure was repeated until the lipid solution was clear. This indicated that lipid vesicles had formed. 100μL of vesicle

solution was placed on freshly cleaved mica. Vesicles were allowed to fuse for 15 minutes. The sample was washed with ultrapure water to remove unfused vesicles. DOTAP bilayers do not easily bind to mica sheets. Therefore, an additional step was taken with DOTAP bilayers: mica sheets were chemically modified with APTES solution, by irrigating mica in APTES for 10 minutes and rinsing it with ultrapure water. Samples of each lipid bilayer (DPPC, DOPG and DOTAP) were imaged with the atomic force microscope to ensure uniformity of the bilayer. One sample of each lipid was rinsed vigourously with ultrapure water, causing "nanoholes" in the lipid bilayer. When imaged, these samples with holes allow us to measure the depth of the holes indicating the thickness of the lipid bilayer. We measured a hole depth of 5nm indicating a correct bilayer height of 5nm.

Amyloid-β Incubation

Amyloid-β (1-42) was purchased from rPeptide Inc. (Bogart, GA). rPeptide has prepared the peptide in an NaCl counter ion in accordance with the Fezoui procedure (Fezoui, et al. 2000). 1 mL of HEPES buffer (50 mmol, pH 7.8) was added to a 0.5mg vial of amyloid-β peptide. The solution was sonicated for 1 minute as directed by rPeptide literature. 100μL amyloid-β of peptide solution was placed on the lipid bilayers and was incubated at room temperature for the defined time periods of 10 minutes, 1 hours, 6 hours, and 24 hours. At the conclusion of incubation time, unbound peptide was gently rinsed with 50μL of ultrapure water three times as described in (Choucair, et al. 2007). Nanopure water was added in sufficient quantity to cover the mica slide during imaging with the atomic force microscope.

For control experiments, 100μL amyloid-β was placed on mica and allowed to adsorb for 5 minutes. Excess peptide was rinsed with 50μL three times.

Atomic Force Microscopy Imaging

Samples were placed in the liquid cells provided by JPK Instruments AG. The liquid cells were filled with nanopure water, covering the entire sample. The liquid cells were placed in the atomic force microscope. All samples were imaged in liquid. To collect images using the JPK Nanowizard II instrument, we used a Veeco DNP-S cantilever designed for liquid cell use. Calibration (laser alignment and tuning) was completed in accordance with the JPK user manual. Images were scanned at a line rate of 0.5Hz and a set point between 0.18-0.30V.

Analysis

Images were processed with JPK image processing software. Images were levelled by subtracting a polynomial fit from the images, and some images were adjusted by adjusting the MinMax z-range to emphasize desired features. For example, if certain features have a variation of height between 2 and 10 nm, but we are only concerned that these features are present, but want to observe the underlying lipid topology as well, we adjusted the z-range to display these features as the same colour (mostly white), while having a contrast for lipid topology differences. In each case, cross sections were taken to show representative height. A few images have been altered by the application of a low pass filter and the replacement of certain pixels by using the mean of neighbouring pixels. These filters were added to improve image quality.

Quantitative analysis of number of oligomers and oligomer surface area was conducted with ImageJ software. The colour AFM image converted to an 8-bit image and the threshold was adjusted to include all higher objects (oligomers and fibrils) and omit the background (bilayer). Particles were than analyzed and the software calculated various statistical values for the number of oligomers, mean particle area, and min and max area.

3.3 Results

3.3.1. **Amyloid-β Incubated in Solution (Control)**

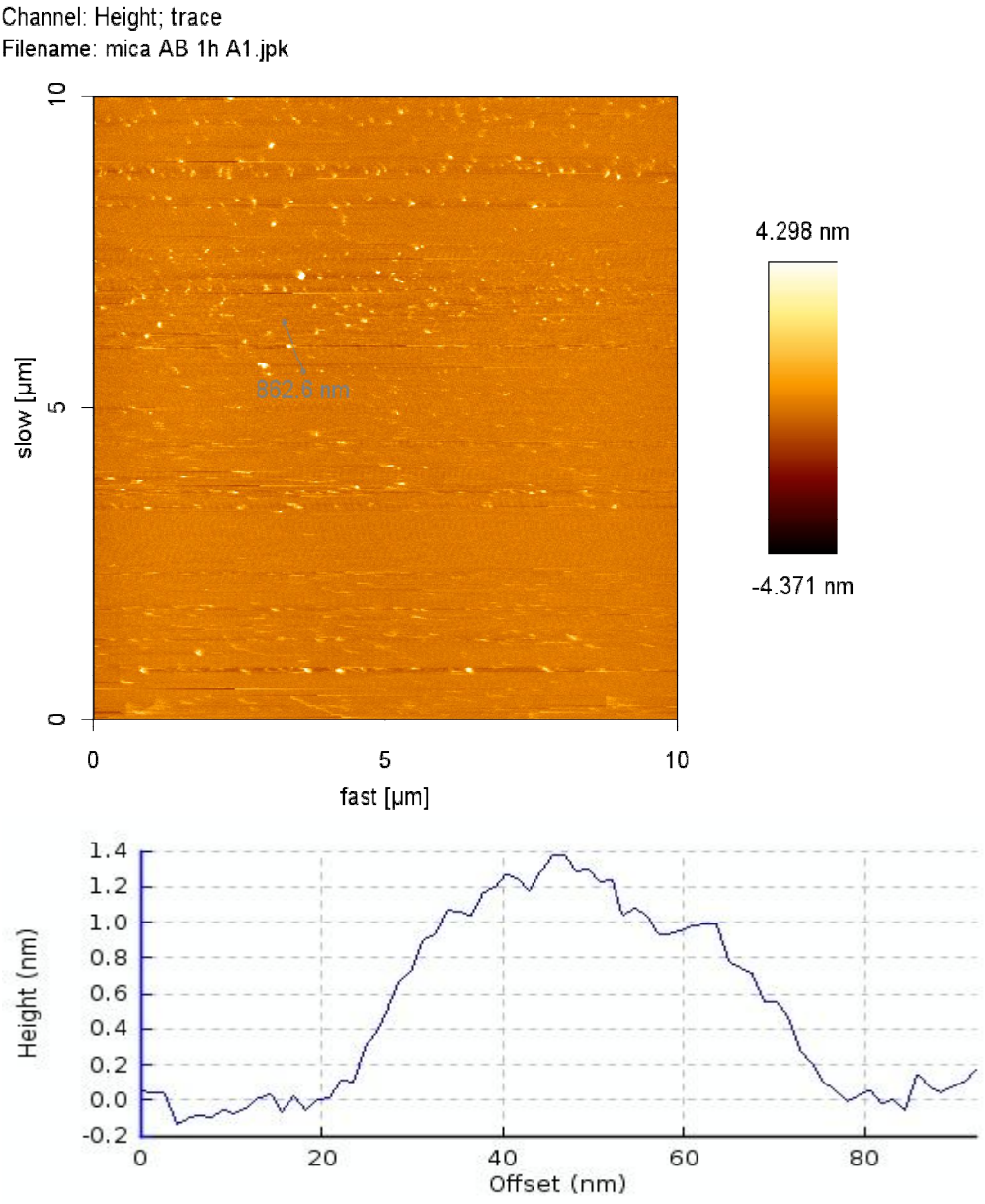

Figure 32 - Amyloid-β incubated in solution 1 hr

In Figure 32 we observe the result of amyloid-β incubated for 1 hr in solution and placed on mica. After 1 hr of incubation, we observe that small amyloid-β oligomers start to form. These oligomers are all circular in shape with a height of between 1 and 3nm.

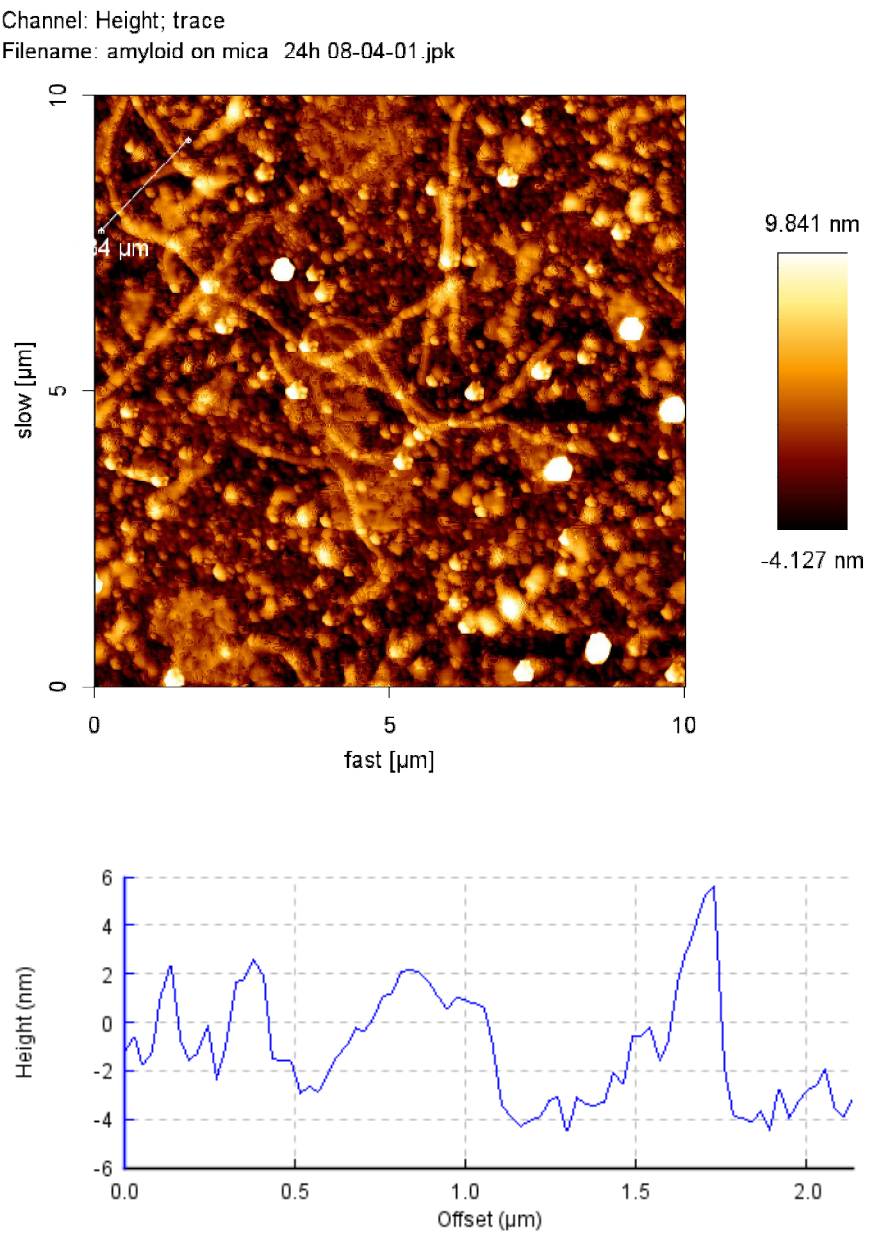

Figure 33 - Amyloid-β incubated in solution 24hr

Figure 33 shows amyloid-β which has been allowed to incubate in solution for 24 hrs. We observe extensive long, thick fibrils, having a length of up to 5 µm and a height of between 2 and 6 nm. Also, we see small spherical aggregates which most likely are oligomers of peptide which have not yet aggregated into fully mature fibril form.

3.3.2. **DPPC**

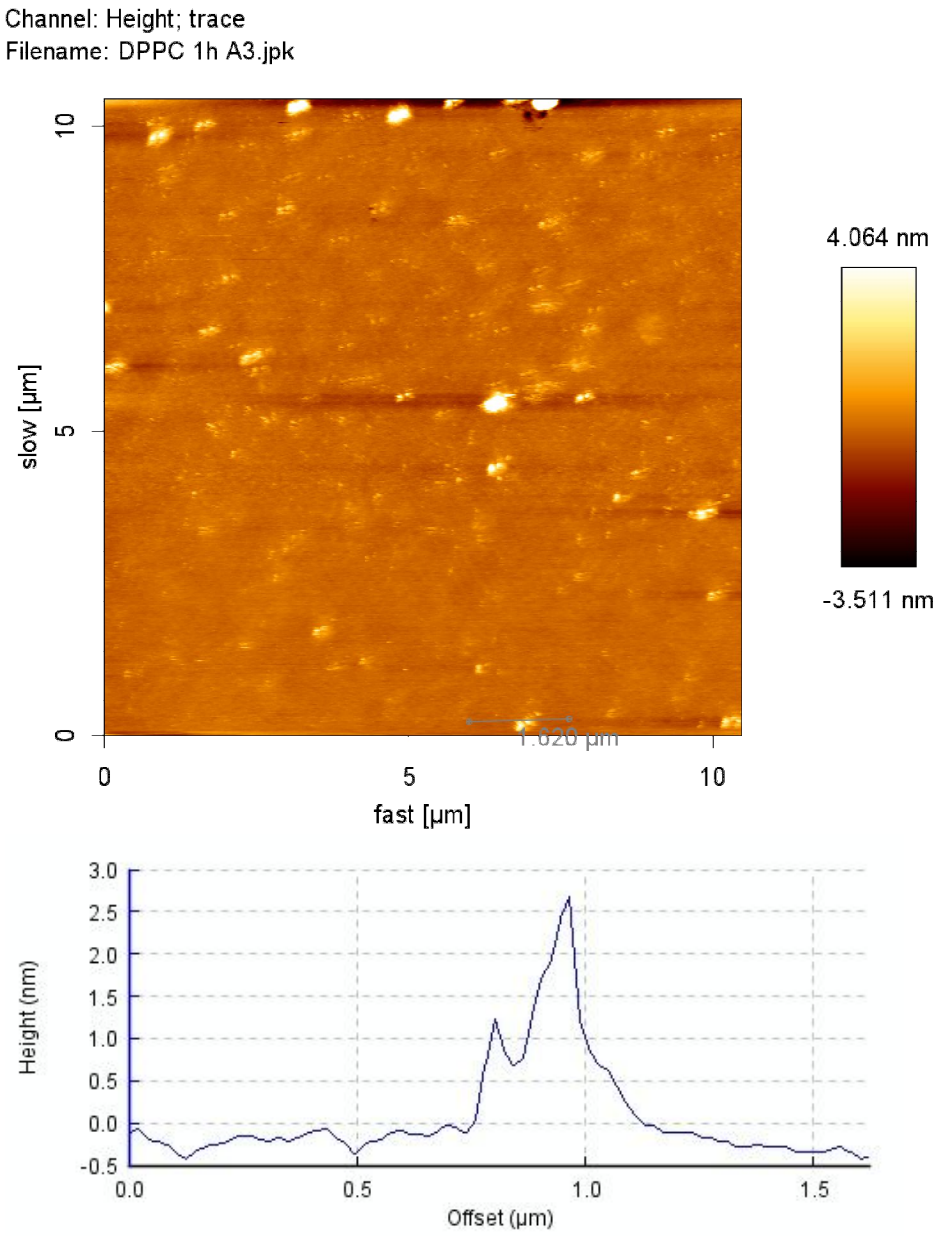

Figure 34 - Amyloid-β incubated on DPPC bilayer 1hr

Figure 34 show amyloid-β incubated on a DPPC bilayer for a period of 1 hr. We observe formation of oligomeric structures of up to 3nm high with a width of between 100-500 nm. Both small and larger oligomers are present and have a mean area of 0.066 μm^2.

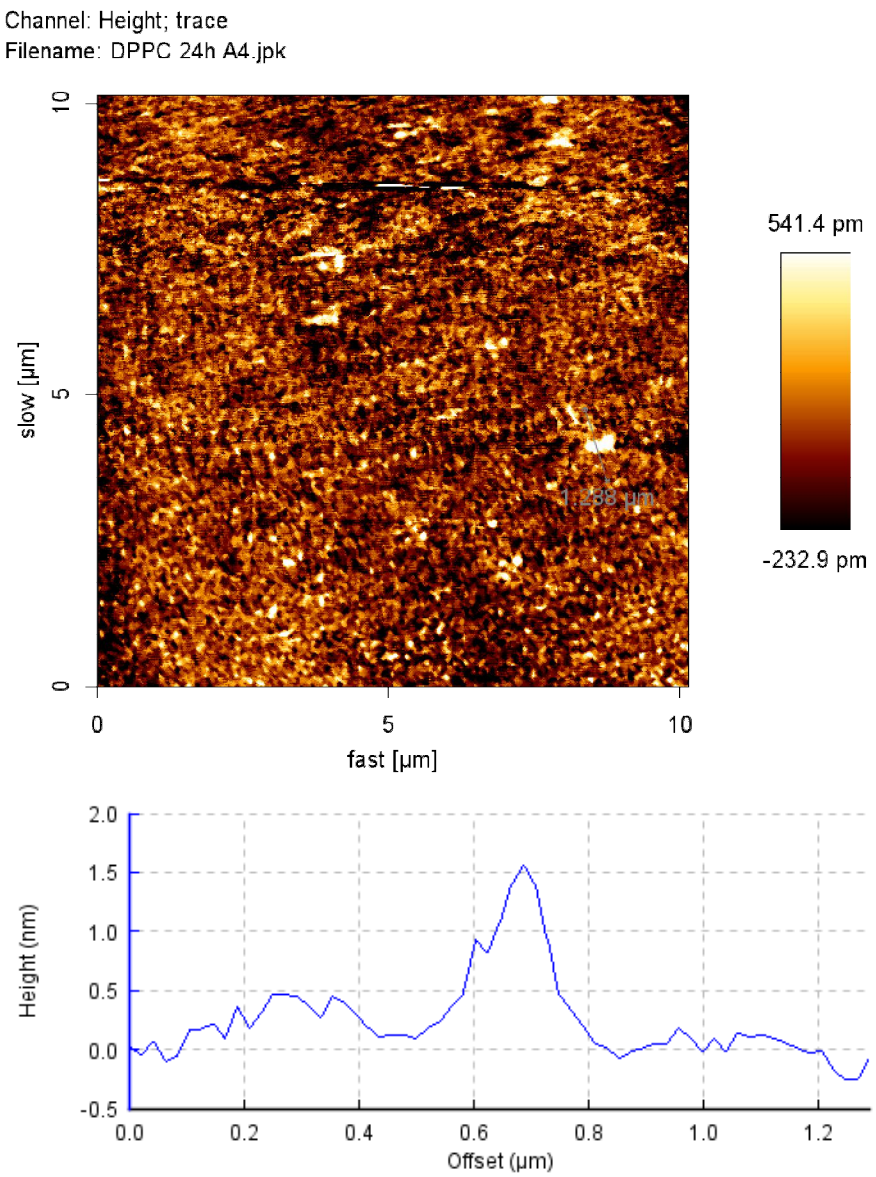

Figure 35 - Amyloid-β incubated on DPPC bilayer 24hr

Figure 35 shows amyloid-β incubated on DPPC for 24 hours. We observe small prolongated oligomers connected to each other, that completely cover the surface of mica and are approximately 0.5-22 nm high and 0.1 µm in length.

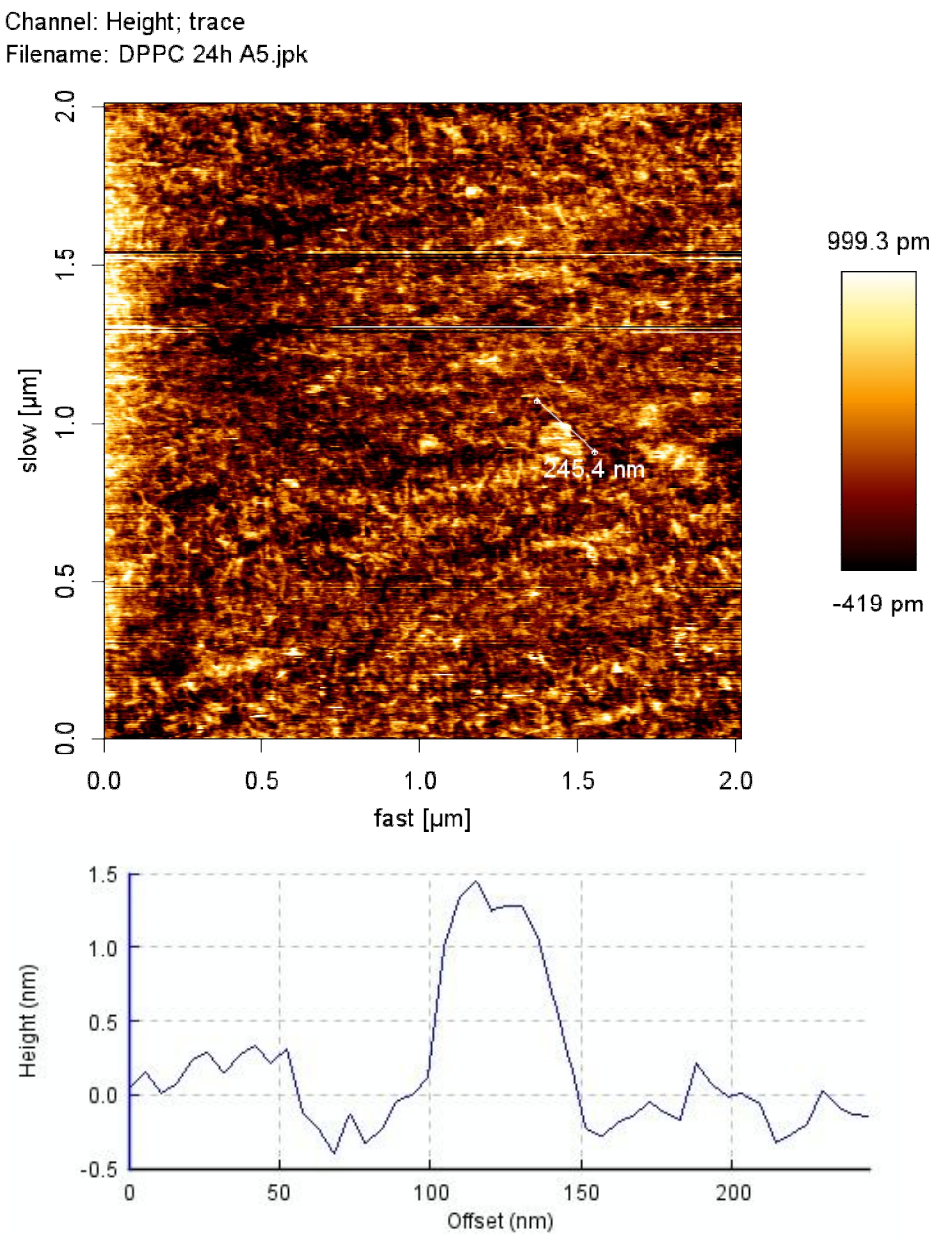

Figure 36 - Amyloid-β incubated on DPPC bilayer 24hr

Figure 36 shows a small scale image of amyloid-β incubated on DPPC bilayers for 24 hours. On close examination, we see very small fibril structures with a height of 0.25nm (see left side of cross section). Larger oligomeric structures approach 1.5nm in height.

3.3.3. **DOPG**

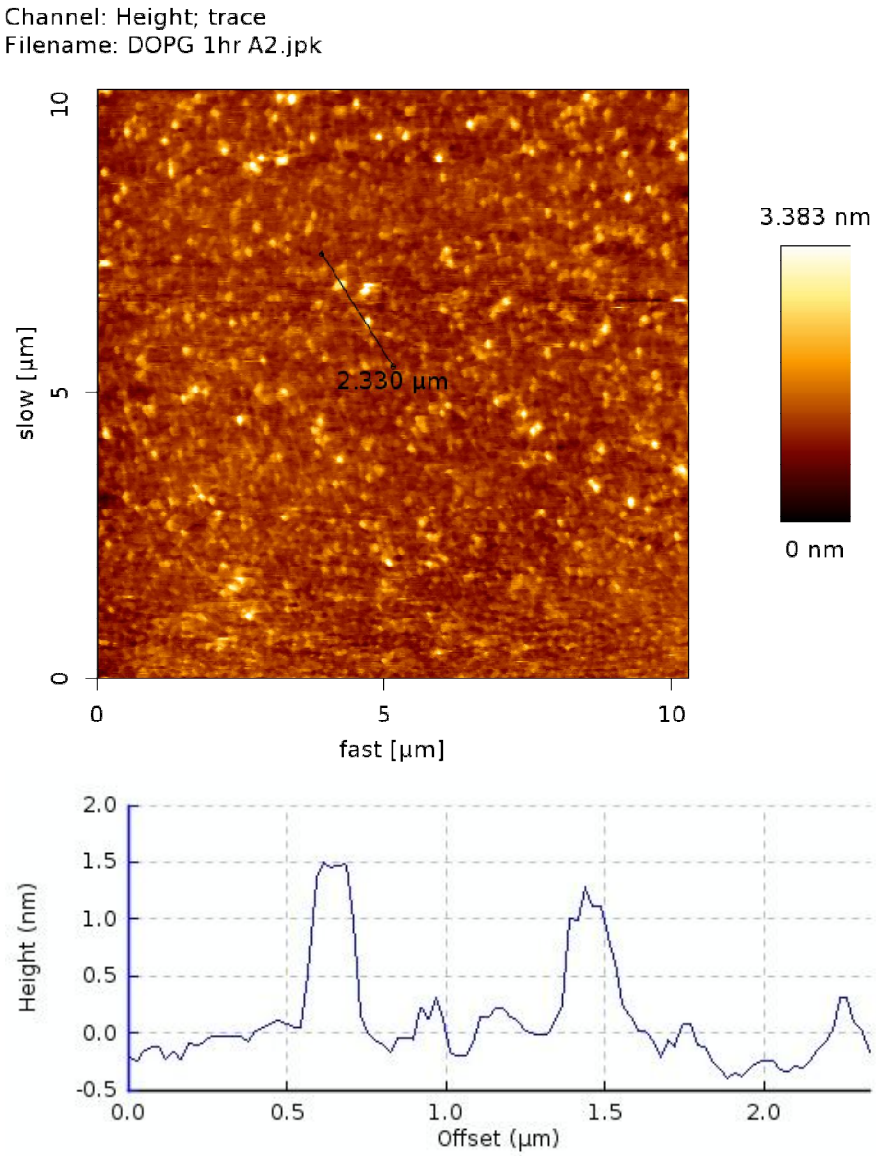

Figure 37 - Amyloid-β incubated on DOPG bilayer 1hr

Figure 37 shows amyloid-β incubated for 1 hour on a DOPG bilayer. We observe numerous, small spherical oligomers with a height of 1-3nm. Oligomers are well distributed. On close examination, we observe some of these oligomers have formed very small fibrils with a height of approximately 0.2nm. They appear spherical and separated from each other, unlike clusters we observed earlier on DPPC bilayer.

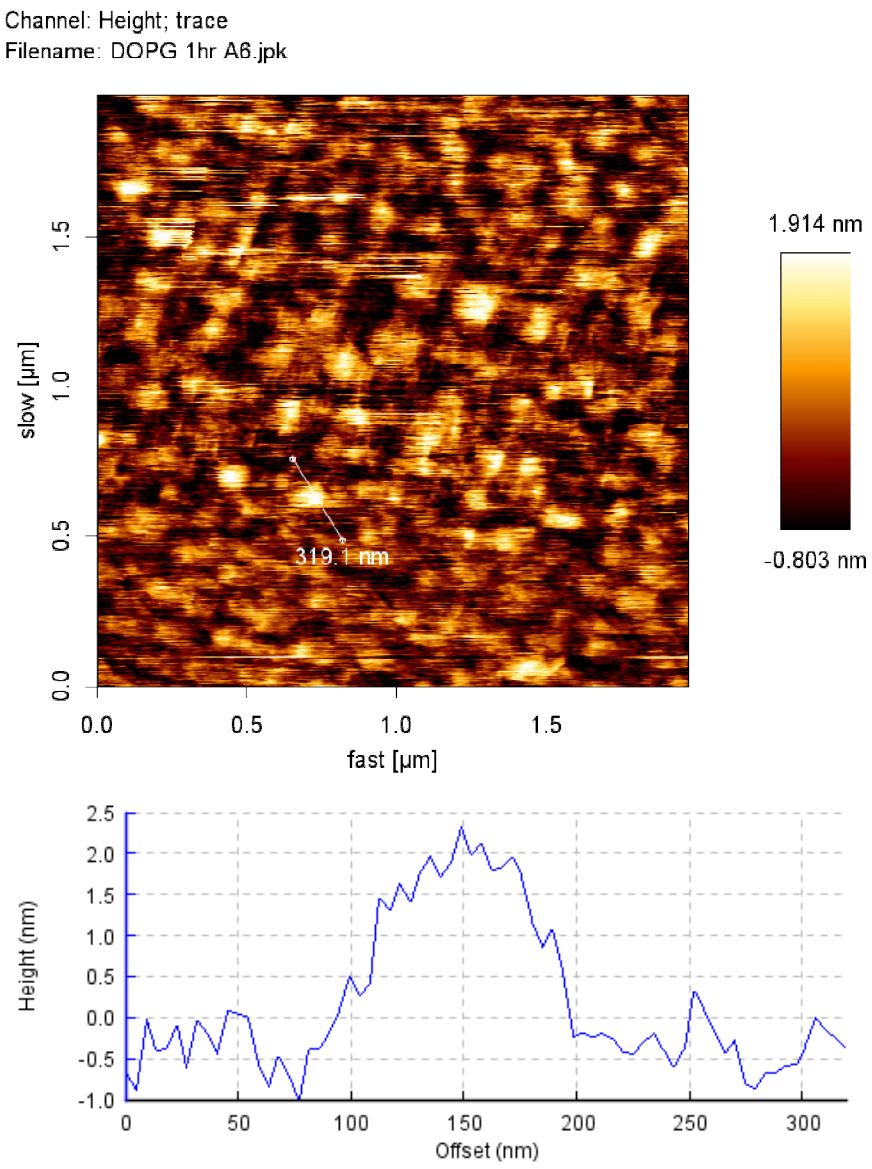

Figure 38 - Amyloid-β incubated on DOPG bilayer 1hr

Figure 38 shows a high resolution image of amyloid-β incubated on a DOPG bilayer for 1 hour. We observe frequent, round oligomers with a height of between 1 and 3 nm. Very small fibrils appear to form in areas outside of the oligomers with a width approaching the lateral resolution of the image. The height appears to be approximately 0.2nm (see left side of cross section).

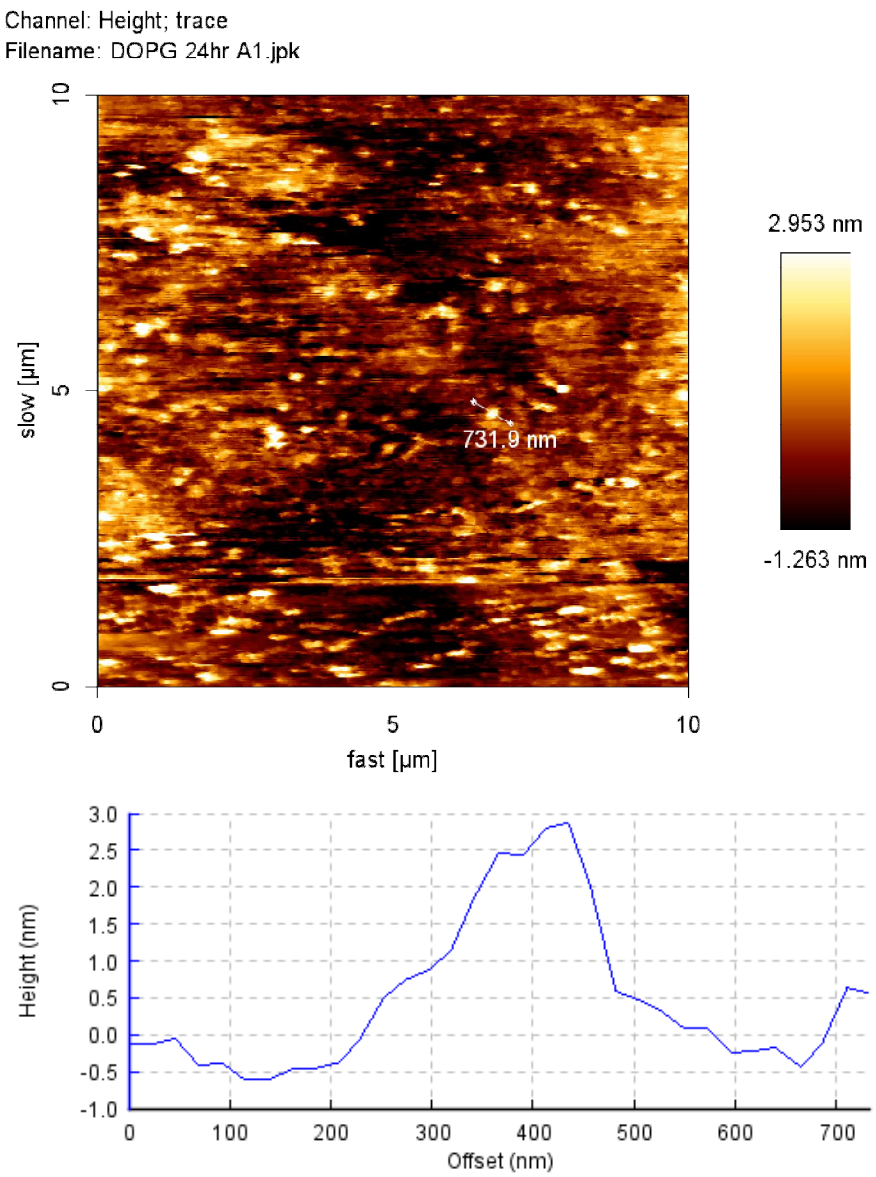

Figure 39 - Amyloid-β incubated on DOPG bilayer 24hr

Figure 39 shows amyloid-β incubated on a DOPG bilayer for 24 hours. We observe numerous elongated oligomers with a height of 3 nm. Occasional small fibril-like structures are seen in the background.

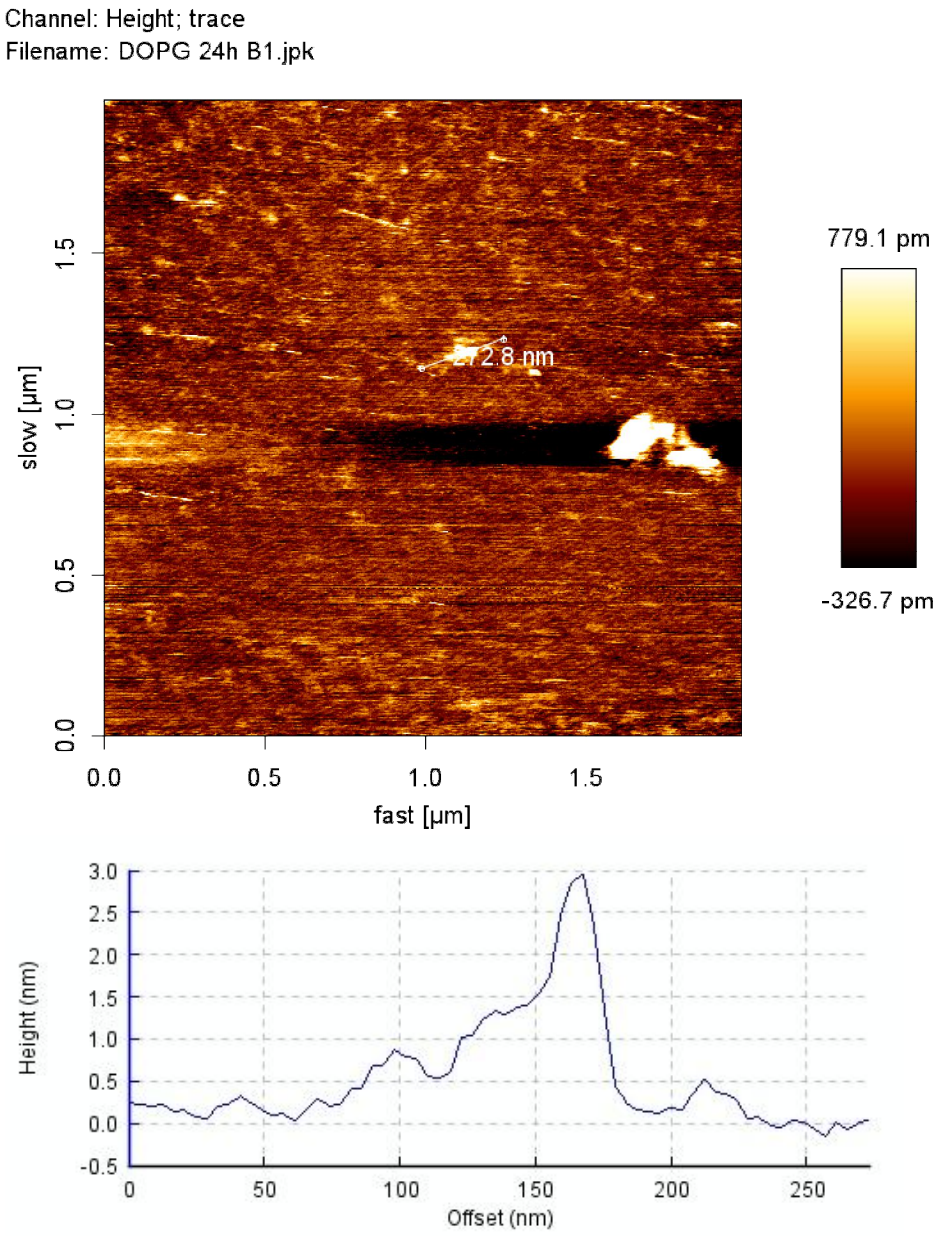

Figure 40 - Amyloid-β incubated on DOPG bilayer 24hr

Figure 40 is a high resolution image of amyloid-β incubated on a DOPG bilayer for 24 hours. We observe few fibril structures with a height of 0.5nm. Fibrils appear to be straight and no longer than 100µm in length. On close examination, 3 fibrils located in the upper left quadrant of Figure 40 appear to have some twist to them.

3.3.4. **DOTAP**

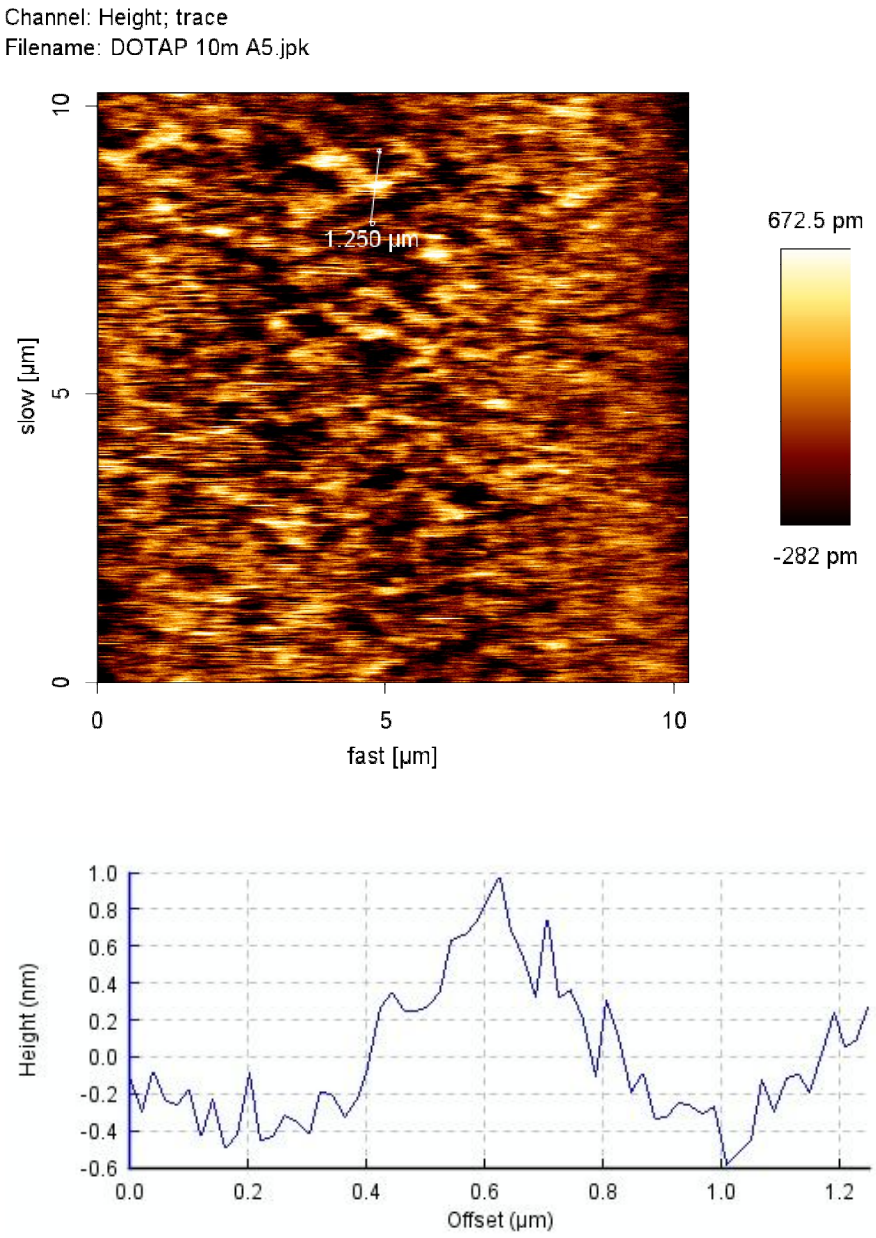

Figure 41 - Amyloid-β incubated on DOTAP bilayer 10min

Figure 41 shows amyloid-β incubated on a DOTAP bilayer for 10 minutes. We observe oligomers with a height of 1nm and mean area of $0.053\mu m^2$. We observe no individual fibrils, but rather interconnected, poorly-defined in structure aggregates.

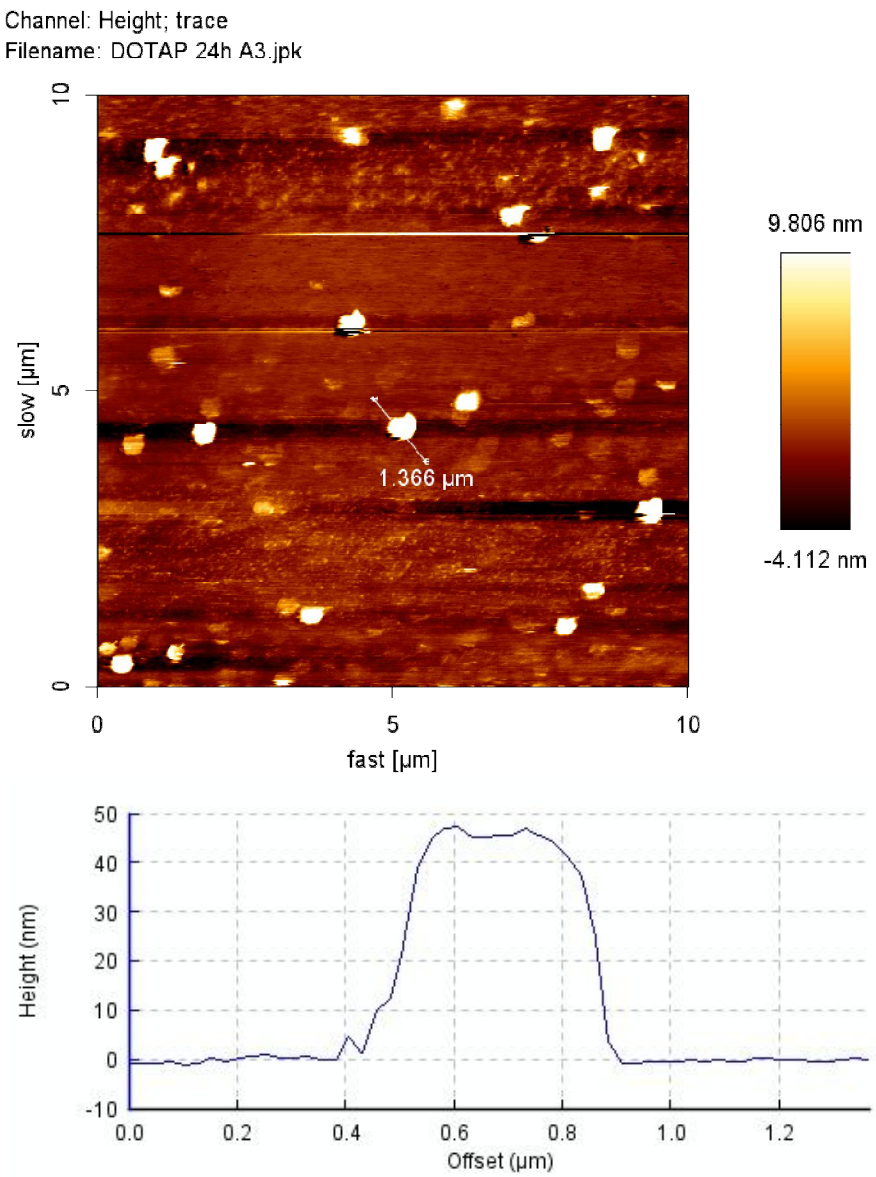

Figure 42 - Amyloid-β incubated on DOTAP bilayer 24hr

Figure 42 shows amyloid-β incubated on a DOTAP bilayer for 24 hours. We observe large round, flat, patch-likeclusters of material reaching up to 80 nm high. Lower clusters reach 20 nm high. We are uncertain whether these clusters are composed of lipids, proteins, or a combination of the two. The top part of the image shows what appear to be small fibrils. These are difficult to resolve because of the large z-range of the image caused by the larger clusters.

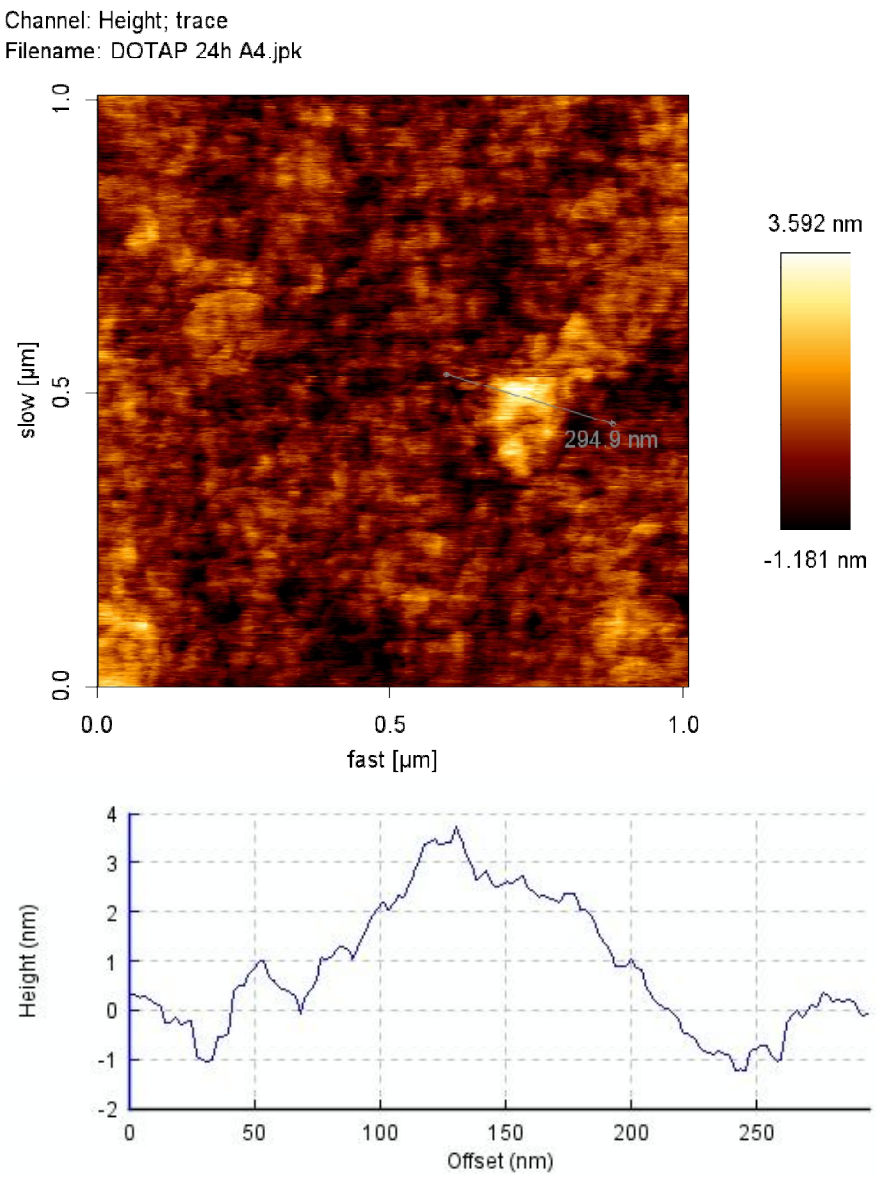

Figure 43 - Amyloid-β incubated on DOTAP bilayer 24hr

Figure 43 shows a high resolution image of amyloid-β incubated on DOTAP bilayers for 24 hours. We observe no single amyloid oligomers but rather entangled plaque-like structures, such as one with a height of 3.5 nm and width of 200 nm, shown on Figure 43 - Amyloid-β incubated on DOTAP bilayer 24hr, cross-section.

3.4 Discussion

Amyloid-β, when cleaved from its precursor protein, is implicated in the neurotoxicological symptoms manifesting as Alzheimer's disease as a result of the misfolding of this peptide. How this protein interacts with lipid cell membranes is essential to understanding the mechanism of action of amyloid-β. Given that extensive work has been done on the misfolding and aggregation of amyloid-β in solution, we compared this aggregation to the aggregation of amyloid-β and growth of amyloid fibrils incubated on lipid bilayers DPPC (neutral), DOPG (anionic) and DOTAP (cationic). While cationic lipids are not present in cell membranes (Ege and Lee 2004), it was important to compare the interactions of amyloid-β between lipids of different charges to better understand the electrostatic interactions between amyloid-β and lipid membranes. We allowed amyloid-β to incubate on lipid bilayers and then used the atomic force microscope to study how amyloid-β interacts with cell membranes. AFM images were compared both qualitatively and quantitatively using ImageJ software to count aggregates and determine their mean size.

The difference in fibril formation between amyloid-β incubated in solution and amyloid-β incubated on lipid bilayers is striking: in solution, we observe extensive fibril formation in which fibrils grow in both length and width with increasing time. For example, area distribution analysis conducted comparing Figure 32 and Figure 33 indicate that while the number of oligomers or fibrils stays constant, the size of the fibrils is radically increased. Figure 32 shows amyloid peptides which have been incubated in solution for 1 hour. A total of 301 oligomers are seen in the image with an average oligomer size of 0.029 μm^2. Figure 33 shows the amyloid peptide after being incubated

for 24 hours in solution. However, while we observe an almost equal number of oligomers: 283, the peptide has aggregated to form large fibrils and oligomers, which average 0.5 μm^2 in area. However, when we allow amyloid-β to incubate on lipid bilayers, we do not see the large fibrils associated with solution incubation. Importantly, both fibrils and spherical oligomers are well resolved when are formed in solution or on supported surfaces (mica). When fibrils are formed on supported lipid bilayers, the structure of fibrils or oligomers are not well resolved, have lower height and seem to fuse with the bilayer. This effect is larger for DOTAP, than DOPG, and smaller on DPPC. This observation suggests that at the initial stage of amyloidosis, small oligomers or even monomers interact strongly with the lipid bilayer. We hypothesize that lipids have a lower packing density when in the fluid phase, compared to lipids the gel phase, therefore peptides insert more readily in fluid phase bilayers than in gel phase bilayers (Ege and Lee 2004). Our results are consistant with this hypothesis: peptide aggregates have larger height and are better resolved on the surface of gel phase DPPC bilayer, than on the surface of fluid phase DOPG and DOTAP bilayers.

Amongst the different lipids, we see differences in their interactions with amyloid-β. In DPPC, we see an increase in both the number of oligomers and the mean size of the oligomers as incubation time increases. We observe the following increase in the number of oligomers (for 10 min, 1hr, 6hr, 24hr respectively): 95, 117, 343, 773. The mean size of the oligomers also increases, ranging from 0.053 μm^2 for a 10 minute sample to 0.084μm^2 at the 6 hour sample. However, by the time 24 hour sample, the mean peptide area is reduced to 0.054μm^2. This decrease is likely due to amyloid-β peptide forming thin fibrils which have much smaller area as compared to oligomers.

In DOPG, we see a constant number of oligomers (approximately 300) and average size regardless of incubation time. The mean peptide area is between 0.055μm^2 and 0.067μm^2. However, Figure 39 demonstrates that approaching a time of 24 hours, amyloid-β incubated in DOPG forms small fibrils which would not be reflected in simply measuring mean oligomer area.

The fibrils-like structures seen in DPPC and DOPG bilayers appear to be significantly smaller, than those seen deposited on mica after solution incubation. Fibrils incubated on DPPC and DOPG bilayers have a height of approximately 0.2nm, which approaches the z-range resolution limit of the AFM. This suggests that these small fibrils have embedded themselves into the lipid bilayer, and only a small top portion is showing. While we believe these structures to be fibrils, it is difficult on this small of a scale to definitely say that these fibril-like structures are in fact amyloid fibrils. Further research using fluorescence may provide a definitive answer.

DOTAP showed mean oligomer area and number of oligomers consistent with DPPC and DOPG bilayers. After 10 minutes of incubation, Figure 41 shows 178 oligomers with a mean area of 0.0528 μm^2. Figure 42 shows peptide incubated on DOTAP for 24hr. We observe a significant disruption of the lipid bilayer indicating a strong interaction between the peptide and the lipid bilayer. This excess material (perhaps DOTAP or DOTAP protein mixtures) reaches a height of up to 60nm. We believe this phenomenon is a result the DOTAP bilayer interacting strongly with the peptides, forming peptide-lipid aggregates. Because of this significant membrane disruption in 24hr samples, quantitative analysis of the number of oligomers was difficult. At high resolution, we were able to observe amyloid oligomers fused with the surface of a

DOTAP bilayer. Figure 43 shows a high resolution image of an amyloid-β oligomer in a DOTAP bilayer incubated for 24 hours. We observe clusters 3nm high allowing us to conclude that there strong interaction of amyloid peptides with the lipids in DOTAP bilayers. We observe that the number of oligomers found in the cationic DOTAP bilayer after 10 minutes, 178, is significantly less than the number of oligomers found in DOPG at a comparable time of 1 hour, 543, but considerably more than the 95 oligomers observed on DPPC.

We believe that when amyloid-β comes in contact with lipids, there is an electrostatic interaction between the peptide and lipid. As the charge of the lipid diverges from neutral, we believe that the electrostatic interaction between lipid and peptide increases and may alter the kinetics of conformational change of amyloid-β. From our data, we believe that the stronger the charge difference between peptide and lipid, the greater the peptide adsorption to the lipid membrane. We base this theory on a couple observations: firstly, the number of oligomers found in anionic DOPG seems to remain constant as incubation time increases. This indicates that amyloid-β adsorbs unto it's a DOPG bilayer almost immediately. However, the adsorbed oligomer count of neutral DPPC increased with increasing incubation time suggesting that as amyloid-β is incubating on the lipid bilayer, it is adsorbed into the bilayer, but does not disrupt the bilayer. Cationic DOTAP was more similar to anionic DOPG: within 10 minutes, a significant number of oligomers were already found embedded onto the cationic bilayer. After 24hr, we notice a significant disruption of the lipid bilayer. Secondly, we observe that peptides incubated on lipid bilayers misfold differently than peptide in solution. In solution, we find only a hydrophobic effect, where we would expect an α-helix-β-sheet

equilibrium to favour the β-sheet conformation. When allowed to incubate on charged lipid bilayers, the peptide experience both electrostatic interactions as well as the hydrophobic effect, driving the peptide into the lipid bilayer. On neutral DPPC, we only have a hydrophobic effect driving the peptide onto the bilayer and no electrostatic interaction. Research by a number of labs have shown that amyloid-β binds preferentially to anionic lipids (Terzi, Holtzmann and Seelig, Self Association of Amyloid beta in solution and binding to lipid membranes 1995) ds. This increase in affinity to anionic DOPG has been attributed to an electrostatic interaction between the amyloid-β peptide and the lipid headgroups (Bokvist, et al. 2004) (Maltseva, et al. 2005) (Ege and Lee 2004) (Ji 2002). Our results, as well as results by Ege show that amyloid-β can bind to cationic lipids just as readily as anionic lipids (Ege and Lee 2004). For our experiments, we dissolved the peptide in HEPES buffer solution at a pH of 7.8, whereas the isoelectric point of amyloid-β is 5.5 (Fezoui, et al. 2000). While the overall net charge of the peptide is negative at relevant pH, the peptide still has local positive and negative charges based on the primary amino acid sequence. Bockvist has theorized that amyloid-β has a local positive charge around Lys28 (Bokvist, et al. 2004). Bockvist showed that when this positively charged part of amyloid-β, comes into contact with anionic DOPG, the amyloid-β is attracted to the negatively charged headgroups on both sides of the bilayer (Bokvist, et al. 2004). This electrostatic effect forces the peptide deep into the bilayer. However, the electrostatic interaction in zwitterionic DPPC is not nearly as strong. Therefore, we see a considerably lower number of oligomers found in the DPPC bilayer. With an increase in incubation time however, the amyloid-β peptide is slowly incorporated into the DPPC bilayer resulting in the increase in oligomers in the lipid

bilayer. At room temperature, DPPC is in a gel phase, whereas DOPG is in a fluid phase. Amyloid-β incorporates into bilayers with lower surface pressures more readily than those with higher surface pressures leading us towards the idea that amyloid-β would incorporate into fluid phase (DOPG and DOTAP) bilayers more readily than DPPC bilayers.

Choucair (Choucair, et al. 2007) used a combination of AFM and Total Internal Reflectance Microscopy (TIRF) to study the effect of amyloid-β insertion on neutral DPPC:DOPC bilayers. Choucair indicates no evidence of amyloid-β insertion into the lipid bilayer, which is also consistent with the theory that because of electrostatic interactions, amyloid-β has difficulty inserting into neutral bilayers.

Using a combination of FTIR and AFM, Sharpe and Forrest showed that insulin had unfolding kinetics highest when adsorbed on cationic lipids, followed by anionic lipids, than followed by bulk solution (Sharpe 2002).Sharpe suggests an explanation for this phenomenon as a thermodynamic interplay of entropic and enthalpic process that direct misfolding kinetics when the peptide is adsorbed to the lipid.

Bockvist has suggested that once incorporated into lipids, amyloid-β is stabilized and prevented from aggregating, inhibiting fibril formation (Bokvist, et al. 2004). This suggestion is consistent with our observation of considerably smaller fibrils. However, it has been shown that the actual oligomers are more toxic than the fibrils, leading us to suggest that this stabilization of amyloid-β in the cell membrane may not actually be beneficial from a neurotoxicological perspective.

Further research into these lipid-amyloid-β interactions should be conducted by allowing amyloid-β to be incubated on solution and allowed to adsorb on various lipid

membranes and imaged. This would allow us to observe with the AFM the two different methods of amyloid-β binding to lipid membranes as Bockvist has suggested (Bokvist, et al. 2004).

Chapter 4
Conclusions

4.1 Overview of Results

In our first experiment, we have demonstrated the effect of amyloid-β and cholesterol on lipid films of DPPC, DPPC-DOPG and BLES. We saw that cholesterol inhibits multilayer formation in all monolayers. Amyloid-β increases multilayer formation in DPPC and DPPC-DOPG, but reduced multilayer formation in BLES. When cholesterol and amyloid-β is added to BLES, 1% amyloid-β has no observable effect, whereas 10% amyloid-β allows BLES to regain some of its surfactant function. Therefore we conclude that amyloid-β alters surface activity of the surfactant BLES and model lipid monolayers, and at lower concentrations helps to counteract the destructive effect of high concentrations of cholesterol.

In our second experiment, we showed that fibril formation of amyloid-β is different on the surfaces of lipid bilayers when compared to fibril formation in solution (protein only interaction). Much larger fibrils are formed in solution compared to what is formed on lipid bilayers. Also, the lipids themselves interact with peptide monomers and oligomers inhibiting larger fibril formation. We showed that amyloid-β interact much strongly with charged (DOPG and DOTAP) than zwitterionic (DPPC). The phase of the bilayer is also important, such as fluid phase bilayers (DOTAP and DOPG) absorb peptide and become distorted easily than gel phase bilayer (DPPC). That is due to the fact that in fluid phase DOPG and DOTAP film, amyloid-β inserts into the bilayer much easier than in gel phase DPPC. This is as a result of the electrostatic interaction between the peptide and lipid bilayer, and the greater fluidity of DOPG and DOTAP than DPPC.

4.2 Future Research

We intend to continue our research into amyloid-β-lipid interactions. We will aim to gather further evidence of the difference between the two different methods of amyloid-β-lipid interactions: monomeric binding into bilayer and fibril binding to bilayer. We intend to use a combination of AFM and fluorescence microscopy to gather these data.

References

Amrein, Matthias, A. von Nahmen, and M. Sieber. "A scanning force- and fluorescence light microscopy study of the structure and function of a model pulmonary surfactant." *European Biophysics Journal 26*, 1997: 349-357.

Astbury, William, and Sylvia Dickinson. "The X-ray interpretation of denaturation and the structure of the seed globulins." *Biochemistry Journal 29*, 1935: 2351-2360.

Balbirnie, M, R Grothe, and Eisenberg, D. "An amyloid forming peptide from yeast prion Sup35 reveals dehydrated beta-sheet structure for amyloid." *PNAS 98*, 2001: 2375-2380.

Bauer, Horst, et al. "Architecture and Polymorphism of Fibrillar Supramolecular Assemblies Produced by in Vitro Aggregation of Human Calcitonin." *Journal Of Stuctural Biology 115*, 1995: 1-15.

Beers, M, C Kim, C Dodia, and A Fisher. "Localization, synthesis, and processing of surfactant protein SP-C in rat lung analyzed by epitope-specific antipeptide antibodies." *Journal of Biological Chemistry 269*, 1994: 20318–20328.

Bokvist, Marcus, Fredrick Lindstrom, Anthony Watts, and Gerhard Grobner. "Two Types of Alzheimer's b-Amyloid (1–40) Peptide Membrane Interactions: Aggregation Preventing Transmembrane Anchoring Versus Accelerated Surface Fibril Formation." *Journal of Molecular Biology 335*, 2004: 1039–1049.

Booth, David, et al. "Instability, unfolding and aggregation of human lysozyme variants underlying amyloid fibrillogenesis." *Nature 385*, 1997: 787-793.

Butterfield, Allan, Yatin, Servet, Sridhar Varadarajan, and Tanuja Koppal. "Amyloid β-peptide-associated free radical oxidative stress, neurotoxicity, and Alzheimer's disease ." *Methods in Enzymology 309*, 1999: 746-768.

Carrell, Robin, and Bibek Gootu. "Conformational changes and disease — serpins, prions and Alzheimer's." *Current Opinions in Structural Biology 8*, 1998: 799-809.

Choucair, A, M Chakrapani, B Chakravarthy, J Katsaras, and Linda Johnston. "Preferential accumulation of amyloid-beta on gel phase domains of lipid bilayers: an AFM and fluorescence study." *Biochemica et Biophysica acta*, 2007: 146-154.

Clements, John. *Alveolar instability associated with altered surface tension. In: Handbook of Physiology. Respiration.* Washington, DC: American Physiology Society, 1964.

Clements, John. "Surface tension of lung extracts." *Prococeedings of the Society of Experimental Biological Medicine 95*, 1957: 170–172.

Cochrane, C, and S Revak. "Pulmonary surfactant protein B (SP-B): structure-function relationships." *Science 254*, 1991: 566–568.

Crewels, L, L van Golde, and H Haagsman. "Review: The Pulmonary Surfactant System: Biochemical and Clinical Aspects." *Lung 175*, 1997: 1-39.

Dante, Silvia, Thomas Hauss, and Norbert Dencher. "Insertion of Externally Administed Amyloid-beta peptide 25-35 and Perturbation of Lipid Bilayers." *Biochemistry 42*, 2003: 13667-13672.

deMello, D, S Heyman, D Phelps, and J Floros. "Immunogold localization of SP-A in lungs of infants dying from respiratory distress syndrom." *American Journal of Pathology 142*, 1993: 1631–1640.

Diaz-Avalos, R, et al. "Cross beta order and diversity in nanocrystals of an amloid forming peptide." *Journal of Molecular Biology 330*, 2003: 1165-1175.

Ding, J, et al. "Effects of Lung Surfactant Proteins, SP-B, SP-C, Palmitic Acid on Monolayer Stability." *Biophysics Journal 80*, 2001: 2262-2272.

Dluhy, R, S Shanmukh, J Leapard, P Kruger, and J Baatz. "Deacylated pulmonary surfactant protein SP-C transforms from alpha-helical to amyloid fibril structure via a pH-dependent mechanism: an infrared structural investigation." *Biophysics Journal 85*, 2003: 2417-2429.

Ege, C, and K Lee. "Insertion of Alzheimers Amyloid Beta into Lipid Monolayer." *Biophysical Journal 87*, 2004: 1732-1740.

Fezoui, Youcef, et al. "An improved method of preparing amyloid beta protein for fibrillogenesis and neurotoxicity experiments." *Amyloid, International Journal of Experimental Clinical Investigation 7*, 2000.

Floros, Jennifer. "Pulmonary Surfactant-Update on Function, Molecular Biology and Clinical Implications." *Current Respiratory Medical Review 1*, 2005: 77.

Giurleo, Jason, Xianglan He, and David Talaga. "β-Lactoglobulin Assembles into Amyloid through sequential Aggregated Intermediates." *Journal of Molecular Biology 381*, 2008: 1332-1348.

Goldsbury, Claire, et al. "Polymorphic Fibrillar Assembly of Human Amylin." *Journal of Structural Biology 119*, 1997: 17-27.

Gregory, T, et al. "Surfactant chemical composition and biophysical activity in acute respiratory distress syndrome." *Journal of Clinical Investigation 88*, 1991: 1976–1986.

Gunasekara, Lasantha, et al. "Pulmonary Surfactant Function is abolished by an elevated proportion of cholesterol." *Biochmica et Biophysica Acta 1737*, 2005: 27-35.

Gustafsson, M, J Thyberg, J, Eliasson, E Naslund, and J Johansson. "Amyloid fibril formation by pulmonary surfactant protein C." *FEBS Letters 464*, 1999: 138-142.

Hallman, M. "The absence of phosphatidylglycerol in surfactant." *Peadeatric Respirology 9*, 1975: 396.

Hane, Francis, Brad Moores, Matthias Amrein, and Zoya Leonenko. "Effect of SP-C on surface potential distribution in pulmonary surfactant: Atomic force microscopy and Kelvin-probe force microscopy study." *Ultramicroscopy*, 2009: In Press.

Harper, J, C Liber, and P Lansbury. *Chemical Biology 4*, 1997: 951-959.

Hawgood, S, J Benson, J Schilling, D Damm, J Clements, and R White. "Nucleotide and amino acid sequences of pulmonary surfactant protein SP 18 and evidence for cooperation between SP 18 and SP 28–36 in surfactant lipid adsorption." *Proceedings of the National Academy of Science 84*, 1987: 66-70.

Holm, B, G Enhorning, and R Notter. "A biophysical mechanism by which plasma proteins inhibit lung surfactant activity." *Chem and Phys of Lipids 49*, 1988: 49-55.

Hoon, Kim Yong, Morio Takizawa, and Tseneo Urisu. *Characterization of Dipalmitoylphosphatidylcholine (DPPC)/Cholesterol Langmuir-Blodgett Monolayers by AFM and FT-IR.*

Ionescu-Zanetti, Cristian, et al. "Monitoring the assembly of Ig light-chain amyloid fibrils by atomic force microscopy." *PNAS 96*, 1999: 13175-13179.

Ji, Shang-Rong, Yi Wu, and Sen-fang Siu. "Cholesterol is an important factor affecting the membrane insertion of b-amyloid peptide (Ab 1–40), which may potentially inhibit the fibril formation." *Journal of Biological Chemistry 277*, 2002: 6273–6279.

Ji, Shang-Rong, Yi Wu, and Sen-fang Siu. "Study of Beta-Amyloid Insertion into Phospholipid Membranes using Monolayer Technique." *Biochemistry (Moscow) 67*, 2002: 1283-1288.

Jimenez, Jose, Ewan Nettleton, Mario Bouchard, Carol Robinson, Christopher Dobson, and Helen Saibil. "The protofilament structure of insulin amyloid fibrils." *PNAS 99*, 2002: 9196–9201.

Johannsen, Jan. "Molecular determinants for amyloid fibril formation: lessons from lung surfactant protein C." *Swiss Med Weekly 133*, 2003: 275-282.

Johannsen, Jan, and Thomas Curstedt. "Molecular Structures and interactions of Pulmonary Surfactant System." *Eurpean Journal of Biochemistry 244*, 1997: 675-693.

Johannson, Jan. "Amyloid Fibrils: Mini-review series." *FEBS Letters 272*, 2005: 5241.

Johansson, Jan, Thomas Curstedt, and B Robertson. "The proteins of the surfactant system." *European Respiratory Journal 7*, 1994: 372-391.

Katsaras, J, D Yang, and R Epand. "Fatty-acid chain tilt angles and directions in dipalmitoylphosphatidylcholine bilayers." *Biophysics Journal*, 1992: 1170–1175.

Keating, Eleonora, et al. "Effect of Cholesterol on the Biophysical and Physiological Properties of a Clinical Pulmonary Surfactant." *Biophysics Journal*, no. 1391-1401 (2007): 1391-1401.

King, Richard. "Pulmonary Surfactant." *Journal of Applied Physiology: Respiratory Enviromental Excercise Physiology 53*, 1982: 1-8.

King, Richard. "Surface active materials from dog lung. II. Composition and physiological correlations." *American Journal of Physiology 223*, 1972: 715-726.

Kirchner, D, C Abraham, and D Selkoe. "X-ray diffraction from intraneuronal paired helical filaments and extraneuronal amyloid fibers in Alzheimer disease indicates cross-beta conformation ." *PNAS 83*, 1986: 503-507.

Koudinov, Alexi, Termirbolat Berezov, and Natalia Koudinova. "Alzheimer's amyloid beta and lipid metabolism: a missing link? ." *FASEB Journal 12*, 1998: 1097-1099.

Kovacs, Helena, Alan Mark, Jan Johansson, and Wilfrid van Gunsteren. "The effect of environment on the stability of an integral membrane helix: Molecular dynamics simulations of surfactant protein C in chloroform, methanol and water." *Journal of Molecular Biology 247*, 1995: 808-822.

Kremer, John, Danial Sklansky, and Murphy Regina. "Profile of Changes in Lipid Bilayer Structure Caused by Beta-Amyloid Peptide." *Biochemistry 40*, 2001: 8563-8571.

Kremer, John, Monica Pallitto, Daniel Sklansky, and Regina Murphy. "Correlation of β-Amyloid Aggregate Size and Hydrophobicity with Decreased Bilayer Fluidity of Model Membranes." *Biochemistry 39*, 2000: 10309-10318.

Leonenko, Zoya, Eric Finot, Vladislav Vassiliev, and Matthias Amrein. "Effect of cholesterol on surfactant film properties: an Atomic Force Microscopy study." *Ultramicroscopy 106*, 2006: 692.

Leonenko, Zoya, et al. "An Elevated Level of Cholesterol Impairs Self-Assembly of Pulmonary Surfactant into a Functional Film." *Biophysical Journal*, 2007: 674-683.

Leonenko, Zoya, Mathias Rodenstein, Jana Dohner, Lukas Eng, and Matthias Amrein. "Surface Potential of Pulmonary Surfactant." *Langmuir 22*, 2006: 10135-10139.

Lin, Hai, Rajinder Bhatia, and Ratneshwar Lal. "Amyloid-beta protein forms ion channels: implications form Alzeimer's diease pathophysiology." *The FASEB Journal 15*, 2001: 2433-2445.

Luhrs, Thorsten, et al. "3D structure of Alzheimer's amyloid-beta(1– 42) fibrils." *PNAS 102*, 2005: 17342–17347.

Maltseva, Elena, Andreas Kerth, Alfred Blume, Helmuth Mowald, and Gerald Brezesinski. "Adsorption of Amyloid b (1–40) Peptide at Phospholipid Monolayers." *ChemBioChem 6*, 2005: 1817 – 1824.

Mathialagan, N. "Low-molecular-weight hydrophobic proteins from bovine pulmonary surfactant." *Biochemie et Biophysica Acta 1045*, 1990: 121-127.

McLaurin, J., and A. Chakrabarty. "Characterization of the interactions of Alzheimer beta-amyloid peptides with phospholipid membranes." *European Journal of Biochemistry 245*, 1997: 355-363.

Morrow, M, S Taneva, G Simatos, L Allwood, and M Keough. "2H NMR studies of the effect of pulmonary surfactant SP-C on the 1,2-dipalmitoyl-sn-glycerol-3-phosphocholine headgroup: a model for transbilayer peptides in surfactant and biological membranes." *Biochemistry 32*, 1993: 11338–11344.

Muller, W, G Eckert, Scheuer, K, N, Maras, A Cairns, and W Gattz. "Effects of β-amyloid peptides on the fluidity of membranes from frontal and parietal lobes of human brain. High potencies of Aβ1-42 and Aβ1-43." *Amyloid 5*, 1998: 10-15.

Nelson, Rebecca, and David Eisenberg. "Recent Atomic Models of Amyloid Fibril Structure." *Current Opinion in Structural Biology*, 2006: 260–265.

Nelson, Rebecca, Micheal Sawaya, Melinda Balbirnie, Anders Madsen, Christian Riekel, and David Eisenberg. "Structure of the cross-beta spine of Amyloid-like Fibrils." *Nature 435*, 2005: 773-778.

Nogee, Lawrance, Alston Dunbar, Susan Wert, Frederic Askin, Aaron Humvas, and Jeffrey Whitsett. "Mutations in the surfactant protein C gene associated with interstitial lung disease." *Chest 121*, 2002: 20S-21S.

Oosterlaken, M. "Characteristics of Lipid insertion into mono molecular layers mediated by surfactant proteins SP-B and SP-C." *Biochemistry 30*, 1991: 10971.

Perez-Gil, J. "Solubility of hydrophobic surfactant proteins in organic solvent/water mixtures: structural studies on SP-B and SP-C in aqueous organic solvents and lipids." *Biochim Biophys Acta 1168*, 1993: 261–270.

Petkova, Aneta, Richard Leapman, Zhihong Guo, Wai-Ming Yau, Mark Mattson, and Robert Tycko. "Self Propogating molecular level polymorphism in Alzheimers beta-amyloid fibrils." *Science 307*, 2005: 262-265.

Petty, T, G Silvers, G Paul, and R Stanford. "Abnormalities in lung elastic properties and surfactant function in Adult Respiratory Distress Syndrome." *Chest 75*, 1979: 571-574.

Poulain, F, and J Clements. "Pulmonary Surfactant Therapy." *Western Journal of Medicine 162*, 1995: 43-50.

Qanbar, R, S Cheng, F Possmayer, and S Schurch. "Role of the palmitoylation of surfactant-associated protein C in surfactant film formation and stability." *American Journal of Physiology 271*, 1996: L572-L580.

Rooney, S, S Young, and C Mendelson. "Molecular and cellular processing of lung surfactant." *The FASEB Journal 8*, 1994: 957-967.

Saitoh, T, et al. "Secreted form of amyloid B protein precursor is involved in the growth regdation of fibroblasts." *Cell 58*, 1989: 615-622.

Selkoe, D. "Toward a comprehensive theory for Alzheimer's disease. Hypothesis: Alzheimer's disease is caused by the cerebral accumulation and cytotoxicity of amyloid beta-protein." *Annals of the New York Academy of Science 924*, 2000: 17-25.

Serpell, Louise. "Alzheimer's amyloid fibrils: structure and assembly." *Biochemie et Biophysica Acta 1502*, 2000: 16-30.

Sharpe, J, J Forrest, and R Jones. "Surface Denaturation and Amyloid Fibril Formation of Insulin at Model Lipid-Water Interfaces." *Biochemistry 41*, 2002: 15810-15819.

Sunde, M, and C Blake. "The Structure of Amyloid Fibrils by Electron Microscopy and X-ray Diffraction." *Advanced Protein Chemistry 50*, 1997: 123-159.

Szyperski, T, G Vandenbussche, Thomas Curstedt, J Ruysschaert, K Wuthrich, and Johansson Jan. " Pulmonary surfactant-associated polypeptide C in a mixed organic solvent transforms from a monomeric alpha-helical state into insoluble beta-sheet aggregates." *Protein Science 7*, 1998: 2533-2540.

Terzi, Evelyn, Gunter Holtzmann, and Joachin Seelig. "Self Association of Amyloid beta in solution and binding to lipid membranes." *Journal of Molecular Biology 252*, 1995: 633–642.

Terzi, Evelyn, Holtzmann, Gunter, and Joachim Seelig. "Alzheimer Amyloid Peptide 25-35: Electrostatic Interactions with Phospholipid Membranes." *Biochemistry 33*, 1994: 7434-7441.

Wüstneck, R. "The influence of SP-B oligomerization and SP-C secondary structure on the interfacial behavior of pulmonary surfactant and the squeeze-out process." *Applied Cardiopulmonary Pathophysiology 13*, 2004: 105-106.